



The University of
Nottingham

UNITED KINGDOM · CHINA · MALAYSIA

**Cavitation based wastewater treatment of
recalcitrant organic pollutants (Dicofol,
BDE-209, HBCD, PFOS, PFOA)**

by

Debabrata Panda, MSc.

**Thesis submitted to the University of Nottingham
for the degree of Doctor of Philosophy**

April 2018

Department of Chemical and Environmental Engineering

Faculty of Engineering

The University of Nottingham

Dedication:

**This PhD dissertation is dedicated to my parents for their
inspiration, vigor, patience and love**

Abstract

Water pollution has been an environmental concern for many years, which have attracted numerous researches for an effective wastewater treatment method to address the issue. Cavitation based wastewater treatments is one of the emerging advanced oxidation processes (AOPs), which has recently drawn attention due to its effectiveness in pollutant removal. But, the effectiveness of cavitation treatment in the elimination of persistent organic pollutants (POPs) is still at an early stage, while considering the wide range of recalcitrant pollutants to be eliminated. Dicofol, Decabromodiphenyl ether (BDE-209), Hexabromocyclododecane (HBCD), perfluorooctanesulfonic acid (PFOS) and Perfluorooctanoic acid (PFOA) are listed or recommended persistent organic pollutants (POPs) under Stockholm convention. For the past several years, numerous reports indicated the detection of above-mentioned POPs in the environmental matrix and hence their elimination via efficient methods is of priority, because of their carcinogenic, endocrine disruptive, hepatotoxic and bioaccumulative nature. POPs are mostly recalcitrant towards conventional treatment methods. Thus, the mineralization of pollutants, treatment duration, energy efficiency etc. are some of the vital concerns to be addressed.

The research investigated the sonochemical based method for the removal of Dicofol, BDE-209, HBCD, PFOS and PFOA (PFOX), whereas hydrodynamic cavitation (HC) was implemented for the removal of Dicofol. The effect of various parameters had been studied distinctively by considering sonication power, HC inlet pressure, treatment duration, pH, reaction solution temperature and initial pollutant concentration. The degradation products were monitored by gas chromatography mass spectrometry (GC-MS), liquid chromatography mass spectroscopy (LC-

MS), high-performance liquid chromatography (HPLC) and liquid chromatography mass spectroscopy (LC-MS) analysis. GC-MS analysis in selected ion monitoring mode (SIM) and liquid chromatography tandem mass spectrometry (LC-MS/MS) in multiple reaction-monitoring mode (MRM), were performed for accurate monitoring of the concentration of parent compounds.

The sonochemical degradation of Dicofol, HBCD, BDE-209, PFOX (PFOS and PFOA) in aqueous media has been investigated using a 20-kHz probe type sonicator with power inputs from 150 to 450 W, whereas the Hydrodynamic cavitation (HC) treatment of Dicofol has been investigated by a liquid whistle reactor (LWR) with an inlet pressure in the range of 3-13 bar. Under optimum conditions of solution pH, reaction temperature, ultrasonic power density and HC inlet pressure, the extent of degradation of Dicofol was found to be 86 % and 100 % within 60 min of ultrasound and HC treatment respectively. Sono-Fenton treatment of BDE-209 demonstrated a complete degradation within 80 min of treatment, whereas sonochemical treatment of PFOX indicated complete disappearance of the parent compounds within 80 min treatment as well. HC treatment of Dicofol illustrated highest mineralization efficiency with 85 % TOC removal within 1 h of treatment. Best mineralization efficiency of sonochemical treatment was achieved for HBCD with 72 % TOC removal within just 40 min of treatment. Overall, cavitation-based wastewater treatments have emerged as potential techniques for the elimination POPs and progressive research is expected to bring out superior treatment efficiency.

Keywords: Cavitation; AOPs; POPs; wastewater; treatment; sonochemical; Hydrodynamic cavitation; Fenton; Dicofol; BDE-209; HBCD; PFOS; PFOA; degradation; mineralization

Acknowledgement

Numerous thanks are owed to those who have supported and inspired me throughout my studies, here at the University of Nottingham, 2014 – 2018.

*I would first like to thank my advisor, **Professor Sivakumar Manickam**, for his wonderful guidance, continuous support, and motivation throughout my PhD career, which enabled me to accomplish one of the important milestones in my career. With respect to his profound understanding in Chemical and Environmental Engineering, I was able to gain a deeper understanding in wastewater treatment and have developed a greater appreciation for the field.*

*I am also thankful to my co-supervisor **Dr. Vasanthi Sethu**, for her valuable guidance, support and suggestions throughout the research work.*

*I would like to give my special thanks to **Mr. Pankaj, Mr. Malaka Kaluarachchi, Ms. Sambath**, for their selfless support during my entire PhD journey.*

Finally, I would like to thank my parents for their continuous support, enthusiasm, and motivation throughout my doctoral program.

Table of contents

Abstract	iii
Acknowledgement	v
Table of contents	vi
List of figures	xii
List of tables	xv
Abbreviations	xvii
Chapter 1: Introduction and Summary	1
1.1 Background and Motivation.....	2
1.2 Objective and Scope.....	4
1.3 Organization of Dissertation.....	5
1.4 References.....	9
Chapter 2: Sonochemical degradation of endocrine-disrupting organochlorine pesticide Dicofol: Investigations on the transformation pathways of dechlorination and the influencing operating parameters	12
Abstract.....	13
2.1 Introduction.....	14
2.2 Experimental.....	16
2.2.1 Materials and equipment.....	16
2.2.2 Sonochemical experiments.....	17
2.3 Analysis.....	17

2.3.1 High performance liquid chromatography (HPLC) analysis.....	17
2.3.2 GC-MS analysis.....	18
2.4 Results and discussion.....	18
2.4.1 HPLC analysis.....	18
2.4.2 GC-MS analysis.....	19
2.4.3 Degradation pathways.....	21
2.4.4 Reaction kinetics of Dicofol.....	23
2.4.5 Effect of initial concentration on the degradation of Dicofol.....	24
2.4.6 Effect of change in pH.....	25
2.4.7 Effect of solution temperature.....	26
2.4.8 Effect of acoustic power on the degradation of Dicofol.....	27
2.4.9 Control experiments.....	29
2.5 Conclusions.....	32
2.6 References.....	33
Chapter 3: Hydrodynamic cavitation assisted degradation of persistent endocrine-disrupting organochlorine pesticide Dicofol: Optimization of operating parameters and investigations on the mechanism of intensification.....	37
Abstract.....	38
3.1 Introduction.....	39
3.2 Experimental.....	40
3.2.1 Materials and equipment.....	40
3.2.2 Experimental set-up.....	40
3.2.2.1 Liquid whistle reactor (LWR).....	40

3.2.3 Experimental methodology.....	41
3.3 Analysis.....	42
3.3.1 High performance liquid chromatography (HPLC) analysis.....	42
3.3.2 GC-MS analysis.....	42
3.3.3 TOC analysis.....	43
3.4 Results and discussion.....	43
3.4.1 Degradation pathways.....	44
3.4.2 Effect of initial pollutant concentration.....	46
3.4.3 Effect of operating temperature.....	48
3.4.4 Effect of inlet pressure.....	49
3.4.5 Effect of change in pH on Dicofol degradation.....	51
3.4.6 Effect of H ₂ O ₂ addition and radical scavengers test.....	53
3.5 Energy efficiency analysis.....	57
3.5.1 Comparison between Hydrodynamic cavitation and Acoustic cavitation	57
3.6 Conclusions.....	58
3.7 Appendix.....	59
3.8 References.....	61
Chapter 4: Heterogeneous Sono-Fenton treatment of Decabromodiphenyl ether (BDE-209):	
Debromination mechanism and transformation pathways.....	65
Abstract.....	66
4.1 Introduction.....	67
4.2 Experimental.....	68
4.2.1 Materials.....	68

4.2.2 Experiment methodology.....	69
4.2.3 Analytical methods.....	70
4.2.4 Debromination rate constants.....	71
4.3 Results and discussion.....	71
4.3.1 Degradation pathways and possible mechanism.....	73
4.3.2 Effect of initial concentration on degradation.....	77
4.3.3 Effect of solution pH on degradation.....	78
4.3.4 Effect of ultrasonic power density on degradation.....	79
4.3.5 Effect of Fenton's reagent loading on degradation.....	80
4.4 Control experiments.....	83
4.5 Comparison of degradation efficiency with different processes.....	84
4.6 Conclusions.....	86
4.7 References.....	87
Chapter 5: Sonolytic mineralization of Hexabromocyclododecane: kinetics and influencing factors.....	92
Abstract.....	93
5.1 Introduction.....	94
5.2 Experimental.....	95
5.2.1 Materials.....	95
5.2.2 Sonochemical experiments.....	96
5.3 Chemical analysis.....	96
5.3.1 HPLC analysis.....	96
5.3.2 GC-MS analysis.....	97

5.3.3 Mineralization study.....	97
5.3.4 Ecotoxicity assessment.....	97
5.4 Results and discussion.....	98
5.4.1 Reaction kinetics of HBCD.....	105
5.4.2 Effect of initial concentration on the degradation of HBCD.....	105
5.4.3 Effect of acoustic power on the degradation of HBCD.....	106
5.4.4 Effect of operating temperature on the degradation of HBCD.....	107
5.4.5 Effect of change in pH on the degradation of HBCD.....	109
5.4.6 Effect of addition of H ₂ O ₂ on the degradation of HBCD.....	110
5.5 Conclusions.....	111
5.6 References.....	113
Chapter 6: Kinetics and mechanism of low frequency ultrasound driven elimination of trace level	
aqueous Perfluorooctanesulfonic acid and Perfluorooctanoic acid.....	118
Abstract.....	119
6.1 Introduction.....	120
6.2 Experimental.....	121
6.2.1 Materials.....	121
6.2.2 Sonochemical experiments.....	122
6.3 Chemical analysis.....	122
6.3.1 LC-MS analysis.....	122
6.3.2 Precautions during detection.....	124
6.4 Results and discussion.....	125
6.4.1 Significance of low frequency for the trace level elimination of PFOX	129

6.4.2 Reaction kinetics of PFOX.....	130
6.4.3 Effect of initial concentration of PFOX on its degradation.....	131
6.4.4 Effect of operating temperature on degradation.....	133
6.4.5 Effect of acoustic power on degradation.....	134
6.4.6 Effect of pH on the degradation of PFOX.....	136
6.5 Conclusions.....	137
6.6 References.....	138
Chapter 7: Overall discussion.....	142
Chapter 8: Conclusions	146

List of figures

Figure 2.1. Chromatographic representation of (a) Dicofol parent compound & degraded products along with Dicofol after (b) 30 min, (c) 60 min of sonication.....	19
Figure 2.2. Mass spectrogram of (a) Dicofol, (b) the degraded product methanone, bis(3-chlorophenyl) and (c) 4-Chlorobenzophenone.....	20
Figure 2.3. Selected ion monitoring (m/z 139) chromatographic representation of Dicofol and peak intensity at (a) 0 min (b) 20 min.....	21
Figure 2.4. The proposed degradation pathways of Dicofol under ultrasonic irradiation	22
Figure 2.5. Degradation of Dicofol at various initial concentrations.....	24
Figure 2.6. Degradation of Dicofol at different pH.....	26
Figure 2.7. Degradation of Dicofol at different temperatures.....	27
Figure 2.8. Degradation of Dicofol at different ultrasonic power levels.....	28
Figure 2.9. Degradation of Dicofol at different H ₂ O ₂ loading.....	30
Figure 2.10. Degradation of Dicofol at various loadings of sodium bicarbonate.....	31
Figure 3.1. Schematic representation of the experimental set-up of LWHCR (1, feed tank; 2, plunger pump; 3, PLC control board; 4, digital pressure gauge.....	41
Figure 3.2. Chromatographic representation of (a) Dicofol at 0 min (b) Degraded products along with Dicofol after 30 min of HC treatment.....	43
Figure 3.3. Selected ion monitoring (m/z 139) chromatographic representation of Dicofol and peak intensity at (a) 0 min (b) 10 min and (c) 30 min of HC treatment.....	44
Figure 3.4. The proposed degradation pathways of Dicofol.....	45
Figure 3.5. Degradation of Dicofol at different initial concentrations.....	47
Figure 3.6. Degradation of Dicofol at various solution temperatures.....	48

Figure 3.7. Schematic of the flow and pressure distribution across the orifice.....	49
Figure 3.8. Degradation of Dicofol at various inlet pressures.....	51
Figure 3.9. Degradation of Dicofol at different pH.....	52
Figure 3.10. The degradation of Dicofol at various H ₂ O ₂ loading.....	53
Figure 3.11. TOC removal of Dicofol during 60 min of HC treatment.....	54
Figure 3.12. Degradation of Dicofol at various loadings of sodium bicarbonate...	56
Figure 4.1. Chromatograms of BDE-209 full scan analysis at (a) 0 min (b) 60 min of treatment.....	72
Figure 4.2. Chromatograms of BDE-209 full scan analysis at 80 min of (a) Fenton and (c) US treatment alone.....	72
Figure 4.3. TOC removal percentage of BDE-209 within 80 min of treatment (Experimental conditions: initial concentration: 20 mg/L; power density: 420 W)	73
Figure 4.4. The proposed degradation pathways of BDE-209 during US/Fenton treatment.....	75
Figure 4.5. Degradation of BDE-209 at different initial concentration.....	77
Figure 4.6. Degradation of BDE-209 at various solution pH.....	78
Figure 4.7. BDE-209 degradation at various ultrasound power density.....	80
Figure 4.8. BDE-209 degradation at various H ₂ O ₂ loading.....	81
Figure 4.9. BDE-209 degradation percentage at various nZVI loading.....	82
Figure 4.10. Degradation of BDE-209 at various loadings of sodium bicarbonate	84
Figure 4.11. The US/Fenton, US and Fenton processes of BDE-209 degradation	85
Figure 5.1. HPLC chromatograph of HBCD at (a) 0 min (b) 30 min of treatment	98
Figure 5.2. Chromatographic representation of (a) HBCD standard.....	99

Figure 5.3. Proposed transformation of HBCD during sonolysis. Dashed line represents the proposed pathways, whereas the solid line represents the identified products during GC-MS analysis.....	100
Figure 5.4. HBCD, (%) Inhibition of <i>Daphnia magna</i> and TOC removal (%)	104
Figure 5.5. Degradation of HBCD at various initial concentrations.....	106
Figure 5.6. Degradation of HBCD at different ultrasonic power levels.....	107
Figure 5.7. Degradation of HBCD at different temperatures.....	108
Figure 5.8. Degradation of HBCD at different pH.....	109
Figure 5.9. Degradation of HBCD at different H ₂ O ₂ loading.....	110
Figure 6.1. Chromatographic representation of (a) ESI mass spectra of PFOS and PFOA parent ions (b) MRM spectra of PFOS and PFOA (c) MRM spectra.....	126
Figure 6.2. (a) Cavitation bubble and PFOX degradation: adsorption and thermal decomposition of PFOX parent compound at bubble-bulk interfacial zone.....	128
Figure 6.3. Degradation of PFOX at various initial concentrations (a) PFOS...	132
Figure 6.4. PFOX degradation percentage at different temperatures.....	134
Figure 6.5. Degradation of PFOX at different ultrasonic power levels.....	135
Figure 6.6. Average percentage degradation of PFOX at different pH.....	136
Figure 7.1. Comparison chart.....	143

List of tables

Table 2.1. Pseudo-first-order rate constants for the degradation of Dicofol.....	31
Table 2.2. Effect of radical scavenger addition on the extent of degradation.....	32
Table 3.1. Flow characteristics of Dicofol at various inlet pressures of HC.....	50
Table 3.2. Pseudo-first-order rate constants for the degradation of Dicofol under different operational parameters.....	52
Table 3.3. Effect of H ₂ O ₂ loading on the extent of degradation and kinetic rate constants for Dicofol.....	54
Table 3.4. Effect of addition of radical scavenger on the extent of degradation and kinetic rate constants.....	56
Table 4.1. Retention time of the chemical standards in the GC-MS.....	74
Table 4.2. The aqueous solubility of PBDE congeners.....	77
Table 4.3. Pseudo-first-order rate constants for the degradation of BDE-209 under different operational parameters.....	82
Table 4.4. Effect of addition of radical scavenger on the extent of degradation and kinetic rate constants.....	84
Table 4.5. Comparison of the combined process of US/Fenton with individual process (US and Fenton)	85
Table 5.1. GC-MS retention time and spectral characteristics of HBCD transformed products.....	100
Table 5.2. Individual chemical bonds of HBCD and their corresponding bond dissociation energies.....	101

Table 5.3. Properties of HBCD.....	101
Table 5.4. Pseudo-first-order rate constants for the degradation of HBCD under different operational parameters.....	111
Table 6.1. Henry's constants of PFOX and their degradants.....	129
Table 6.2. Pseudo-first-order rate constants for PFOX under different initial concentration.....	133
Table 6.3. pKa values of PFOX and their degradants.....	137

Abbreviations

POP	Persistent organic pollutant
HPLC	High performance liquid chromatography
GC-MS	Gas chromatography mass spectroscopy
EDC	Endocrine disrupting compound
BCF	Bioconcentration factor
LOD	Limit of detection
LOQ	Limit of quantification
Fig	Figure
min	Minute
h	Hour
W	Watt
kHz	Kilohertz
°C	Celsius
SIM	Selected Ion Monitoring
Ph	Phenol
CB	Chlorobenzene
NB	Nitrobenzene

PNP	P-nitrophenol
2,4-DCP	2,4-dichlorophenol
HC	Hydrodynamic cavitation
LWR	Liquid whistle reactor
TOC	Total organic carbon
LWHCR	Liquid whistle hydrodynamic cavitation reactor
VFD	Variable frequency drive
VWD	Variable Wavelength Detector
UV	Ultraviolet
DBP	4,4'-Dichlorobenzophenone
MPa	Megapascal
AOP	Advanced oxidation process
LPH	Liters Per Hour
BDE-209	Decabromodiphenyl ether
US	Ultrasound
PBDE	Polybrominated diphenyl ether
EPA	Environmental protection agency
AFP	Advanced heterogeneous Fenton process

THF	Tetrahydrofuran
amu	Atomic mass unit
NIST	National Institute of Standards and Technology
nZVI	Nano zero valent iron
H ₂ O ₂	Hydrogen Peroxide
HBCD	Hexabromocyclododecane
PS	Polystyrene
ppm	Parts per million
PFOS	Perfluorooctanesulfonic acid
PFOA	Perfluorooctanoic acid
PTFE	Polytetrafluoroethylene
LC-MS/MS	Liquid chromatography tandem mass spectroscopy
ESI	Electrospray ionization
API	Atmospheric Pressure Ionization
MRM	Multiple reaction monitoring
CID	Collision-induced dissociation
PFC	Perfluorinated compound
TIC	Total ion chromatogram

Chapter 1

Introduction and Summary

1.1 Background and Motivation

Rapid industrialization, ever growing human food consumption and the need of associated agricultural growth have resulted in the increased use of numerous harmful chemicals. Associated hazardous pollutants can enter the environment either by direct or indirect emission sources such as use of commercial products, manufacturing processes, degradation of precursor substances or release of wastewater. Exposure of persistent organic pollutants (POPs) above a certain limit can lead to severe consequences for humans and aquatic lives.

With the constant increase in pesticides use, the World Health Organization (WHO, 1992) reported three million pesticide poisonings annually, resulting in 220,000 deaths worldwide (Thundiyl et al., 2008). Dicofol is one of the acaricide/miticide, widely used for variety of crops, which has been identified as a potential candidate to be included under POP protocol and is reported to be an endocrine disrupter (Hoekstra et al., 2006; Li et al., 2014). There is mounting evidence on the link of exposure of pesticides and the associated human chronic diseases such as cancer, diabetes, Parkinson, Alzheimer, cardiovascular and kidney diseases (Mostafalou and Abdollahi, 2013).

The application of brominated flame retardants (BFRs) such as HBCD ranges from upholstery textiles to polystyrene (PS) based consumer products. Considering the detrimental consequences of HBCD for humans and animals, the associated countries of Stockholm convention commenced a ban on its application that to be effective in 2019 (Hogue, 2013). Apart from HBCD, BFRs such as Decabromodiphenyl ether (BDE-209) is regarded as an endocrine disrupting chemical (EDC) (Kharlyngdoh et al., 2015), which is used as a flame retardant in different electrical as well as textile applications. Till now, this is the major technical polybrominated diphenyl ether (PBDE) to be used. PBDE congeners including BDE-209 are detected worldwide, resulting in significant environmental issues (Thuresson et al., 2005).

Perfluorooctanoic acid (PFOA) and perfluorooctanesulfonic acid (PFOS), altogether called PFOX, are under the family of perfluorinated surfactants (PFSs). For the past 50 years, they have been used in various applications including cosmetics, insecticides, stain repellants, fabric protectors, production of firefighting foams and fluoropolymers such as polytetrafluoroethylene (PTFE/Teflon). Various studies reported the persistency of PFOX in the environment and serious health problems because of its carcinogenic, hepatotoxic and neoplastic nature (Alexander and Olsen, 2007; Xiao et al., 2015).

Complete elimination of recalcitrant pollutants is vital because of the associated adverse health concerns, but most of the POPs are resistant towards conventional treatment technologies such as biodegradation, adsorption, filtration, sedimentation and chlorination. For example, PFOS and PFOA are difficult to eliminate via conventional treatment methods owing to their stable structure (Kato et al., 2013). Even though nanofiltration and reverse osmosis had shown to remove numerous pollutants from wastewater, but subsequent incineration is necessary for complete destruction of the dissolved waste (Li et al., 2012; Zhang et al., 2006). Also, the degradation of pollutants may generate short chain byproducts with higher toxicity compared to the parent compound (Luo et al., 2011; Trovó et al., 2012) and hence mineralization of pollutant is essential for complete elimination. Advanced oxidation processes (AOPs) such as cavitation-based techniques have emerged as the most effective treatment methods for the elimination of recalcitrant pollutants. If the cavitation event occurs due to the passage of ultrasonic waves in the liquid medium, then it is termed as acoustic cavitation, whereas if it occurs due to the pressure variations in the flowing liquid with respect to change in the geometry of constriction, then it is called as hydrodynamic cavitation (HC). Introduction of ultrasonic waves of certain frequencies (20-1000 kHz) can create bubbles followed by the collapse events (Brennen 1995). In case of HC, when the

liquid passes through the constriction the velocity of the liquid increases at the expense of local pressure and the pressure around the point of vena contracta falls below the threshold pressure (usually vapor pressure of the medium at the operating temperature), resulting in the formation of cavities. At the downstream of the constriction, as the liquid jet expands, the pressure recovers, and this results in the collapse of cavities (Moholkar and Pandit, 1997). The collapse of cavities can generate temperatures up to 5,000 K inside the bubble core along with the production of highly reactive free radicals such as H^{\bullet} , OH^{\bullet} , O^{\bullet} owing to the homolytic cleavage of water molecules and dissolved gases such as oxygen (Didenko et al. 1999). While pyrolysis in the bubble core and to a lesser extent at bubble-liquid interfacial region have been reported to be effective for the mineralization of hydrophobic pollutants, at the same time, the generated oxidizing free radicals are responsible for the degradation of polar organic compounds (Nam et al. 2003).

While cavitation-based treatments have great potential to improve and revolutionize water treatment technology, there is imminent concern regarding the efficiency in the removal of recalcitrant pollutants. Since POPs possess unique properties, they may pose challenges during cavitation-based wastewater treatment processes. Therefore, this research addresses detailed fundamental mechanisms and degradation pathways regarding the removal of POPs via sonochemical and HC based treatment processes.

1.2 Objectives and Scope

The goal of this doctoral research was to investigate the cavitation-based (sonochemical and hydrodynamic cavitation) treatment of recalcitrant organic pollutants such as Dicofol, BDE-209, HBCD, PFOS and PFOA. The fundamental mechanism governing the removal of pollutants in model solutions were investigated and respective degradation pathways were extensively studied.

The scope of this study involves treatment of five recalcitrant pollutants and the optimization of operating parameters for best possible removal efficiency.

The first objective was to optimize analytical instruments such as HPLC, LC-MS, GC-MS and TOC with respect to the available standards and to compare the standardized data with experimental outcomes. The second objective is to conduct experiments for respective pollutants under a range of operational parameters. The general parameters under consideration include pH, reaction solution temperature, ultrasound intensity, inlet pressure of HC, initial concentration of pollutant and the addition of H₂O₂. The last objective was to evaluate the outcomes of treatments with respect to obtained experimental data to establish the degradation mechanism and to draw the transformation pathways. The study involved 1) comparison of individual process outcomes (US, Fenton and US/Fenton) 2) calculation of synergistic index 3) deciding energy efficiency with respect to sonochemical and HC treatment.

1.3 Organization of Dissertation

This entire PhD dissertation is composed of six chapters, including the Introduction section (Chapter 1). Following the Chapter 1 Introduction, Chapter 2 titled “Sonochemical degradation of endocrine-disrupting organochlorine pesticide Dicofol: Investigations on the transformation pathways of dechlorination and the influencing operating parameters,” discusses the optimum conditions to be undertaken for the highest rate of sonochemical degradation of Dicofol. Degradation products were monitored via High performance liquid chromatography (HPLC) and Gas chromatography coupled with mass spectroscopy (GC-MS) analysis. Control experiments and radical scavenger test determined the predominant cavitation degradation region and degradation mechanism was illustrated with respect to the detected degradation products.

Chapter 3, entitled “Hydrodynamic cavitation assisted degradation of persistent endocrine-disrupting organochlorine pesticide Dicofol: Optimization of operating parameters and Investigations on the mechanism of intensification” investigated on a liquid whistle hydrodynamic cavitation reactor (LWHCR) for Dicofol removal. Process intensification was achieved via optimization of essential parameters such as inlet pressure, initial concentration of Dicofol, solution temperature, pH and addition of H₂O₂. Results showed that under optimum conditions, the complete removal of Dicofol was achieved within 1 h of treatment and total organic carbon (TOC) analysis demonstrated significant mineralization efficiency within the treatment time. Also, a comparison between hydrodynamic cavitation and acoustic cavitation was performed to determine the energy efficiency with respect to the degradation yield.

Chapter 4, titled “Heterogeneous Sono-Fenton treatment of Decabromodiphenyl ether (BDE-209): Debromination mechanism and transformation pathways” illustrates the experimental outcomes of combined ultrasound and advanced Fenton process for the removal of Decabromodiphenyl ether (BDE-209). The effects of vital parameters (i.e. pH, pollutant concentration, ultrasonic power density, Fenton’s reagent loading) were studied to see impact on the degradation rate. Most of the degradation products were determined quantitatively via GC-MS analysis, whereas the concentration of parent compound was also monitored via HPLC analysis. The degradation mechanism during the combined process indicated the thermal decomposition of pollutants at bubble-vapor interface along with reductive debromination at the surface of iron. Lastly, a comparison study among ultrasound, Fenton and Sono-Fenton treatment methods was conducted to calculate the synergistic index.

Chapter 5, titled “Sonolytic mineralization of Hexabromocyclododecane: kinetics and influencing factors” investigated the sonochemical mineralization of Hexabromocyclododecane (HBCD).

HPLC, GC-MS and TOC analysis were performed to demonstrate the presence of degradation products and mineralization efficiency. Also, the ecotoxicity of HBCD and its transformed products were evaluated via *Daphnia magna* bioassay test. A complete degradation of HBCD was achieved within 40 min of sonochemical treatment at optimum conditions.

Chapter 6, titled “Kinetics and Mechanism of Low Frequency Ultrasound Driven Elimination of Trace Level Aqueous Perfluorooctanesulfonic acid and Perfluorooctanoic acid” demonstrated sonochemical treatment of Perfluorooctanesulfonic acid (PFOS) and Perfluorooctanoic acid (PFOA) and essential precautions to be opted during Liquid chromatography mass spectroscopy (LC-MS) analysis. The relation between initial concentration of pollutant and the frequency of sonication was established with respect to previous reported results. LC-MS analysis in multiple reaction monitoring (MRM) mode was performed for the quantification of parent as well as degradation products.

Part of the work reported in this dissertation has been published or submitted. With respect to the outcomes of this research, below is a list of published manuscripts:

Published:

(1) **Debabrata Panda**, Sivakumar Manickam, Recent advancements in the sonophotocatalysis (SPC) and doped- sonophotocatalysis (DSPC) for the treatment of recalcitrant hazardous organic water pollutants, *Ultrasonics Sonochemistry* 36 (2017), 481–496.

(2) **Debabrata Panda**, Sivakumar Manickam, Sonochemical degradation of endocrine-disrupting organochlorine pesticide Dicofol: Investigations on the transformation pathways of dechlorination and the influencing operating parameters, *Chemosphere* 204 (2018), 101-108.

(3) **Debabrata Panda**, Sivakumar Manickam, Hydrodynamic cavitation assisted degradation of persistent endocrine-disrupting organochlorine pesticide Dicofol: Optimization of operating

parameters and investigations on the mechanism of intensification, *Ultrasonics Sonochemistry*, 2018.

(4) **Debabrata Panda**, Sivakumar Manickam, Heterogeneous Sono-Fenton treatment of Decabromodiphenyl ether (BDE-209): Debromination mechanism and transformation pathways, *Separation and purification technology*, 2018.

Submitted:

(1) **Debabrata Panda**, Sivakumar Manickam, “Sonolytic mineralization of Hexabromocyclododecane: kinetics and influencing factors”.

(Manuscript submitted to: Journal of Cleaner Production)

(2) **Debabrata Panda**, Sivakumar Manickam, “Kinetics and Mechanism of Low Frequency Ultrasound Driven Elimination of Trace Level Aqueous Perfluorooctanesulfonic acid and Perfluorooctanoic acid”.

(Manuscript submitted to: Water, Air, & Soil Pollution)

1.4 References

- WHO, 1992. *Our Planet, Our Health; Report of the WHO commission on health and environment*, WHO: Geneva, Switzerland.
- Thundiyil, J. G., Stober, J., Besbelli, N., Pronczuk, J., 2008. Acute pesticide poisoning: a proposed classification tool, *Bulletin of the World Health Organisation* 86, 205-209.
- Hoekstra, P. F., Burnison, B. K., Garrison, A. W., Neheli, T., Muir, D. C. G., 2006. Estrogenic activity of dicofol with the human estrogen receptor: Isomer- and enantiomer-specific implications, *Chemosphere* 64, 174–177.
- Li, S., Tian, Y., Ding, Q., Liu, W., 2014. The release of persistent organic pollutants from a closed system dicofol production process, *Chemosphere* 94, 164–168.
- Mostafalou, S., Abdollahi, M., 2013. Pesticides and human chronic diseases: Evidences, mechanisms, and perspectives, *Toxicol. Appl. Pharmacol.* 268, 157–177.
- Hogue, C., 2013. Global ban for flame retardant, *Chem. Eng. News* 91, 6.
- Kharlyngdoh, J. B., Pradhan, A., Asnake, S., Walstad, A., Ivarsson, P., Olsson, P. E., 2015. Identification of a group of brominated flame retardants as novel androgen receptor antagonists and potential neuronal and endocrine disrupters, *Environ. Int.* 74, 60–70.
- Thuresson, K., Bergman, Å., Jakobsson, K., 2005. Occupational exposure to commercial decabromodiphenyl ether in workers manufacturing or handling flame-retarded rubber, *Environ. Sci. Technol.* 39, 1980–1986.
- Alexander, B. H., Olsen, G. W., 2007. Bladder cancer in Perfluorooctanesulfonyl Fluoride manufacturing workers, *Ann. Epidemiol.* 17, 471-478.

- Xiao, F., Simcik, M. F., Halbach, T. R., Gulliver, J. S., 2015. Perfluorooctane sulfonate (PFOS) and perfluorooctanoate (PFOA) in soils and groundwater of a U.S. metropolitan area: Migration and implications for human exposure, *Water Res.* 72, 64–74.
- Kato, K., Wong, L. Y., Basden, B. J., Calafat, A. M., 2013. Effect of temperature and duration of storage on the stability of polyfluoroalkyl chemicals in human serum, *Chemosphere.* 91, 115–117.
- Li, X. Y., Zhang, L. W., Wang, C. W., 2012. Review of Disposal of Concentrate Streams from Nanofiltration (NF) or Reverse Osmosis (RO) Membrane Process, *Adv. Mater. Res.* 518–523, 3470–3475.
- Zhang, G., Ji, S., Xi, B., 2006. Feasibility study of treatment of amoxicillin wastewater with a combination of extraction, Fenton oxidation and reverse osmosis, *Desalination.* 196, 32–42.
- Luo, S., Yang, S., Xue, Y., Liang, F., Sun, C., 2011. Two-stage reduction/subsequent oxidation treatment of 2,2',4,4'-tetrabromodiphenyl ether in aqueous solutions: Kinetic, pathway and toxicity, *J. Hazard. Mater.* 192, 1795–1803.
- Trovó, A. G., Pupo Nogueira, R. F., Agüera, A., Fernandez-Alba, A. R., Malato, S., 2012. Paracetamol degradation intermediates and toxicity during photo-Fenton treatment using different iron species, *Water Res.* 46, 5374–5380.
- Brennen, C. E., 1995. Cavitation and bubble dynamics.
- Moholkar, V. S., Pandit, A. B., 1997. Bubble behavior in hydrodynamic cavitation: effect of turbulence, *AIChEJ.* 43, 1641–1648.
- Didenko, Y. T., McNamara III, W. B., Suslick, K. S., 1999. Hot spot conditions during cavitation in water, *J. Am. Chem. Soc.* 121, 191–204.

Nam, S. N., Han, S. K., Kang, J. W., Choi, H., 2003. Kinetics and mechanisms of the sonolytic destruction of non-volatile organic compounds: Investigation of the sonochemical reaction zone using several OH• monitoring techniques, *Ultrason. Sonochem.* 10, 139–147.

Chapter 2

Sonochemical degradation of endocrine-disrupting organochlorine pesticide Dicofol: Investigations on the transformation pathways of dechlorination and the influencing operating parameters

Abstract

Dicofol, an extensively used organochlorine pesticide and a recommended Stockholm convention persistent organic pollutant (POP) candidate is well known for its endocrine disruptive properties. The sonochemical degradation of Dicofol in aqueous media has been investigated using a 20-kHz probe type sonicator with power inputs from 150 to 450 W. The degradation rate was determined as a function of concentration of Dicofol, solution pH, bulk phase temperature, ultrasonic power density and H₂O₂ addition. At optimum operating conditions, the pseudo-first-order degradation rate constant (k) was determined to be 0.032 min⁻¹ and the extent of degradation was found to be 86 % within 60 min of ultrasound treatment. High performance liquid chromatography (HPLC) and Gas chromatography coupled with mass spectroscopy (GC-MS) analysis indicated the presence of degraded products. The obtained results of Dicofol degradation and control experiments in the presence of H₂O₂ and radical scavenger test suggest thermal decomposition along with radical attack at bubble-vapor interface to be the dominant degradation pathway.

2.1 Introduction

Pesticides are extensively used worldwide in agriculture to prevent damage caused by various pests. Even though the use of pesticides brings undeniable benefits in agricultural production and assists mitigating the food scarcity to meet ever growing human consumption, but on the other hand it brings several environmental and health consequences due to their toxic, bioaccumulative and endocrine disruptive nature (Mostafalou and Abdollahi, 2013; Mckinlay et al., 2008; Mnif et al., 2011). Among them, organochlorine pesticides are a cause of concern due to their global use (Tiemann, 2008). Dicofol is one of the extensively used organochlorine pesticide which is applied for foliar applications and predominantly for cotton, apple, citrus crops along with several others such as beans, peppers, tomatoes and ornamental crops (US EPA,1998). Since mid-1950s, Dicofol has been used worldwide as miticide, pesticide and acaricide, while the East-Southeast Asia, Mediterranean coast along with Northern-Central America are reported to be as dominant consumers.

Considering the adverse consequences, Dicofol has been proposed as a persistent organic pollutant under Stockholm Convention (UNEP, 2013) and it has been nominated as a potential “endocrine disrupting compound” (EDC) (US EPA,1998). The principal release of Dicofol to the environment might result from the production units or via professional and private use. Due to its high bioconcentration factor (BCF) of >5000 and long-range environmental transport, Dicofol satisfies the criteria for bioaccumulation and is considered to be highly toxic to aquatic organisms (US EPA,1998). The half-lives of Dicofol elimination from bluegill sunfish and mammals are reported to be 33 days and 14 days respectively (US EPA, 1998). Stockholm convention report suggests that there are evidences of estrogenic activity and reproductive effects on fish, birds, rats and dogs

(US EPA, 1998). Studies found out the development of Hodgins disease, leukemia and autism disorders in children following its residential exposure (UNEP, 2015).

US EPA reported that the photodegradation of Dicofol is not expected to be a significant route of degradation in the environment (UNEP, 2015). Guo et al. (2009) reported 72.5% removal of Dicofol under photocatalytic conditions, whereas the efficiency of Dicofol degradation under ultraviolet irradiation alone is negligible compared to Ag/TiO₂-NT/UV photocatalytic treatment. Binbin et al. (2008) reported a complete removal of Dicofol within 2 h of irradiation in the presence of TiO₂-NPs photocatalyst and high pressure (400 W) mercury lamp. Even though photocatalytic treatment has shown effectiveness in Dicofol removal, but the requirement of catalyst and intense UV light are major drawbacks compared to sonochemical treatment. Ren et al. (2011) investigated the theoretical photodegradation mechanism of Dicofol by density functional theory, but the relevance of this study is questionable with respect to US EPA investigation. Even though biodegradation (Osman et al., 2008; Oliveira et al., 2012) has been reported to be successful in removing Dicofol, but the requirement of a comparatively longer duration of treatment time (28 days for 96% degradation) and incomplete degradation are the major drawbacks. Based on persistence, bioconcentration, high aquatic toxicity, extensive occurrence in environment, along with the endocrine disrupting nature of Dicofol, the employment of an effective wastewater treatment technique is of significance for its elimination. In this context, in our investigation, the proposed sonochemical treatment provides advantages over the previously employed techniques that include faster and effective removal of Dicofol with efficient utilization of energy. Several investigations on the sonochemical degradation of recalcitrant pesticides such as DDT, dichlorvos and alachlor etc. indicated the competence of sonolysis in achieving their successful removal (Thangavadivel et al., 2009; Patil and Gogate, 2015; Bagal and Gogate, 2012). Ultrasound-based

wastewater treatment offers a faster rate of pollutant removal, requires a minimal space and can be operated at low maintenance and hence could be a viable wastewater treatment technology.

In the present work, the sonochemical degradation of Dicofol has been performed to investigate the degradation pathways. Besides, the effects of operational parameters such as ultrasonic power, concentration of Dicofol, pH, solution temperature and H₂O₂ addition on the extent of Dicofol degradation were also investigated. High performance liquid chromatography (HPLC) and Gas chromatography-mass spectrometry (GC-MS) analysis have been employed to monitor the concentration of Dicofol during sonochemical treatment and to identify the degraded products, respectively. Calibration curves for Dicofol at concentrations from 1.35 to 405 µM were constructed and a good linearity was observed. To the best of our knowledge, we believe that this is the first reported investigation on the sonochemical treatment of Dicofol for its efficient removal.

2.2 EXPERIMENTAL

2.2.1 Materials and equipment

Dicofol [2,2,2-Trichloro-1,1-bis(4-chlorophenyl) ethanol (C₁₄H₉Cl₅O), 99.3%, CAS Number 115-32-2], Hydrogen peroxide (H₂O₂), Sodium bicarbonate (99.5%), n-hexane, Methanol (HPLC grade) were purchased from Sigma Aldrich (Malaysia). Ultra-pure deionized water of 15 MΩ.cm resistivity was obtained from a water purification system (PURELAB Option-R, ELGA, UK) and used throughout this study. All other chemicals used in this study were of the highest grade available. Agilent nylon syringe filter of 0.45 µm pore size and 5 ml syringes were purchased from IT Tech Research (M) Sdn. Bhd. (Malaysia). For the analysis, High performance liquid chromatography (HPLC, Agilent 1200 infinity) and Gas chromatograph (GC-MS, Perkin Elmer CLARUS SQ8 S/CLARUS 680) were employed. A temperature-controlled water bath (Julabo Labortechnik GmbH, Germany) system was used to maintain the temperature of reaction solution.

2.2.2 Sonochemical experiments

A co-solvent approach of using methanol along with water for the sonication of Dicofol was adopted because of low aqueous solubility of Dicofol. Extraction of the sonicated sample by n-hexane was performed before GC-MS analysis due to the limitation of analytical instrument. Stock solution of Dicofol in methanol was prepared and was stored at 2 °C. Working standard solutions were prepared regularly by the dilution of stock in methanol and water to the desired concentration. The pH of solution was varied between 3 to 7 throughout the experiment, while excluding higher pH (>7) due to hydrolysis of Dicofol at alkaline pH (US EPA, 1998).

Sonochemical treatment was performed in a 100-mL reactor using a 20 kHz ultrasonic probe (Cole-Parmer Instruments, Illinois, USA) and the applied ultrasonic power range was varied between 150 to 450 W. Calorimetric procedures (Koda et al., 2003) were adopted to verify the actual ultrasonic power and the energy dissipated by the transducer into the solution. The temperature of reaction mixture was maintained between 10-40 °C using a chiller. At selected time intervals, 2 ml aliquots were withdrawn to analyze the final concentration of Dicofol as well as to detect the degraded products. Sonication was performed for 60 min and aliquots were withdrawn at 0, 5, 10, 20, 30, 40, 60 min for HPLC and GC-MS analyses. Each experiment was repeated three times and the standard deviation of the triplicate experiments has been considered.

2.3 Analysis

2.3.1 High performance liquid chromatography (HPLC) analysis

Optimization of HPLC parameters for Dicofol analysis was conducted prior to the injection of sonicated sample and to construct the standard curve and Dicofol stock solutions were prepared in the concentration range of 1.35-405 µM. The limit of detection (LOD) and limit of quantification

(LOQ) were decided based on the signal to noise responses. The HPLC response was linear for Dicofol in the range of 0.5 to 150 ppm. The LOD and LOQ were 0.27 and 1.35 μM , respectively. Samples were injected onto an Agilent HPLC system equipped with an online degasser, quaternary LC pump (Agilent infinity model 1260) and an Agilent infinity 1260 VWD UV detector for the separation on a CORTECSTM C18 column (4.6 mm \times 100 mm, 2.7 μm). The Agilent ChemStation software was used for instrument control, data acquisition, and data analysis. The Dicofol elution was carried out at a column temperature of 30 $^{\circ}\text{C}$ using an isocratic gradient composed of solvent A (methanol) and solution B (4 μM aqueous acetic acid) in 80:20 ratio and the detection was carried out at a wavelength of 229 nm. The injection volume and flow rate were 20 μL and 1.4 ml/min respectively. The retention time of Dicofol was 3.5-3.6 min.

2.3.2 GC-MS analysis

Sonicated samples followed by extraction through n-hexane were subjected to Gas chromatography coupled with mass spectrometry (GC-MS) analysis equipped with a PerkinElmer Elite 5-MS capillary column (length: 30 m, I.D: 0.25 mm, Film thickness: 0.25 μm). The injector temperature was at 200 $^{\circ}\text{C}$, the flow rate was 1.0 mL/min and the injection volume was 1 μL . The oven temperature was at 50 $^{\circ}\text{C}$ for 1 min, which was then increased at 25 $^{\circ}\text{C}/\text{min}$ to 125 $^{\circ}\text{C}$ for 0 min and 10 $^{\circ}\text{C}/\text{min}$ to 300 $^{\circ}\text{C}$ for 1 min. The GC interface and the source were at 280 $^{\circ}\text{C}$ and at 300 $^{\circ}\text{C}$ respectively.

2.4 Results and discussion

2.4.1 HPLC analysis

In the present investigation, HPLC chromatogram (Fig. 2.1) indicated the presence of several peaks in the ultrasound-treated solution in comparison with the untreated Dicofol, justifying the formation of numerous degraded components. The degraded products of Dicofol were observed to

appear after 20 min of sonication followed by a gradual decrease in the concentration of parent compound with treatment time. Also, a decline in the peak intensity of degraded products was observed after 30 min of sonochemical treatment, indicating the removal of degraded short chain intermediates with treatment time. The retention time of Dicofol was noted to be 3.5-3.6 min.

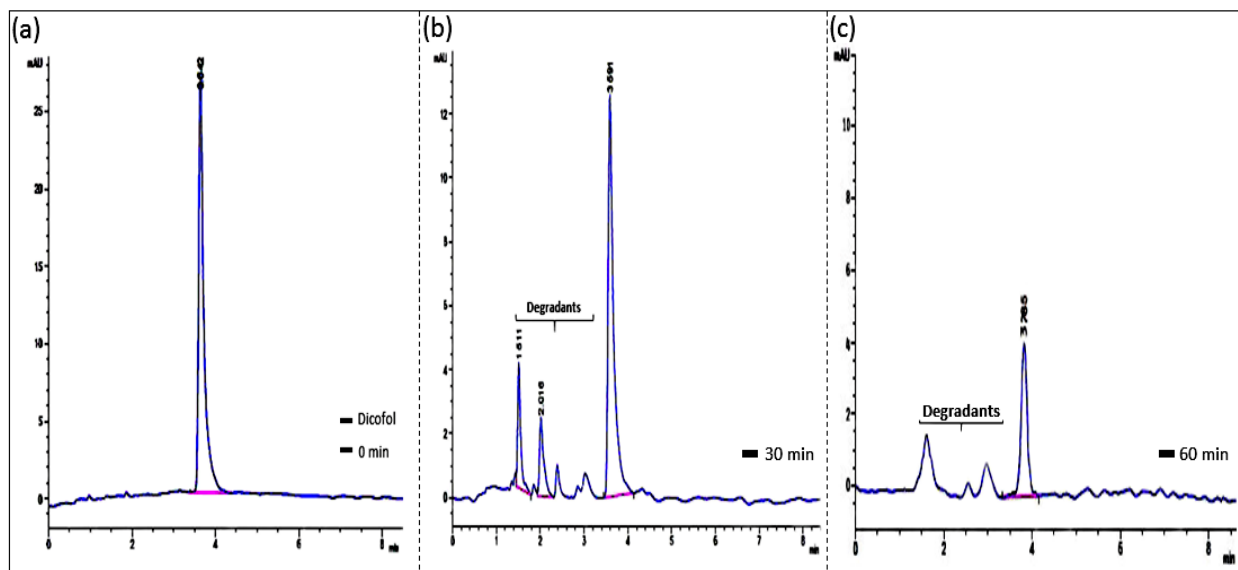


Figure 2.1. Chromatographic representation of (a) Dicofol parent compound & degraded products along with Dicofol after (b) 30 min (c) 60 min of sonication

2.4.2 GC-MS analysis

Three degraded products of Dicofol have been detected via qualitative GC-MS analysis. 3,3'-Dichlorobenzophenone/methanone, bis(3-chlorophenyl) - ($C_{13}H_8Cl_2O$), 4-Chlorobenzophenone ($C_{13}H_9ClO$) and Benzophenone ($C_{13}H_{10}O$) were identified via GC-MS analysis in full scan mode after 20 min of sonication and a gradual decrease in the peak intensity of degradants with treatment time was observed. GC-MS analysis in the Selected Ion Monitoring (SIM) mode was performed for the target ion (m/z 139) to accurately monitor the concentration of Dicofol, which indicated the decline in its concentration with treatment time. Fig. 2.2 represents the mass spectrogram of Dicofol and the degraded products identified via GCMS NIST library during full scan analysis,

whereas Fig. 2.3 demonstrates the gradual decrease in the peak intensity of Dicofol with treatment time monitored via GC-MS SIM mode.

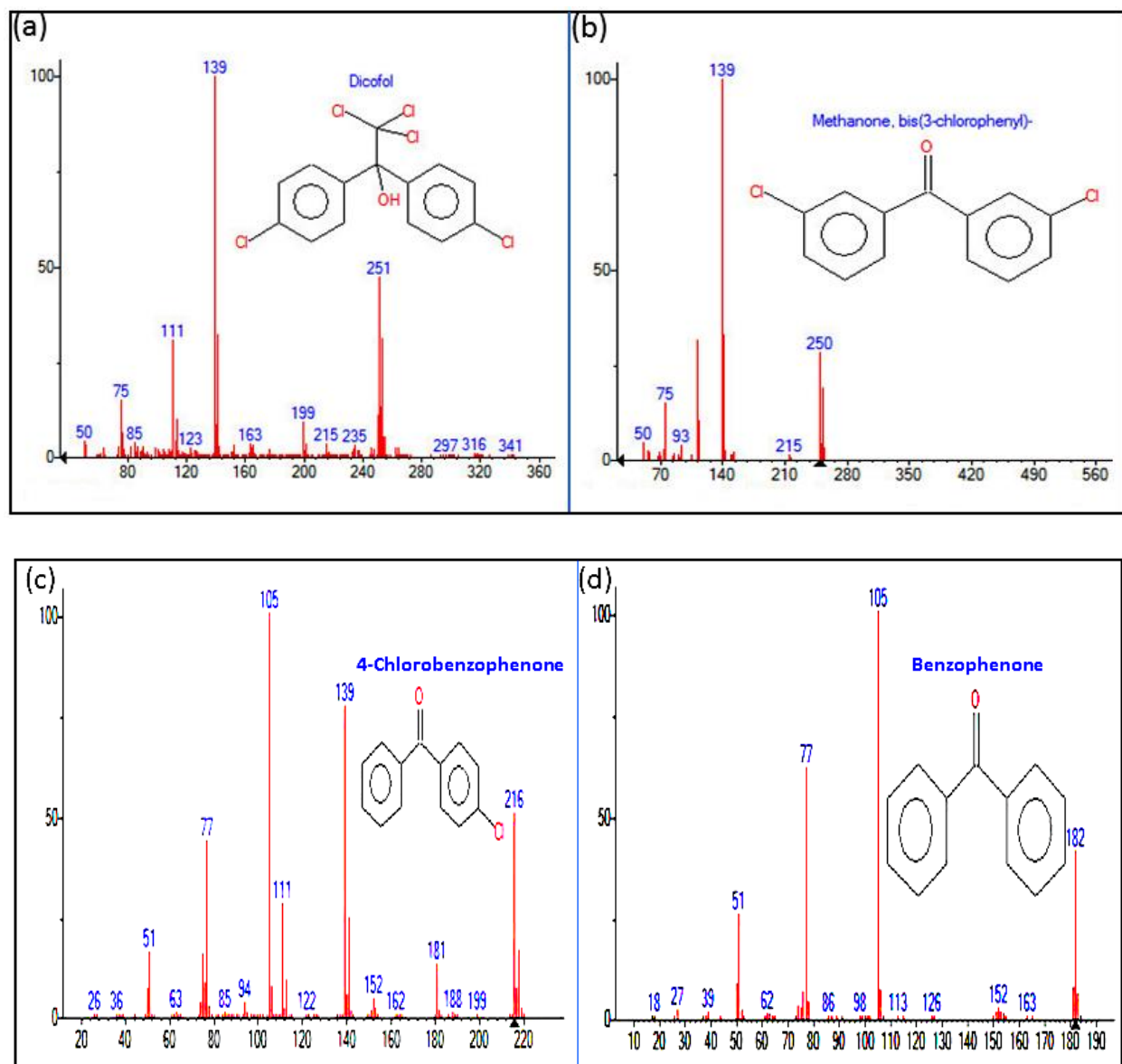


Figure 2.2. Mass spectrogram of (a) Dicofol and (b) the degraded product methanone, bis(3-chlorophenyl) – (c) 4-Chlorobenzophenone (d) Benzophenone identified by GC-MS NIST library match

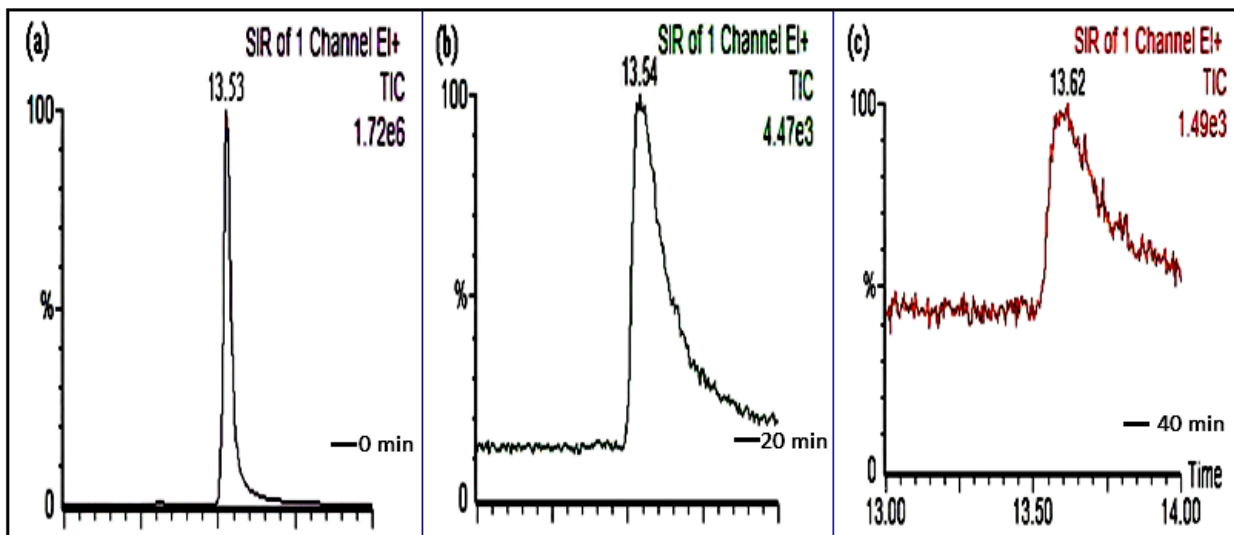


Figure 2.3. Selected ion monitoring (m/z 139) chromatographic representation of Dicofol and peak intensity at (a) 0 min (b) 20 min and (c) 40 min of sonochemical treatment

2.4.3 Degradation pathways

Based on the identified degradants of Dicofol, the possible degradation pathways are represented in Fig. 2.4. Volatility and solubility of pollutants play a vital role in deciding the predominant cavitation region for their optimum degradation. Based on Henry's law constant of Dicofol (2.4×10^{-7} atm m^3 /mol), it is considered to be semi-volatile and according to $\log K_{ow}$ of Dicofol (5.02), it is essentially a hydrophobic substance. Since Dicofol is a semi-volatile molecule, pyrolysis inside the cavitation bubbles should be excluded, whereas due to hydrophobic nature of Dicofol, the transport of pollutants to the bubble interfacial region could be dominant. Thus, interfacial region appears to be the predominant site for the degradation of Dicofol. Conceptually, degradation of Dicofol can be considered into three predominant fundamental steps. The first step involves the diffusion and adsorption of Dicofol to the transient cavitating bubble-liquid interface followed by a second step involving thermal decomposition along with radical attack on the degraded molecules at the interfacial region and subsequent pyrolytic degradation of intermediates inside the bubble core as the last step. According to the proposed scheme (Fig. 2.4), the initial degradation of Dicofol involves the loss of CCl_3 moiety via thermal decomposition at the bubble-water

interface and subsequent radical attack to form 3,3'-Dichlorobenzophenone, as the presence of highly reactive oxygen species are also dominant at the interfacial region. The detection of 4-Chlorobenzophenone and Benzophenone indicated successive removal of chloride atom from the aromatic ring of 3,3'-Dichlorobenzophenone and 4-Chlorobenzophenone respectively, following a subsequent radical attack to form the intermediates.

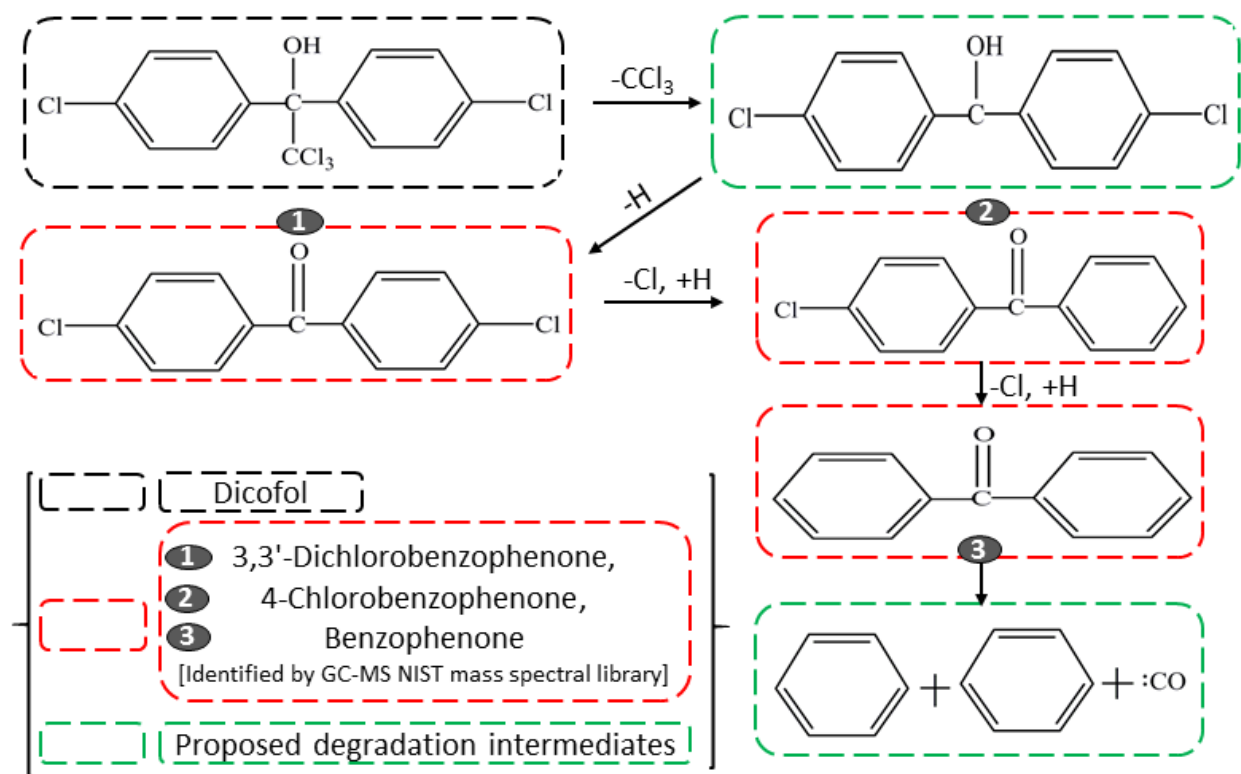
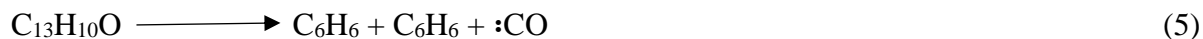


Figure 2.4. The proposed degradation pathways of Dicofol under ultrasonic irradiation

At later stage of degradation, the short chain aromatic intermediates are expected to enter the bubble core and undergo a series of pyrolytic reactions leading to carbon monoxide and other mineralized products according to the following equations (1-5).





The proposed dissociation reactions of Dicofol (eqns. 1-5) are expected to follow the order of bond dissociation energy: for example, C-C (607 kJ/mol) and C-O (1076 kJ/mol), which lead to the cleavage of CCl_3 moiety with the initiation of thermal decomposition of Dicofol. The aromatic rings being the most inert are assumed to dissociate at a later stage of degradation. Brown carbonaceous particles were observed visually after 50 min of sonication under optimized parameters suggesting the mineralization of Dicofol. These observations of formation of carbonaceous particles via pyrolytic conditions during sonolysis are consistent with the results as observed by Hart et al. (1990) and González-García et al. (2010), where they noted the formation of carbonaceous particles during sonolysis of acetylene and chlorinated organocompounds. Sivasankar and Moholkar (2009) reported the degradation of phenol (Ph), chlorobenzene (CB), nitrobenzene (NB), p-nitrophenol (PNP) and 2,4-dichlorophenol (2,4-DCP) based on their water solubility and volatility. Reported results suggested that phenol (Ph) is not expected to evaporate into the bubble due to its nonvolatile nature and high solubility and hence the degradation mechanism of Ph is expected to be hydroxylation, whereas CB is expected to evaporate into the bubble and undergo pyrolytic decomposition due to its volatile and hydrophobic nature. But semi-volatile and hydrophobic pollutants such as Dicofol are expected to follow bubble-liquid interfacial region as the predominant region of degradation with mixed probability of thermal decomposition and free radical attack.

2.4.4 Reaction kinetics of Dicofol

Considering all the studied parameters during the sonochemical treatment of Dicofol, the experimental data fit well to the pseudo-first-order kinetic model. Based on Eqn. 6, plots of C_t

versus irradiation time (t) were produced as shown in Figs. 2.5-2.9 using the data obtained during different operating parameters.

$$C_t = C_0 e^{-kt} \quad (6)$$

Where, k is the apparent rate constant; C_0 and C_t are the concentrations of Dicofol at time “0” and at “t” respectively. Table 2.1 lists the values of pseudo-first order degradation rate constant (k), and the linear regression coefficient (R^2) for all the operating parameters.

2.4.5 Effect of initial concentration on the degradation of Dicofol

The efficacy of pollutant degradation can be significantly affected by its initial concentration. The extent of pyrolytic destruction of semi-volatile pollutants is dependent on their concentration and hydrophobicity, which defines their ability to migrate towards the bubble-liquid interface and to accumulate (Serpone et al., 1994). The concentration of Dicofol was varied from 5.4 to 54 μM while maintaining the solution temperature at 20 $^\circ\text{C}$, pH at 3 and with a power density of 375 W.

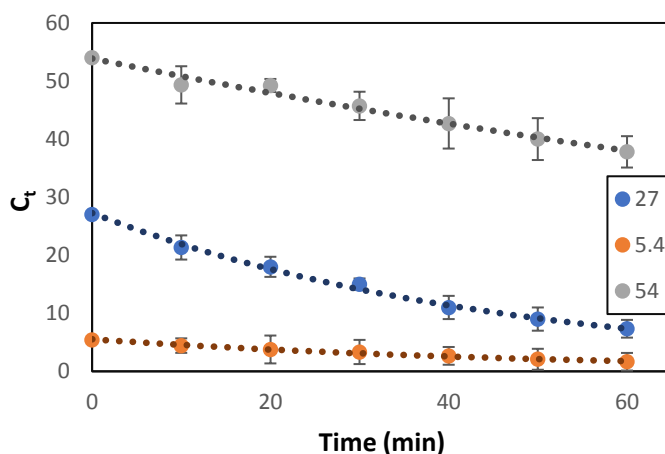


Figure 2.5. Degradation of Dicofol at various initial concentrations: (●) 5.4 μM (●) 27 μM (●) 54 μM

The degradation rate scarcely increased above and below 27 μM , indicating as the optimum concentration for the highest rate of degradation. From Table 2.1, it is evident that the rate constant decreased from 0.022 to 0.006 min^{-1} for an increase in the concentration from 27 to 54 μM . Above

the optimum concentration of Dicofol, the surface of bubbles is expected to be saturated and hence a decline in the degradation rate was witnessed, whereas below the optimum value a decline in the degradation rate was also observed. A rise in the pollutant concentration up to the optimum value can lead to a higher degradation rate due to the rise in the interfacial pollutant concentration, whereas at low concentration a decline in the degradation rate indicates lesser evaporation of pollutant into the bubble-vapor interfacial region. Some authors reported that in case of non-volatile and semi-volatile pollutants, thermal decomposition at interfacial region is predominant at higher solute concentration, whereas radical reactions predominate at lower solute concentration (González-García et al., 2010). As the degradation of Dicofol beyond the optimum value was observed to be hindered, thermal decomposition along with radical attack at interfacial region is expected to be the dominant pathway at the optimum concentration. Mendez-Arriaga et al. (2008) observed an optimum concentration of 5 mg/L for Ibuprofen followed by a relatively constant degradation rate at its higher concentrations demonstrating the existence of optimum concentration for the highest rate of pollutant degradation.

2.4.6 Effect of change in pH

Sonochemical degradation of Dicofol was conducted at different initial solution pH in the range of 3-7, while maintaining Dicofol concentration of 27 μ M, solution temperature at 20 °C and power density of 375 W. The results indicated that the rate of degradation increased (Table 2.1) with a decrease in solution pH and the highest rate of Dicofol degradation was achieved at pH 3 (Fig. 2.6), which can be attributed to the faster transport of pollutants towards bubble interfacial region due to their enhanced hydrophobic nature at acidic conditions.

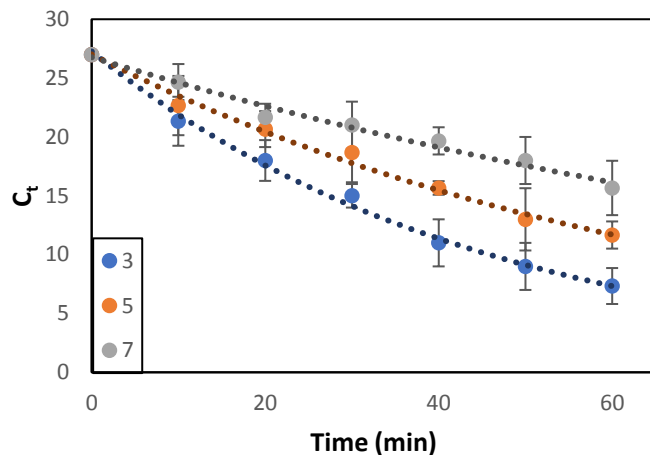


Figure 2.6. Degradation of Dicofol at different pH: (●) 3, (●) 5, (●) 7

Also, several previous reports suggested acidic medium for the highest rate of pollutant removal via sonochemical treatment, owing to increased hydrophobicity of protonated species, resulting in an enhanced accumulation of molecules at the bubble interfacial region (Wei et al., 2016). Golash and Gogate (2012) reported an increase in the removal of dichlorvos with a change in pH from 8 to 2. Similarly, the extent of alachlor degradation increased from 45 to 86% with a decrease in its initial pH from 11 to 3 within 2 h of treatment (Bagal and Gogate, 2012).

2.4.7 Effect of solution temperature

A change in the solution temperature during cavitation affects the cavitation intensity owing to the variation in the physiochemical properties of the liquid medium (Golash and Gogate, 2012). By using the cooling system, the solution temperature was controlled to vary over a range of 10-40 °C, while maintaining the concentration of Dicofol solution as 27 μM. The solution temperature of 20 °C has been found to be the optimum for the highest rate of Dicofol degradation and the degradation rate constant decreased to 0.009 min⁻¹ and 0.008 min⁻¹ (Table 2.1) with a change in the solution temperature to 10 °C and 30 °C, respectively.

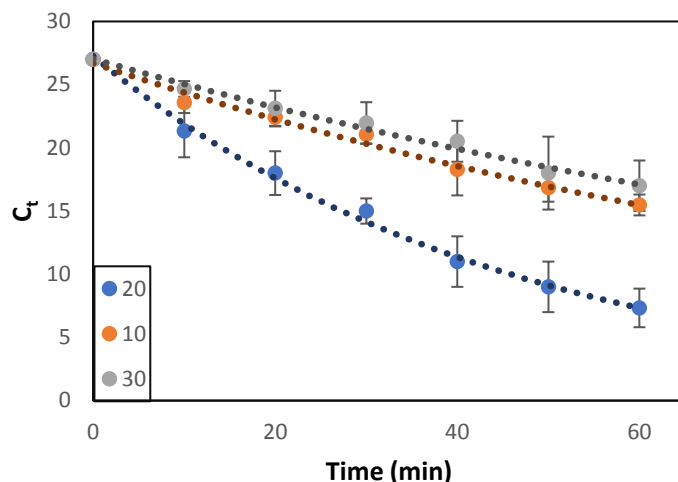


Figure 2.7. Degradation of Dicofol at different temperatures: (●) 10 °C (●) 20 °C (●) 30 °C

Varying the solution temperature affects the cavitation intensity and the type of cavities formed (gaseous or vaporous) as well as affecting the kinetic rate constant of the components subjected to degradation (Evgenidou et al., 2005). According to the studies on bubble dynamics, a linear decrease in the collapse pressure is witnessed with a rise in the bulk liquid temperature (Gogate et al., 2003). At high temperature, semi-volatile or nonvolatile molecules may migrate easily from the bulk solution to the interfacial regions, but at the same time a decline in the formation of gaseous nuclei and bubble collapse intensity could result. Lin et al. (2015) and Yang et al. (2013) reported on the detrimental effect of higher sonochemical reaction temperatures on the degradation of PFOS and PFOA, whereas Jiang et al. (2006) reported an optimum temperature for the degradation of 4-chlorophenol, demonstrating that an optimum temperature for the highest rate of degradation is pollutant specific.

2.4.8 Effect of acoustic power on the degradation of Dicofol

The generation of number of active cavitation bubbles can be significantly altered depending on the extent of applied ultrasound power (Merouani et al., 2010). The correlation between sonochemical reactions and the applied power can be illustrated as follows: (1) the rate and the

generation of number of active bubbles increase with an increase in the power density, (2) an increase in the size of individual bubbles with an increase in power density, resulting in higher collapse temperature because of the conversion of higher available potential energy into heat (Kanthale et al., 2008), (3) an increase in the mixing intensity results with an increase in power density because of the turbulence produced from cavitation effects. The effect of acoustic power on the degradation of Dicofol was monitored by varying the power (150-450 W) at a solution temperature of 20 °C, while maintaining pH at 3 and Dicofol concentration of 27 μM to decide the optimum condition. Fig. 2.8 shows the power dependence of Dicofol degradation.

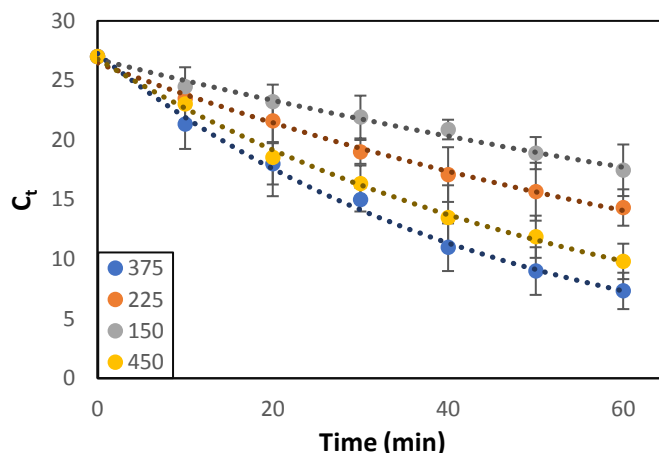


Figure 2.8. Degradation of Dicofol at different ultrasonic power levels: (●) 150 W (●) 225 W (●) 375 (●) 450 W

It was observed that the degradation enhanced with a rise in acoustic power up to 375 W with the degradation rate constant of 0.022 min^{-1} , beyond which a decline in the degradation rate (Table 2.1) was observed. By increasing the power, the energy of cavitation enhanced following a more violent implosion. It has been reported that an increase in the acoustic intensity up to a maximum of 8.4 W/cm^2 and 110 W/cm^2 enhanced the degradation efficiency of Ofloxacin and Nitrotoluenes (Panda and Manickam, 2017) beyond which a decline in the degradation rate was observed. The optimum power dissipation for effective pollutant removal is dependent on reactor configuration

and the pollutant employed. Cavitation events could be affected or reduced marginally beyond the optimum power intensity, because of an excessive production of heat during sonication, leading to a less violent bubble collapse.

2.4.9 Control experiments

Control and sonochemical experiments in the presence of H_2O_2 in the range of 1000 to 10000 μM were performed to verify the role of hydrogen peroxide for oxidative degradation of Dicofol. While degradation was not observed during the addition of H_2O_2 alone, a slight increase in degradation rate was witnessed during the combination of sonication, up to a H_2O_2 loading of 5000 μM , beyond which it decreased. The addition of H_2O_2 can lead to additional oxidative degradation pathways while acting as a radical promoter, but at the same time it can also act as a scavenger beyond the optimum concentration. The H_2O_2 effect is predominant in the bulk solution phase, where the reaction between pollutant and active radicals follows the removal of OH, rather than at bubble interfacial region, where recombination of active radicals along with thermal decomposition dominates. Based on Eq. (6), Fig. 2.9 demonstrated the pseudo-first-order degradation of Dicofol with different H_2O_2 loading in comparison with degradation without H_2O_2 addition, while maintaining an acoustic power of 375 W, a solution temperature of 20 °C, a pH of 3 and an initial Dicofol concentration of 27 μM .

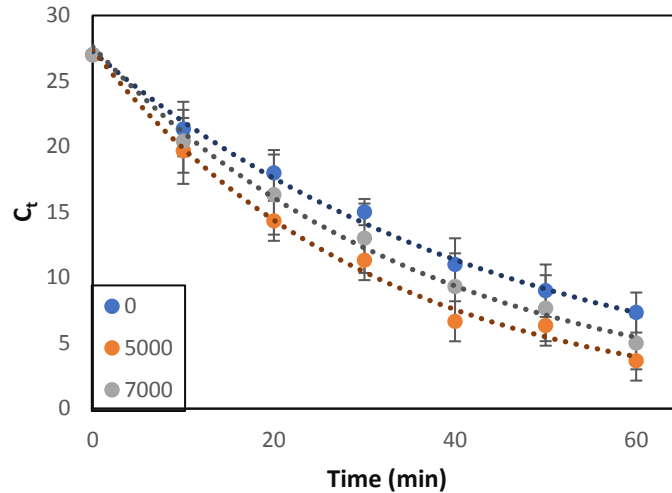


Figure 2.9. Degradation of Dicofol at different H_2O_2 loading: (●) 0 μM (●) 5000 μM (●) 7000 μM

The rate constant (k) enhances only up to 0.032 min^{-1} in comparison to the degradation rate constant of 0.022 min^{-1} (Table 2.1) for Dicofol without H_2O_2 , suggesting a minor degradation taking place in the bulk solution. This could be attributed to radical driven degradation up to the optimum loading. The reduced degradation beyond optimum H_2O_2 addition depicts its role of scavenging of OH radical (Eq. 7).



Gogate (2008) stated that the combined effect of H_2O_2 and ultrasound is dependent on the type of pollutants and the interaction of free radicals over a specified period. Merouani et al. (2010) also reported on the presence of optimum concentration of H_2O_2 and a slight enhancement of degradation rate by the addition of H_2O_2 for the degradation of Rhodamine B.

The role of free radical reaction can be decided with respect to the pollutant degradation rate in the presence of scavengers. To obtain further information regarding the cavitation reaction zone, sodium bicarbonate was chosen, which is known as the free radical scavenger for bulk phase solution (Liao et al., 2001). Experiments with sodium bicarbonate loading (0.5 & 2 g/L) were

conducted, while maintaining all other optimum parameters. The rate constant decreased only marginally (Table 2.2) in the presence of bicarbonate ions for both loading, indicating interfacial region as the predominant degradation zone with lesser extent of radical reaction in the bulk solution. Yao et al. (2010) also reported similar result for parathion degradation in the presence of sodium bicarbonate, where the reaction zones are predominantly the interfacial region. Fig. 2.10 demonstrates the percentage of Dicofol degradation with the addition of scavenger.

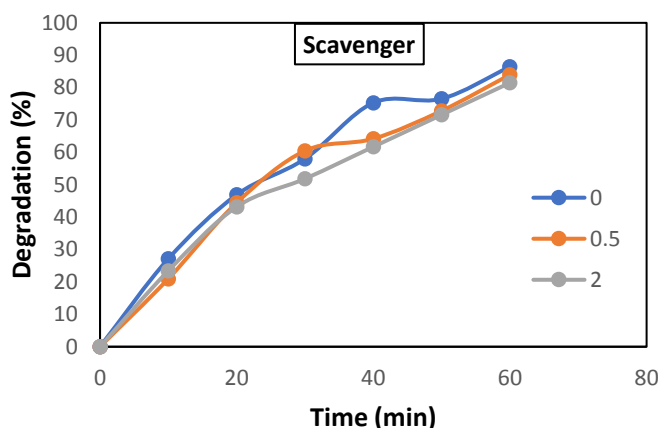


Figure 2.10. Degradation of Dicofol at various loadings of sodium bicarbonate: (●) 0 (●) 0.5 (●) 2 g/L

Table 2.1. Pseudo-first-order rate constants for the degradation of Dicofol under different operational parameters

Parameter		K (min^{-1})	R^2
Initial concentration (μM)	5.4	0.019	0.98
	27	0.022	0.99
	54	0.006	0.98
pH	3	0.022	0.99
	5	0.014	0.98
	7	0.008	0.98
Solution temperature ($^{\circ}\text{C}$)	10	0.009	0.98
	20	0.022	0.99
	30	0.008	0.98
Acoustic Power (W)	150	0.007	0.98
	225	0.011	0.99

	375	0.022	0.99
	450	0.017	0.99
H ₂ O ₂ loading (μM)	0	0.022	0.99
	5000	0.032	0.98
	7000	0.027	0.99

Table 2.2. Effect of radical scavenger addition on the extent of degradation and kinetic rate constants

Sodium bicarbonate loading (g/L)	Extent of degradation (%)	Rate constant k (min ⁻¹)	R ²
0	86	0.032	0.98
0.5	84	0.029	0.98
2	81	0.027	0.98

2.5 Conclusions

In the present study, the sonochemical degradation of Dicofol has been accomplished and the main conclusions observed from this investigation are:

- The removal of Dicofol has proven to be effective and efficient under sonochemical-based treatment.
- HPLC and GC-MS analyses justified the formation of degraded products during sonication.
- Thermal decomposition along with radical attack at bubble-vapor interphase is assumed to be the dominant degradation pathway.
- The highest rate of degradation was achieved under optimum parameters of acoustic power, solution temperature, pH, pollutant concentration and the addition of H₂O₂.
- Formation of carbonaceous particles suggested the mineralization of Dicofol.

2.6 References

- Mostafalou, S., Abdollahi, M., 2013. Pesticides and human chronic diseases: evidences, mechanisms, and perspectives, *Toxicol. Appl. Pharmacol.* 268, 157–177.
- Mckinlay, R., Plant, J. A., Bell, J. N. B., Voulvoulis, N., 2008. Endocrine disrupting pesticides: Implications for risk assessment, *Environ. Intern.* 34,168–183.
- Mnif, W., Hassine, A. I. H., Bouaziz, A., Bartegi, A., Thomas, O., Roig, B., 2011. Effect of endocrine disruptor pesticides: a review, *Int. J. Environ. Res. Public Health.* 8, 2265–2303.
- Tiemann, U., 2008. In vivo and in vitro effects of the organochlorine pesticides DDT, TCPM, methoxychlor, and lindane on the female reproductive tract of mammals: a review, *Reproduct. Toxicol.* 25, 316–326.
- US EPA,1998. Reregistration eligibility decision (RED) Dicofol, *Prev. Pestic. Toxic Subst. EPA* 738-R-98-018.
- UNEP, 2013. Proposal to list dicofol in annexes A, B and/or C to the stockholm convention on persistent organic pollutants note, *Stock. Conv. Persistent Org. Pollut.* 1–6.
- UNEP, 2015. Draft risk profile: dicofol.
- Guo, G., Yu, B., Yu, P., Chen, X., 2009. Synthesis and photocatalytic applications of Ag /TiO₂ - nanotubes, *Talanta.* 79, 570–575.
- Binbin, Y., JingBin, Z., LiFen, G., XiaoQing, Y., Limei, Z., Xi, C., 2008. Photocatalytic degradation investigation of dicofol, *Sci. Bull.* 53, 27–32.
- Ren, X., Sun, Y., Zhu, L., Cui, Z., 2011. Theoretical studies on the OH-initiated photodegradation mechanism of dicofol, *Comput. Theor. Chem.* 963, 365–370.
- Osman, K. A., Ibrahim, G. H., Askar, A. I., Alkhail, A. R. A., 2008. Biodegradation kinetics of dicofol by selected microorganisms, *Pest. Biochem. Physio.* 91, 180–185.

- Oliveira, J. L. M., Silva, D. P., Martins, E. M., Langenbach, T., Dezotti, M., 2012. Biodegradation of 14C-dicofol in wastewater aerobic treatment and sludge anaerobic biodigestion, *Environ. Technol.* 33, 695-701.
- Thangavadivel, K., Megharaj, M., Smart, R. S. C., Lesniewski, P. J., Naidu, R., 2009. Application of high frequency ultrasound in the destruction of DDT in contaminated sand and water, *J. Hazard. Mater.* 168, 1380–1386.
- Patil, P. N., Gogate, P. R., 2015. Degradation of dichlorvos using hybrid advanced oxidation processes based on ultrasound, *J. Water Process Eng.* 8, e58–e65.
- Bagal, M. V., Gogate, P. R., 2012. Sonochemical degradation of alachlor in the presence of process intensifying additives, *Sep. Purif. Technol.* 90, 92–100.
- Serpone, N., Terzian, R., Hidaka, H., Pelizzetti, E., 1994. Ultrasonic induced dehalogenation and oxidation of 2-, 3-, and 4-chlorophenol in air-equilibrated aqueous media. Similarities with irradiated semiconductor particulates, *J. Phys. Chem.* 98, 2634-2640.
- Mendez-Arriaga, F., Torres-Palma, R. A., Petrier, C., Esplugas, S., Gimenez, J., Pulgarin, C., 2008. Ultrasonic treatment of water contaminated with ibuprofen, *Water Res.* 42, 4243–4248.
- Merouani, S., Hamdaoui, O., Saoudi, F., Chiha, M., 2010. Sonochemical degradation of rhodamine B in aqueous phase: effects of additives, *Chem. Eng. J.* 158, 550–557.
- Koda, S., Kimura, T., Kondo, T., Mitome, H., 2003. A standard method to calibrate sonochemical efficiency of an individual reaction system, *Ultrason. Sonochem.* 10, 149–156.
- Hart, E. J., Fischer, C. H., Henglein, A., 1990. Pyrolysis of acetylene in sonolytic cavitation bubbles in aqueous solution, *J. Phys. Chem.* 94, 284-290.

- González-García, J., Sáez, V., Tudela, I., Díez-García, M. I., Esclapez, M. D., Louisnard, O., 2010. Sonochemical treatment of water polluted by chlorinated organocompounds, a review. *Water*. 2, 28–74.
- Sivasankar, T., Moholkar, V. S., 2009. Physical insights into the sonochemical degradation of recalcitrant organic pollutants with cavitation bubble dynamics, *Ultrason. Sonochem.* 16, 769–781.
- Wei, Z., Spinney, R., Ke, R., Yang, Z, Xiao, R., 2016. Effect of pH on the sonochemical degradation of organic pollutants, *Environ. Chem. Lett.* 14, 163-182.
- Golash, N., Gogate, P. R., 2012. Degradation of dichlorvos containing wastewaters using sonochemical reactors, *Ultrason. Sonochem.* 19, 1051–1060.
- Evgenidou, E., Fytianos, K., Poulios, I., 2005. Semiconductor-sensitized photodegradation of dichlorvos in water using TiO₂ and ZnO as catalysts, *Appl. Catal. B Environ.* 59, 81–89.
- Gogate, P. R., Wilhelm, A. M., Pandit, A. B., 2003. Some aspects of the design of sonochemical reactors, *Ultrason. Sonochem.* 10, 325–330.
- Lin, J. C., Lo, S. L., Hu, C. Y., Lee, Y. C., Kuo, J., 2015. Enhanced sonochemical degradation of perfluorooctanoic acid by sulfate ions, *Ultrason. Sonochem.* 22, 542–547.
- Yang, S. W., Sun, J., Hu, Y., Cheng, J., Liang, X., 2013. Effect of vacuum ultraviolet on ultrasonic defluorination of aqueous perfluorooctanesulfonate, *Chem. Eng. J.* 234, 106–114.
- Jiang, Y., Petrier, C., Waite, T.D., 2006. Sonolysis of 4-chlorophenol in aqueous solution: effects of substrate concentration, aqueous temperature and ultrasonic frequency, *Ultrason. Sonochem.* 13, 415–422.
- Kanthale, P., Ashokkumar, M., Grieser, F., 2008. Sonoluminescence, sonochemistry (H₂O₂ yield) and bubble dynamics: frequency and power effects, *Ultrason. Sonochem.* 15, 143–150.

- Panda, D., Manickam, S., 2017. Recent advancements in the sonophotocatalysis (SPC) and doped-sonophotocatalysis (DSPC) for the treatment of recalcitrant hazardous organic water pollutants, *Ultrason. Sonochem.* 36, 481–496.
- Gogate, P. R., 2008. Treatment of wastewater streams containing phenolic compounds using hybrid techniques based on cavitation. A review of the current status and the way forward, *Ultrason. Sonochem.* 15, 1–15.
- Liao, C., Kang, S., Wu, F., 2001. Hydroxyl radical scavenging role of chloride and bicarbonate ions in the H₂O₂/UV process, *Chemosphere.* 44, 1193–1200.
- Yao, J. J., Gao, N. Y., Li, C., Li, L., Xu, B., 2010. Mechanism and kinetics of parathion degradation under ultrasonic irradiation, *J. Hazard. Mater.* 175, 138–145.

Chapter 3

Hydrodynamic cavitation assisted degradation of persistent endocrine-disrupting organochlorine pesticide Dicofol: Optimization of operating parameters and Investigations on the mechanism of intensification

Abstract

Dicofol, a recommended Stockholm convention persistent organic pollutants (POPs) candidate is well known for its endocrine disruptive properties and has been extensively used as an organochlorine pesticide worldwide. The Hydrodynamic cavitation (HC) treatment of Dicofol in aqueous media induced by a liquid whistle reactor (LWR) has been investigated while considering important parameters such as inlet pressure, initial concentration of Dicofol, solution temperature, pH, addition of H₂O₂ and radical scavenger for the extent of degradation. The pseudo-first-order degradation rate constant (k) was determined to be 0.073 min⁻¹ with a degradation yield of 1.26×10^{-5} mg/J at optimum operating conditions and a complete removal of Dicofol was achieved within 1 h of treatment. Considering the removal rate and energy efficiency, the optimal inlet pressure was found to be 7 bar, resulting in a cavitation number of 0.17. High performance liquid chromatography (HPLC) and Gas chromatography mass spectroscopy (GC-MS) analyses indicated a sharp decline in the concentration of Dicofol with treatment time and indicated the presence of degraded products. An 85 % total organic carbon (TOC) removal was achieved within 1 h of treatment time, demonstrating successful mineralization of Dicofol. The obtained results suggest that the degradation of Dicofol followed thermal decomposition and successive recombination reactions at bubble-vapor interface.

3.1 Introduction

Dicofol has been associated with numerous disease due to its endocrine disruptive nature (US EPA,1998) and hence an effective waste water treatment method is needed for its elimination. The hydrodynamic cavitation-based treatment in this investigation has demonstrated better removal efficiency as compared to previous reported results. Cavitation can be produced in the liquid medium through pressure variations by introducing constrictions in the liquid flow and according to Bernoulli's equation (Lohse, 2003) when the liquid passes through the constriction, the kinetic energy/velocity increases at the expense of pressure and when the pressure at orifice equals or falls below the vapor pressure of the liquid, vaporous cavities are formed. In the case of liquid whistle hydrodynamic cavitation reactor (LWHCR), the high velocity liquid jet generated due to the presence of orifice, is projected over the edge of the knifelike stainless-steel blade, enabling it to vibrate at ultrasonic frequencies. As a result, intense cavitation is obtained due to the local pressure changes around the orifice and due to the mechanical ultrasonic vibrations as well. LWHCR was employed for water disinfection (Chand et al., 2007), treatment of industrial wastewater effluents (Chakinala et al., 2008) and several other hydrodynamic cavitation reactor set-ups have shown to achieve cavitating conditions at larger scale as compared to acoustic cavitation (Gogate and Pandit, 2005) and hence has the potential for large-scale applications due to its easy scale-up.

In the present work, the degradation of Dicofol was performed using hydrodynamic cavitation. Circular orifice plate was employed as the cavitating device of HC reactor. We believe that this is the first reported investigation utilizing HC cavitation for the effective removal of Dicofol.

3.2 EXPERIMENTAL

3.2.1 Materials and equipment

Dicofol [2,2,2-Trichloro-1,1-bis(4-chlorophenyl) ethanol ($C_{14}H_9Cl_5O$), 99.3%, CAS Number 115-32-2], Methanol (HPLC grade), Glacial acetic acid (HPLC grade), Potassium hydrogen phthalate (>99%), Hydrogen peroxide (H_2O_2), n-hexane and Sodium bicarbonate (99.5%) were purchased from Sigma Aldrich (Malaysia). Ultra-pure deionized water of 15 M Ω cm resistivity was obtained from a water purification system (PURELAB Option-R, ELGA, UK) and was used throughout the experiment. Agilent nylon syringe filter of 0.45 μ m pore size and 5 ml syringes were purchased from IT Tech Research (M) Sdn. Bhd. (Malaysia).

3.2.2 Experimental set-up

3.2.2.1 Liquid whistle reactor (LWR)

The experimental set-up of the liquid whistle hydrodynamic cavitation reactor (LWHCR), called Benchtop SonolatorTM 2000 (Sonic corporation, CT, USA) is shown in Fig. 3.1, comprises a Model A CIP SonolatorTM, a 2 HP motor, a plunger pump (Giant industries, model P220A, power consumption 2.2 kW, speed 1460 rpm), an Hitachi variable frequency drive (VFD) inverter, feed tank of 5 L capacity, flow meter and pressure measuring gauges. The cavitation chamber (length, 0.078 m, width, 0.044 m, height, 0.044 m) has the orifice plate (orifice area, 7.74×10^{-7} m², diameter 0.0016 m) and a blade (length 0.0268 m; width 0.0222 m; thickness 0.015 m) (Figure 1). A maximum discharge pressure of 2000 psi (138 bar) could be employed by the pump.

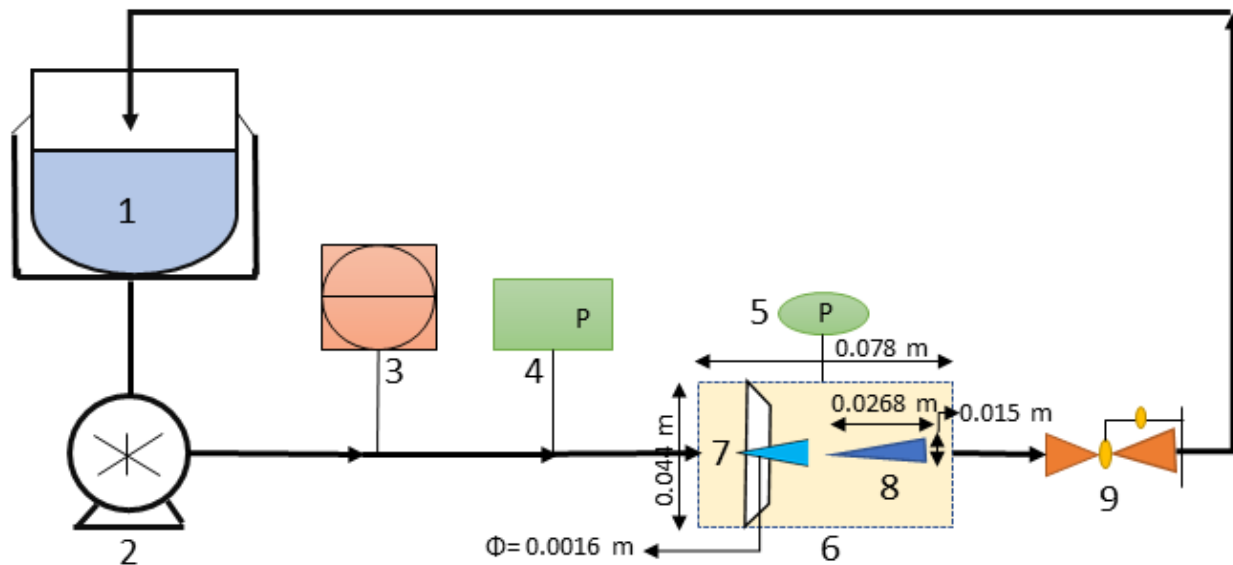


Figure 3.1. Schematic representation of the experimental set-up of LWHCR (1, feed tank; 2, plunger pump; 3, PLC control board; 4, digital pressure gauge; 5, analog pressure gauge; 6, cavitation chamber; 7, orifice; 8, blade; 9, back-pressure valve)

3.2.3 Experimental methodology

A stock solution of Dicofol in methanol was prepared and was stored at 2 °C after performing acidification by acetic acid. Preparation of working standard solutions were performed regularly by the dilution of stock solution in methanol and water to the desired concentration. Experiments were performed at pH 3, except for those conducted to examine the effect of solution pH, while excluding higher pH (>7) due to hydrolysis of Dicofol at alkaline pH (US EPA, 1998). The acidification of solution was performed by the addition of glacial acetic acid. For the treatment, 2 L Dicofol solution of desired concentration was placed in the feed tank. Due to Dicofol's low aqueous solubility, a co-solvent approach of using methanol along with water was adopted. Experiments were conducted up to 120 min and the samples were withdrawn at regular intervals for High performance liquid chromatography (HPLC), Gas chromatography mass spectroscopy (GC-MS) and Total organic carbon (TOC) analyses. For GC-MS analysis, the extraction of samples was performed by n-hexane. The inlet pressure was adjusted to 5 bar for initial

experiments, excluding runs conducted to investigate the effect of inlet pressure. Experiments were conducted in triplicates and the standard deviations were included. Calibration curves for Dicofol at the concentrations from 1 to 150 ppm were obtained with a good linearity.

3.3 Analysis

3.3.1 High performance liquid chromatography (HPLC) analysis

Dicofol standard was used for the optimization of HPLC parameters, which has been followed for the entire analysis. The limit of detection (LOD) and limit of quantification (LOQ) for Dicofol were noted to be 0.54 and 1.80 mg/L respectively and a good signal to noise ratio was observed. Samples were injected onto an Agilent HPLC system equipped with an online degasser, quaternary LC pump (infinity model 1260), an infinity 1260 VWD UV detector for the separation on a CORTECS™ C18 column (4.6 mm × 100 mm, 2.7 μm). The Agilent ChemStation software was used for instrument control, data acquisition and data analysis. The Dicofol elution was carried out at a column temperature of 30 °C using an isocratic gradient composed of solvent A (methanol) and solution B (5 mM aqueous acetic acid) in 80:20 ratio and was detected at a wavelength of 229 nm. The injection volume and flow rate were 20 μL and 1.4 ml/min respectively.

3.3.2 GC-MS analysis

Treated samples followed by extraction through n-hexane were subjected to Gas chromatography mass spectrometry (GC-MS, Perkin Elmer CLARUS SQ8 S/CLARUS 680) equipped with a PerkinElmer Elite 5-MS capillary column (length: 30 m, I.D: 0.25 mm, film thickness: 0.25 μm) and the determination of intermediates was performed qualitatively. The injector temperature was at 200 °C, the flow rate was 1.0 mL/min and the injection volume was 1 μL. The oven temperature was at 50 °C for 1 min, which was then increased at 25 °C/min to 125 °C for 0 min and 10 °C/min to 300 °C for 1 min. The GC interface and the source were at 280 °C and 300 °C respectively.

3.3.3 TOC analysis

To determine the extent of Dicofol mineralization, the decay in total organic carbon (TOC) content was monitored using a TOC analyzer (Shimadzu TOC 5050A) equipped with an ASI5000 autosampler. Prior to analysis, all the liquid samples, including blanks and standards were acidified to pH 2 using hydrochloric acid and instrument calibration was performed using potassium hydrogen phthalate standards. The inorganic carbon was removed by sparging the samples with air.

3.4 Results and discussion

HPLC analysis demonstrated a decline in the concentration of Dicofol with treatment time, along with the appearance of degraded products. A complete disappearance of parent compound along with degraded products was observed within 60 min of HC treatment. Fig. 3.2 illustrates the chromatographic comparison of Dicofol at 0 and 30 min of treatment. The detection of parent compound and comparison between chromatographs were performed with respect to the retention time of Dicofol standard, which was noted to be at 7-8 min.

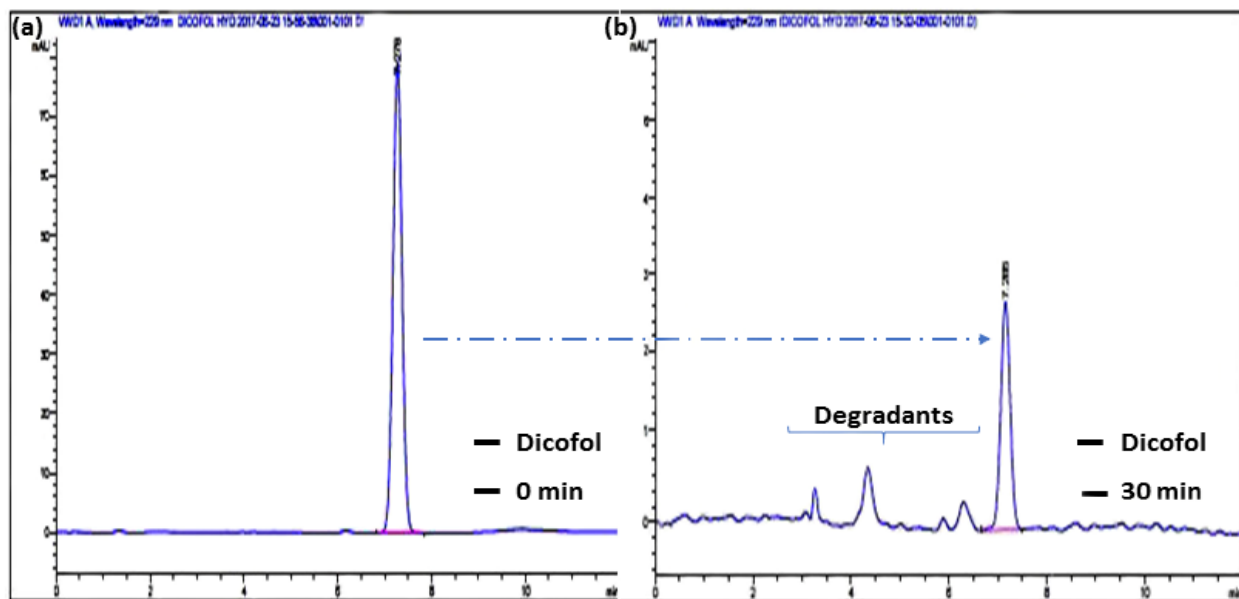


Figure 3.2. Chromatographic representation of (a) Dicofol at 0 min (b) Degraded products along with Dicofol after 30 min of HC treatment

GC-MS analysis in full scan mode indicated the presence of Kelthane acetate ($C_{16}H_{11}Cl_5O_2$) as the transformed product and 4,4'-Dichlorobenzophenone (DBP, $C_{13}H_8Cl_2O$) as the degraded product, via GCMS NIST library matching. GC-MS analysis in Selected Ion Monitoring (SIM) mode for the target ion (m/z 139) was performed to monitor Dicofol concentration over treatment time. As indicated in Fig. 3.3, a gradual decrease in Dicofol concentration was witnessed with respect to the chromatogram peak intensity. The peak intensity gradually decreased with treatment time and a complete disappearance of Dicofol was observed after 60 min of HC treatment.

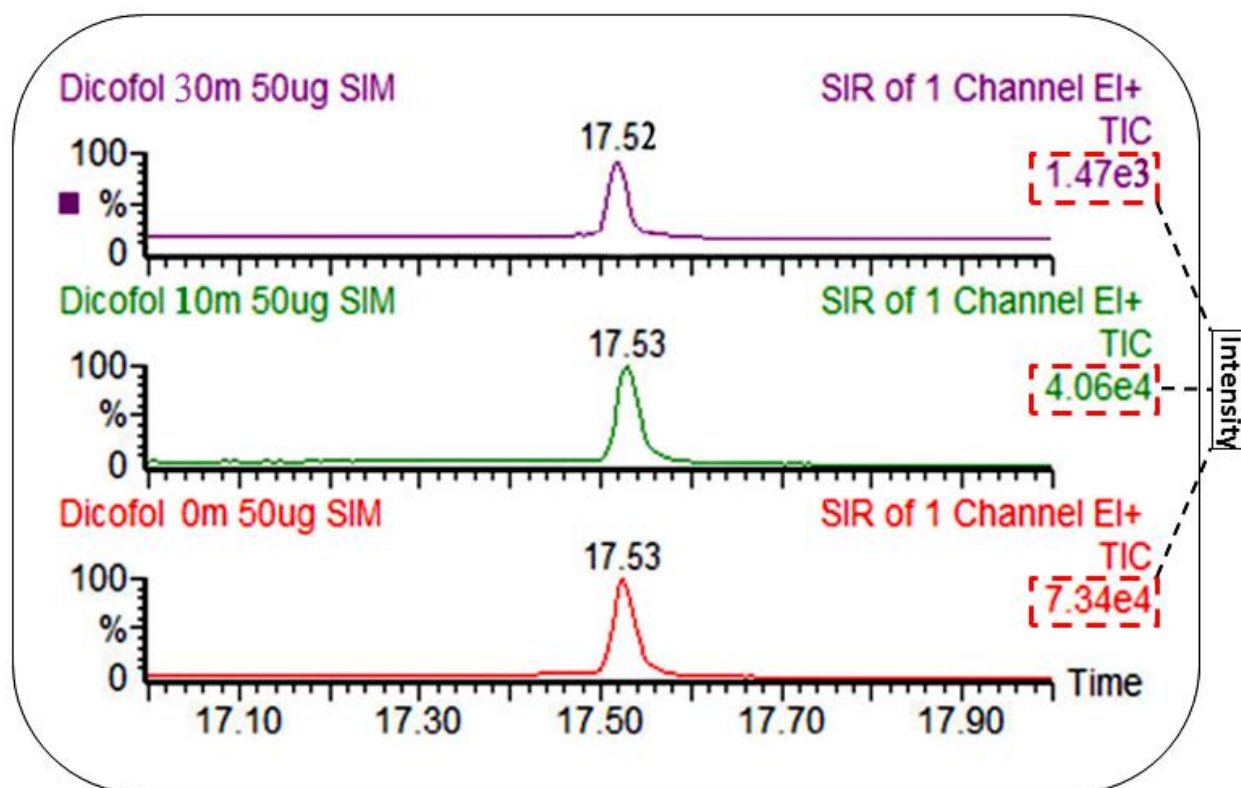


Figure 3.3. Selected ion monitoring (m/z 139) chromatographic representation of Dicofol and peak intensity at (a) 0 min (b) 10 min and (c) 30 min of HC treatment

3.4.1 Degradation pathways

The possible degradation mechanism of Dicofol is represented in Fig. 3.4, which is based on the outcomes obtained from HPLC and GC-MS analyses. The formation of transformed product, Kelthane acetate could be due to an initial decomposition of Dicofol or radical attack to lose a

hydrogen atom following subsequent recombination reaction with acetyl moiety (C_2H_3O) which could have been generated from the degradation of acetic acid.

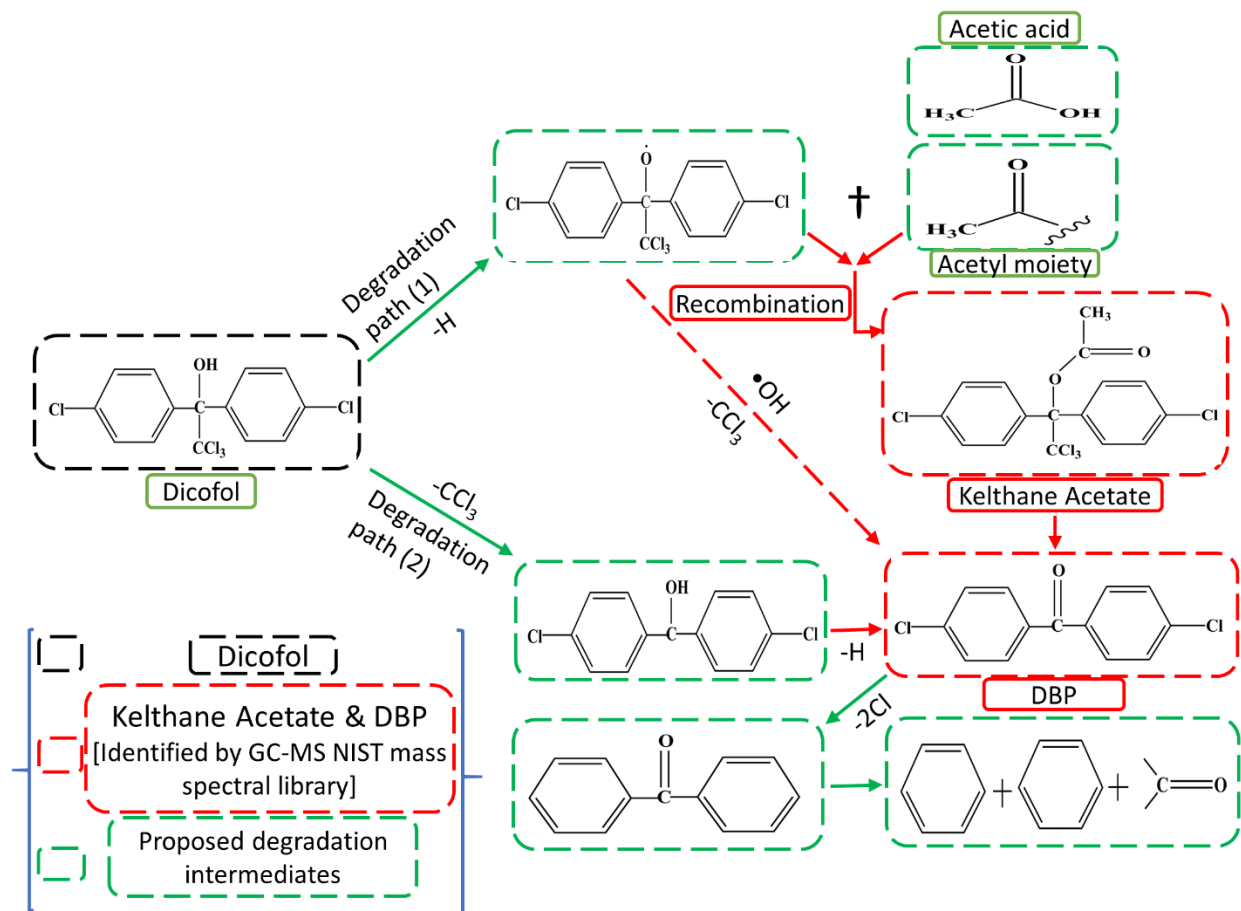
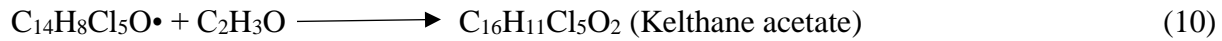
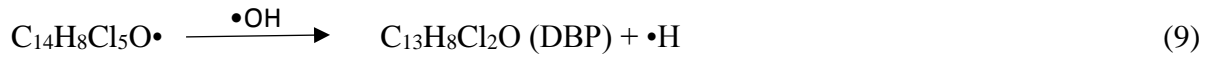


Figure 3.4. The proposed degradation pathways of Dicofol after subjecting to HC treatment

As proposed in Fig. 3.4, the degradation could follow different paths (degradation path 1 or 2), leading to the formation of short chain products as illustrated by equations (1-7) and the detection of degraded product, DBP also indicated either degradation path 1 or 2 for its formation. Binbin et al. (2008) and Wang et al. (2015), also reported the formation of degradant DBP via hydroxyl radical ($\bullet OH$) mediated oxidative degradation of Dicofol during photocatalytic and cellulase/Fenton's based catalytic treatments. While reported results suggested degradation path 1

(Eq.8 & 9) for the formation of DBP, thermal decomposition type cleavage of CCl₃ moiety as the degradation initiator is proposed as the alternative degradation pathway in our studies.

Degradation path 1:



Degradation path 2:



During HC based treatment, short chain degradation products are expected to follow bond dissociation energy order and hence aromatic rings are assumed to dissociate at a later stage for being the most inert. The aromatic intermediates are expected to enter the bubble core and undergo a series of pyrolytic reactions leading to carbon monoxide and other mineralized products, while excluding any oxidative transformation pathways.

3.4.2 Effect of initial pollutant concentration

To determine the effect of initial concentration of pollutant on the rate of degradation and to investigate the order of reaction kinetics, experiments were performed for a range of initial concentration (20-100 mg/L) of Dicofol. The operating inlet pressure of 5 bar, the solution temperature of 20 °C and the solution pH of 3 were kept constant during experiments. Rates were

calculated at different initial concentration of Dicofol and were determined to follow pseudo-first-order kinetic model, which can be expressed as follows:

$$C_t = C_0 e^{-kt} \quad (15)$$

Where, k is the apparent rate constant and C_0 , C_t are the concentrations of Dicofol at time “0” and “ t ” respectively. Fig. 3.5 depicts the variation in degradation with respect to the initial concentration of Dicofol.

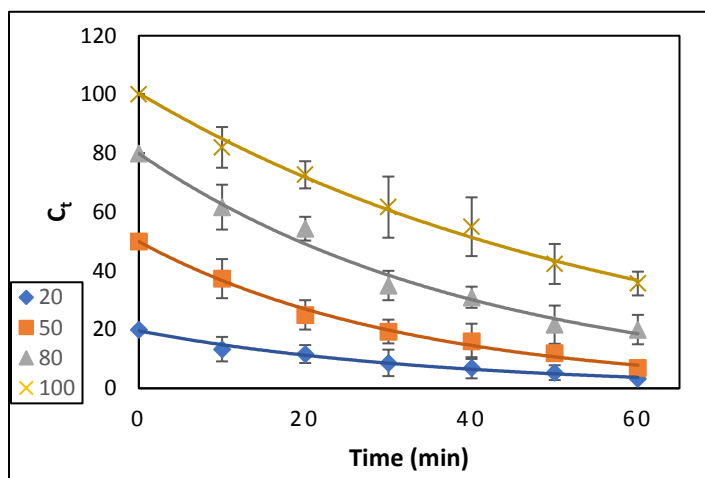


Figure 3.5. Degradation of Dicofol at different initial concentrations: (◆) 20 (■) 50 (▲) 80 (×) 100 mg/L

The extent of degradation decreased with an increase in the initial dicofol concentration above 50 mg/L. From Table 3.2, it is evident that the rate constant decreased from 0.031 to 0.017 min⁻¹ for an increase in concentration from 50 to 100 mg/L. The observed decline in the degradation above optimum value can be attributed to the fact that a higher concentration of pollutant can lead to the saturation of cavity interfacial region along with lack of generated radicals induced by HC to oxidize all pollutant (Merouani et al., 2010). Similarly, Patil et al. (2014) reported that the pseudo-first-order rate constant for imidacloprid degradation decreased with an increase in its concentration above 20 mg/L.

3.4.3 Effect of operating temperature

To investigate the effect of solution temperature on the degradation rate of Dicofol, experiments were conducted in the temperature range of 20-40 °C, while maintaining the concentration of dicofol as 50 mg/L, an inlet pressure of 5 bar and a solution pH of 3. The obtained results (Fig. 3.6) suggested 30 °C to be the optimum value for highest rate of degradation.

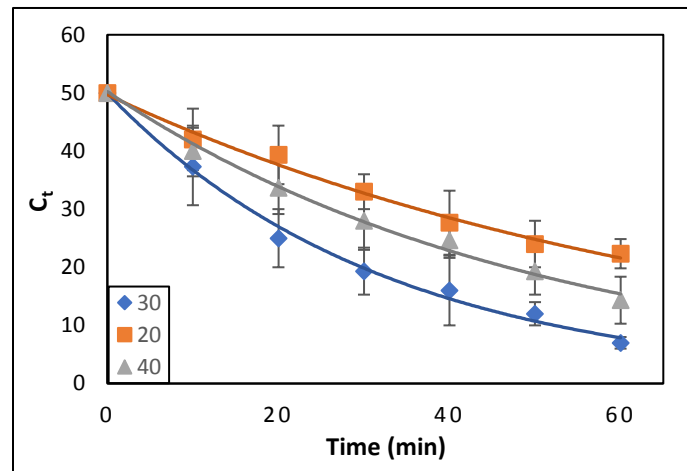


Figure 3.6. Degradation of Dicofol at various solution temperatures: (■) 20 (◆) 30 (▲) 40 °C

Wang et al. (2009) reported similar observations for alachlor degradation with an increase in the temperature up to an optimum value of 40 °C. Bubble dynamics demonstrates that the cavitation intensity and the generation of cavity nuclei reduced with the rise of liquid temperature, because of a decline in the liquid properties such as viscosity, surface tension and gas solubility, resulting in the formation of vaporous cavities (Gogate et al., 2003). But, on the other hand, a rise in the temperature up to the optimum value can enhance the presence of pollutants in collapsing cavities. Similarly, Bagal et al. (2013) reported a temperature of 35 °C as the optimum value for 2,4-dinitrophenol degradation, beyond which the degradation rate decreased marginally.

3.4.4 Effect of inlet pressure

The removal of pollutants by HC depends on the type of cavities (gaseous or vaporous) produced which is dependent on the inlet pressure and cavitation number. The hydraulic characteristics of orifice were studied considering the volumetric flow rate at different inlet pressures and cavitation numbers were estimated according to Eqn. 16. The cavitation number is defined as,

$$C_v = \frac{P_2 - P_v}{\frac{1}{2}\rho v_0^2} \quad (16)$$

Where, P_2 is the fully recovered downstream pressure, P_v is the saturated vapor pressure of the liquid, ρ is the density of liquid and v_0 is the average velocity of liquid at the constriction of orifice. Fig. 3.7 illustrates pressure distribution across the orifice.

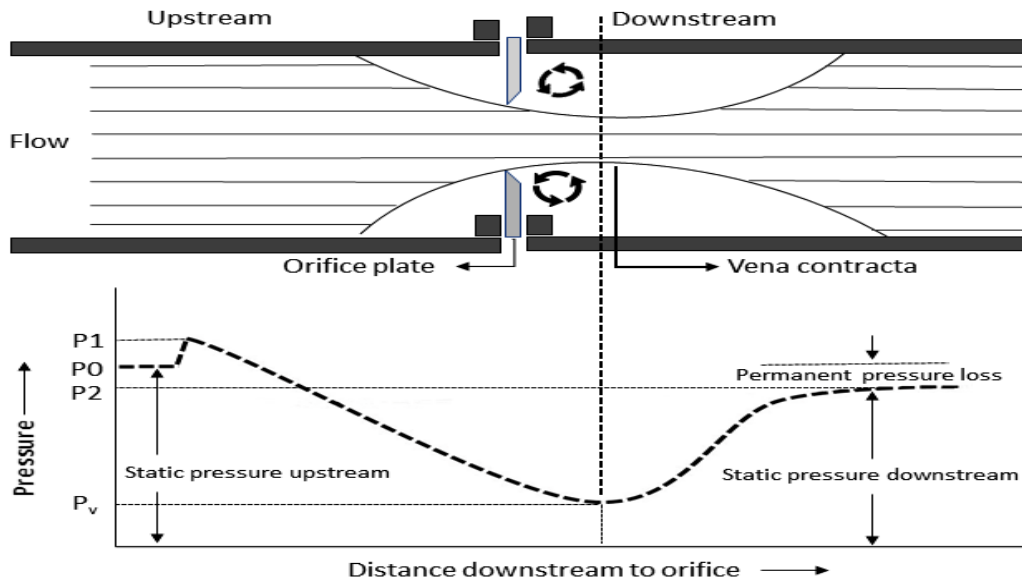


Figure 3.7. Schematic of the flow and pressure distribution across the orifice

The initiation of cavitation starts at a threshold cavitation number known as cavitation inception number (Senthilkumar et al., 2000; Saharan et al., 2011). With an increase in inlet pressure, the volumetric flow rate through the orifice increases and the velocity at the constriction of orifice also increases, resulting in a decline in cavitation number (Gore et al., 2014). Generally, cavitation occurs at $C_v \leq 1$, but cavities can also be formed at a value greater than 1 owing to the presence

of dissolved gases and other solid particles in the liquid (Saharan et al., 2011). The inlet pressure was varied from 3 to 13 bar to determine the optimum pressure for Dicofol degradation, while maintaining the concentration of dicofol as 50 mg/L, the solution temperature at 30 °C and the pH at 3. The established relationship between inlet pressure, volumetric flow rate, cavitation number are represented in Table 3.1 (refer APPENDIX A for detailed calculations).

Table 3.1. Flow characteristics of Dicofol at various inlet pressures of HC

Inlet pressure (bar)	Volumetric flow rate (V) (LPH)	Velocity (v_0) (m/s)	Cavitation number (C_v)
3	133	18.47	0.57
5	182	25.16	0.31
7	246	34.07	0.17
9	288	39.81	0.12
13	382	53.18	0.07

It has been observed that the extent of degradation reached maximum at an inlet pressure of 7 bar (Fig. 3.8). With an increase in inlet pressure and a decrease in cavitation number below 1, the intensity of cavity collapse increases with the generation of larger quantum of active radicals and temperature. But, beyond an inlet pressure of 7 bar, the extent of degradation of Dicofol (Table 3.2) decreased, indicating super cavitation, where indiscriminate and rapid growth of bubbles take place at the downstream of orifice constriction which leads to choked cavitation (Mishra and Gogate, 2010).

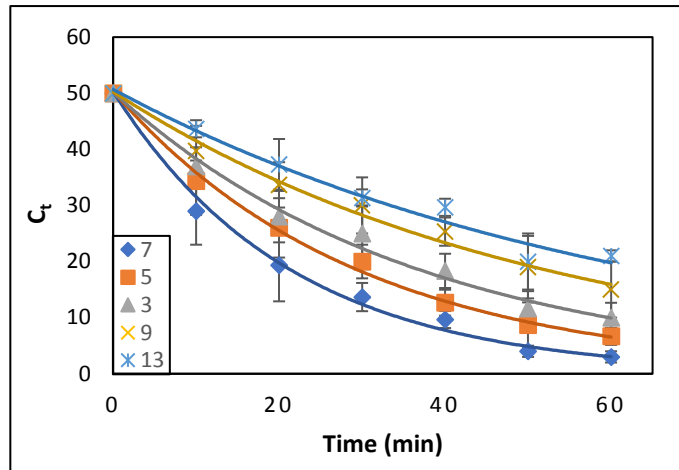


Figure 3.8. Degradation of Dicofol at various inlet pressures: (▲) 3 (■) 5 (◆) 7 (×) 9 (✕) 13 bar

Similar observations were reported by Saharan et al. (2011) for the degradation of reactive red 120 dye and have demonstrated that beyond an optimum inlet pressure choked cavitation has resulted in the decline of degradation. Wang et al. (2009) have reported an increase in the degradation rate of alachlor with an increase in the inlet pressures from 0.2 to 0.6 MPa, while using swirling jet cavitation. Joshi et al. (2012) investigated the degradation of dichlorvos using an orifice plate as the cavitating device and reported that the degradation rate increases up to 4 bar, indicating the presence of an optimum inlet pressure for the removal of pollutant.

3.4.5 Effect of change in pH on Dicofol degradation

HC degradation of Dicofol was conducted at different initial solution pH in the range of 3-7, while maintaining Dicofol concentration of 50 mg/L, solution temperature at 30 °C and operating inlet pressure at 7 bar. The results indicated that the rate of degradation increased with a decrease in solution pH and the highest rate of Dicofol degradation was achieved at pH 3 (Fig. 3.9), which can be attributed to faster transport of pollutants towards bubble interfacial region due to their enhanced hydrophobic nature at acidic conditions (Wei et al., 2016).

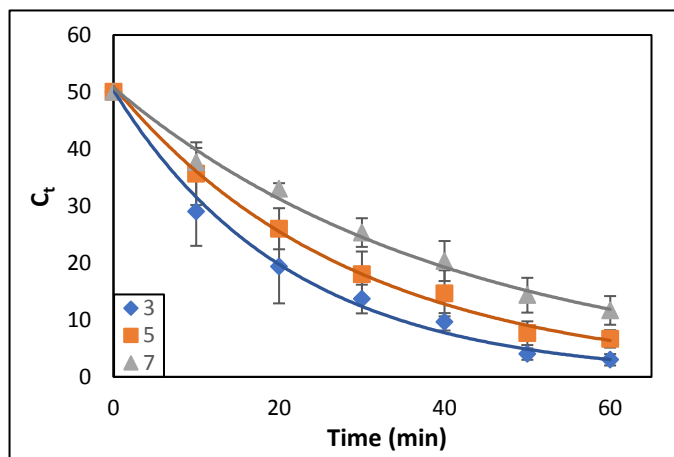


Figure 3.9. Degradation of Dicofol at different pH: (◆) 3, (■) 5, (▲) 7

Also, several previous reports suggested acidic medium for the highest rate of pollutant removal via hydrodynamic cavitation treatment. Bagal et al. (2014) reported a rise in diclofenac sodium removal from 14.7 to 26.8 % with a change in pH from 7.5 to 4. Similarly, the highest rate of imidacloprid removal was reported at an optimum pH of 3 (Patil et al., 2014), whereas under alkaline conditions the extent of degradation was significantly lower.

Table 3.2. Pseudo-first-order rate constants for the degradation of Dicofol under different operational parameters

Parameter		k (min ⁻¹)	R ²
Initial concentration (ppm)	20	0.028	0.98
	50	0.031	0.98
	80	0.024	0.98
	100	0.017	0.99
Inlet pressure (bar)	3	0.027	0.98
	5	0.034	0.99
	7	0.047	0.98
	9	0.019	0.98
	13	0.016	0.95
pH	3	0.047	0.98
	5	0.035	0.98
	7	0.024	0.99
Solution temperature (°C)	20	0.014	0.98
	30	0.031	0.98
	40	0.020	0.98

3.4.6 Effect of H₂O₂ addition and radical scavengers test

For advanced oxidation processes (AOPs), addition of hydrogen peroxide has been opted as an additional source of hydroxyl radicals for the intensification of degradation process. Effect of hydrogen peroxide on the extent of Dicofol degradation has been investigated and the loading of H₂O₂ was considered with respect to an optimum concentration of Dicofol. Three ratios of Dicofol: H₂O₂ such as (1:0.5), (1:1) and (1:2) were investigated, while maintaining the Dicofol concentration of 50 mg/L, inlet pressure at 7 bar, pH at 3 and solution temperature at 30 °C. A significant enhancement in the degradation rate was not observed and the rate increased up to the loading of 50 mg/L resulting in a complete removal of Dicofol within 60 min of treatment. Beyond the optimum loading, the scavenging action of hydrogen peroxide for the generated free radicals can be explained as per Eq. 17.



As H₂O₂ effect is predominant in the solution bulk phase, an increase in the Dicofol degradation rate indicates bulk phase radical attack to lesser extent and the rate constant (k) enhanced only up to 0.073 min⁻¹ in comparison to Dicofol degradation rate constant of 0.047 min⁻¹ without H₂O₂.

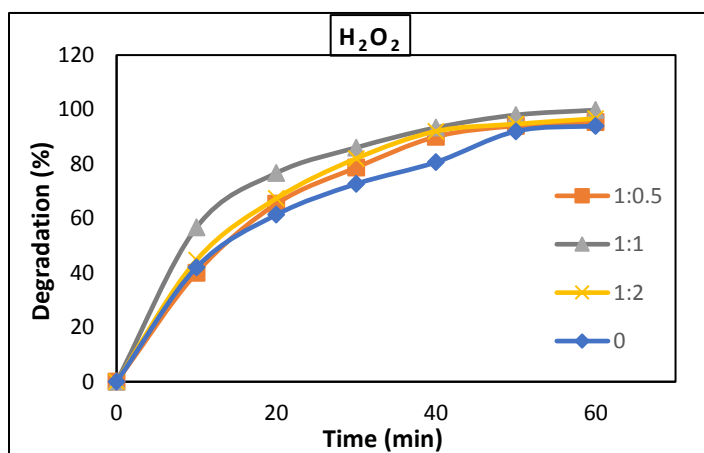


Figure 3.10. The degradation of Dicofol at various H₂O₂ loading: (◆) 0, (■) 25, (▲) 50, (×) 100 mg/L

Table 3.3. Effect of H₂O₂ loading on the extent of degradation and kinetic rate constants for Dicofol

H ₂ O ₂ loading (mg/L)	Extent of degradation (%)	Rate constant k (min ⁻¹)	R ²
0	94	0.047	0.98
25	95	0.054	0.99
50	100	0.073	0.98
100	96	0.058	0.99

Gore et al. (2014) and Saharan et al. (2012) also reported a similar role of hydrogen peroxide for the degradation of reactive orange 4 and acid red 88, where the decolorization rate decreased above an optimum value of H₂O₂ addition. Fig. 3.10 demonstrates the effect of H₂O₂ on the removal of Dicofol, indicating a faster removal of Dicofol within 60 min for a H₂O₂ loading of 50 mg/L.

To evaluate the mineralization efficiency, TOC analysis was performed at 50 mg/L of hydrogen peroxide loading, while maintaining all other parameters at optimum values, which indicated significant mineralization of Dicofol within 60 min of treatment. Fig. 3.11 plots the percentage of TOC removal, demonstrating 85 % removal at the optimum conditions.

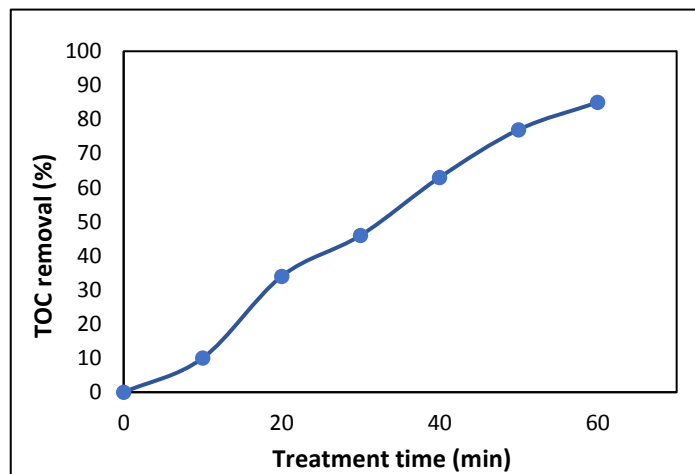


Figure 3.11. TOC removal of Dicofol during 60 min of HC treatment (Experimental conditions: initial pollutant concentration: 50 mg/L; solution temperature: 30 °C; inlet pressure: 7 bar; pH: 3; H₂O₂ loading: 50 mg/L)

While combined advanced oxidation processes such as sonophotocatalysis, and ultrasound assisted electrochemical oxidation of Phenolic compound (Silva et al., 2007) and Perfluorooctanoate (Zhao et al., 2013), have demonstrated 98 % and 86 % of TOC removal respectively, the effectiveness of LWHCR in Dicofol mineralization indicated its superior removal efficiency, which could be attributed to the more intense cavitation events compared to other AOPs.

It is assumed that the degradation of Dicofol would mainly occur at the interfacial region and to obtain information regarding the reaction zone, sodium bicarbonate was chosen which is a free radical scavenger for the bulk phase solution (Liao et al., 2001). The involvement of free radical reaction can be decided if the degradation rate of pollutants declines in the presence of scavengers. Different sets of experiments were conducted for the loading of sodium bicarbonate i.e. 1 g/L, 2 g/L and 5 g/L, while maintaining all other optimum parameters. The rate constant decreased marginally in the presence of bicarbonate ions for the entire loading, indicating interfacial region as the predominant degradation zone with lesser extent of radical reaction in the bulk solution. Yao et al. (2010) also reported similar result for parathion degradation in the presence of sodium bicarbonate, where the reaction zones are predominantly the interfacial region. Fig.3.12 demonstrates the percentage of Dicofol degradation during the addition of radical scavenger.

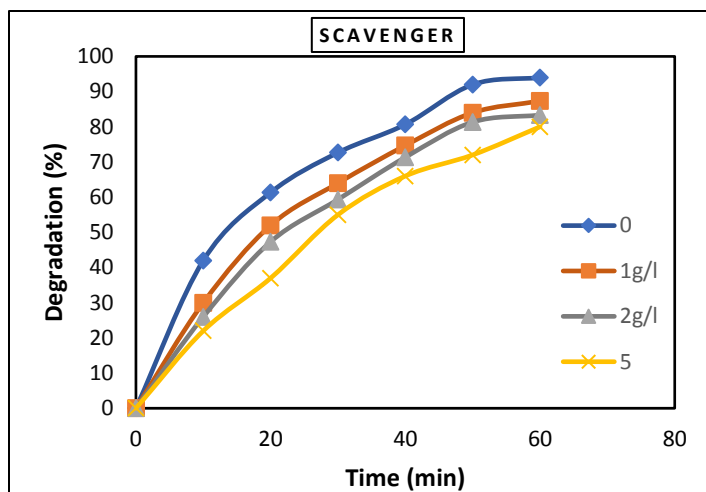


Figure 3.12. Degradation of Dicofol at various loadings of sodium bicarbonate: (◆) 0, (■) 1, (▲) 2, (×) 5 g/L

Table 3.4. Effect of addition of radical scavenger on the extent of degradation and kinetic rate constants

Sodium bicarbonate loading (g/L)	Extent of degradation (%)	Rate constant k (min^{-1})	R^2
0	94	0.047	0.98
1	87	0.035	0.99
2	83	0.031	0.99
5	80	0.027	0.99

The $\log K_{ow}$ and Henry's law constant of Dicofol are 5.02 and 2.4×10^{-7} atm m^3/mol , respectively, indicating hydrophobic and semi-volatile nature of Dicofol. Also, the vapor pressure of Dicofol is 3.98×10^{-7} mmHg at 25 °C, and thus falling under the category of gas/particulate mixture, thereby expected to transport into vapor-liquid interphase rather than being present in the bulk phase, which is in line with our outcomes of scavenger studies. Thus, thermal decomposition at the interfacial region is assumed to be the dominant degradation pathway, following radical attack as the secondary transformation mechanism.

3.5 Energy efficiency analysis

The energy efficiency of HC cavitation can be evaluated based on the degradation yield which can be defined as the extent of degradation per unit energy consumed (mg/J). The degradation yield is expressed as below:

$$\text{Degradation yield (mg/J)} = \frac{\text{Amount of pollutant degraded}}{(P_m t)/V} \quad (18)$$

Where, P_m is the power of the pump, t is the operation time, and V is the volume of pollutant solution.

3.5.1 Comparison between Hydrodynamic cavitation and Acoustic cavitation

Till date, Acoustic cavitation has been implemented for successful removal of numerous pollutants (Panda and Manickam, 2017), but large-scale industrial application has encountered with numerous difficulties with respect to energy efficiencies, reactor construction etc. Based on our previous work of acoustic cavitation based Dicofol removal, a comparison on the effectiveness of both modes of cavitation treatment has been attempted. While ultrasonic generator is the main energy consuming component for acoustic cavitation, the major energy consuming component of hydrodynamic cavitation is the pump, which is employed for the circulation of solution through the reactor. Experiments were conducted at a fixed initial concentration of Dicofol (50 mg/L), at pH 3 for 60 min of treatment for both types of cavitation reactors. A 20-kHz probe type sonicator with a supplied power of 375 W was employed for the sonochemical treatment of Dicofol. Considering the maximum degradation obtained under the optimum conditions, the degradation yield obtained for acoustic and hydrodynamic cavitation were calculated to be 1.07×10^{-6} and 1.26×10^{-5} (mg/J) respectively, which was determined following Eq. 18 (refer APPENDIX B for detailed calculations), demonstrating degradation yield for HC to be 12 times higher than acoustic cavitation. Senthilkumar et al. (2000) and Sivakumar et al. (2002) reported HC degradation yield

to be 3 times and 12 times higher than acoustic cavitation respectively. The degradation yield of HC was even reported to be 20 times higher than acoustic cavitation for methyl parathion degradation (Patil and Gogate, 2012) and hence can be considered as more energy efficient cavitating condition generator.

3.6 Conclusions

The present work has demonstrated that hydrodynamic cavitation can be used efficiently for the removal of Dicofol. Process intensification has been achieved effectively while considering the addition of H₂O₂ and the optimization of essential parameters such as inlet pressure, solution temperature and initial concentration of Dicofol. Following vital conclusions can be drawn from the present work:

- HPLC and GC-MS analyses have demonstrated the formation of degraded products.
- The degradation of Dicofol increased with an increase in the inlet pressure up to an optimum value of 7 bar beyond which a decline in the degradation was witnessed.
- The extent of degradation increases marginally with the addition of hydrogen peroxide up to the loading of 50 mg/L.
- Experiments conducted in the presence of sodium bicarbonate as radical scavenger demonstrated interfacial region to be the dominant degradation zone for Dicofol.
- Under optimum conditions, TOC removal reached 85 % within 60 min of treatment, illustrating the significant mineralization of Dicofol.
- Comparison between acoustic and hydrodynamic degradation yield, demonstrates HC to be more energy efficient.

3.7 APPENDIX

A: THE ESTIMATION OF HYDRAULIC CHARACTERISTICS: TABLE 1

Calculation of cavitation number for an inlet pressure of 7 bar

- Inlet fluid pressure = 802145 Pa
- Downstream pressure (P_2) = 102145Pa
- Vapor pressure of water at 30 °C (P_v) = 4242.14 Pa
- Volumetric flow rate (V) = 246 LPH = 6.85×10^{-5} m³/s
- Diameter of the orifice constriction (d_0) = 1.6 mm

Flow area:

$$(a_0) = \frac{\pi}{4} d_0^2 = \frac{\pi}{4} \times (1.6 \times 10^{-3})^2 = 2.01 \times 10^{-6} \text{ m}^2$$

Velocity at the throat of the orifice:

$$(v_0) = \left(\frac{V}{a_0} \right) = \left(\frac{6.85 \times 10^{-5}}{2.01 \times 10^{-6}} \right) = 34.07 \text{ m/s}$$

Cavitation number:

$$(C_v) = \frac{P_2 - P_v}{\frac{1}{2} \rho v_0^2} = \frac{(102145 - 4242.14)}{\left(\frac{1}{2} \times 1000 \times 34.07^2 \right)} = 0.17$$

B: THE ESTIMATION OF DEGRADATION YIELD

Calculation of degradation yield:

Conditions for Acoustic cavitation:

- Ultrasonic horn frequency - 20 kHz
- Reaction volume - 100 ml
- Supplied electric power – 375 W
- Treatment time – 60 min
- Percentage degradation obtained – 29 %
- Dicofol concentration – 50 mg/L

$$\text{Degradation obtained (mg/L)} = \frac{29 \times 50}{100} = 14.5 \text{ mg/L}$$

$$\text{Energy density (J/L)} = \frac{375 \times 60 \times 60}{0.1} \text{ (J/L)} = 13500000 \text{ J/L}$$

$$\text{Degradation yield} = \frac{14.5 \left(\frac{\text{mg}}{\text{L}}\right)}{13500000 \left(\frac{\text{J}}{\text{L}}\right)} = 1.07 \times 10^{-6} \text{ (mg/J)}$$

Conditions for Hydrodynamic cavitation:

- Reaction volume – 2 L
- Power rating of pump (P_m) – 2.2 kW (2200 W)
- Treatment time – 60 min
- Concentration = 50 mg/L
- Percentage of degradation = 100 %

$$\text{Degradation obtained (mg/L)} = \frac{100 \times 50}{100} = 50 \text{ mg/L}$$

$$\text{Energy density (J/L)} = \frac{2200 \times 60 \times 60}{2} \text{ (J/L)} = 3960000 \text{ J/L}$$

$$\text{Degradation yield} = \frac{50 \left(\frac{\text{mg}}{\text{L}}\right)}{3960000 \left(\frac{\text{J}}{\text{L}}\right)} = 1.26 \times 10^{-5} \text{ (mg/J)}$$

3.8 References

- US EPA, 1998. Dicofol: reregistration eligibility decision (RED), *Prev. Pestic. Toxic Subst. EPA* 738-R-98-018.
- Binbin, Y., JingBin, Z., LiFen, G., XiaoQing, Y., Limei, Z., Xi, C., 2008. Photocatalytic degradation investigation of dicofol, *Sci. Bull.* 53, 27–32.
- Lohse, D., 2003. Bubble puzzles, *Phys. Today* 56, 36–41.
- Chand, R., Bremner, D. H., Namkung, K. C., Collier, P. J., Gogate, P. R., 2007. Water disinfection using the novel approach of ozone and a liquid whistle reactor, *Biochem. Eng. J.* 35, 357–364.
- Chakinala, A. G., Gogate, P. R., Burgess, A. E., Bremner, D. H., 2008. Treatment of industrial wastewater effluents using hydrodynamic cavitation and the advanced Fenton process, *Ultrason. Sonochem.* 15, 49–54.
- Gogate, P. R., Pandit, A. B., 2005. A review and assessment of hydrodynamic cavitation as a technology for the future, *Ultrason. Sonochem.* 12, 21–27.
- Wang, Z., Yang, T., Zhai, Z., Zhang, B., Zhang, J., 2015. Reaction mechanism of dicofol removal by cellulase, *J. Environ. Sci.* 36, 22–28.
- Merouani, S., Hamdaoui, O., Saoudi, F., Chiha, M., 2010. Sonochemical degradation of rhodamine B in aqueous phase: effects of additives, *Chem. Eng. J.* 158, 550–557.
- Patil, P. N., Bote, S. D., Gogate, P. R., 2014. Degradation of imidacloprid using combined advanced oxidation processes based on hydrodynamic cavitation, *Ultrason. Sonochem.* 21, 1770–1777.
- Wang, X., Zhang, Y., 2009. Degradation of alachlor in aqueous solution by using hydrodynamic cavitation, *J. Hazard. Mater.* 161, 202–207.

- Gogate, P. R., Wilhelm, A. M., Pandit, A. B., 2003. Some aspects of the design of sonochemical reactors. *Ultrason. Sonochem.* 10, 325–330.
- Bagal, M. V., Gogate, P. R., 2013. Degradation of 2,4-dinitrophenol using a combination of hydrodynamic cavitation, chemical and advanced oxidation processes, *Ultrason. Sonochem.* 20, 1226–1235.
- Senthilkumar, P., Sivakumar, M., Pandit, A. B., 2000. Experimental quantification of chemical effects of hydrodynamic cavitation, *Chem. Eng. Sci.* 55, 1633– 1639.
- Saharan, V. K., Badve, M. P., Pandit, A. B., 2011. Degradation of reactive red 120 dye using hydrodynamic cavitation, *Chem. Eng. J.* 178, 100–107.
- Gore, M. M., Saharan, V. K., Pinjari, D. V., Chavan, P. V., Pandit, A. B., 2014. Degradation of reactive orange 4 dye using hydrodynamic cavitation based hybrid techniques, *Ultrason. Sonochem.* 21, 1075–1082.
- Mishra, K. P., Gogate, P. R., 2010. Intensification of degradation of rhodamine B using hydrodynamic cavitation in the presence of additives, *Sep. Purif. Technol.* 75, 385–391.
- Saharan, V. K., Badve, M. P., Pandit, A. B., 2011. Degradation of reactive red 120 dye using hydrodynamic cavitation, *Chem. Eng. J.* 178, 100–107.
- Joshi, R. K., Gogate, P. R., 2012. Degradation of dichlorvos using hydrodynamic cavitation based treatment strategies, *Ultrason. Sonochem.* 19, 532– 539.
- Wei, Z., Spinney, R., Ke, R., Yang, Z, Xiao, R., 2016. Effect of pH on the sonochemical degradation of organic pollutants. *Environ. Chem. Lett.* 14, 163-182.
- Bagal, M. V., Gogate, P. R., 2014. Degradation of diclofenac sodium using combined processes based on hydrodynamic cavitation and heterogeneous photocatalysis, *Ultrason. Sonochem.* 21, 1035–1043.

- Gore, M. M., Saharan, V. K., Pinjari, D. V., Chavan, P. V., Pandit, A. B., 2014. Degradation of reactive orange 4 dye using hydrodynamic cavitation based hybrid techniques, *Ultrason. Sonochem.* 21, 1075–1082.
- Saharan, V. K., Pandit, A. B., Satish Kumar, P. S., Anandan, S., 2012. Hydrodynamic cavitation as an advanced oxidation technique for the degradation of acid red 88 dye, *Ind. Eng. Chem. Res.* 51, 1981–1989.
- Silva, M. T., Nouli, E., Xekoukoulotakis, N. P., Mantzavinos, D., 2007. Sonophotocatalytic/H₂O₂ degradation of phenolic compounds in agro-industrial effluents, *Cataly. Today.* 124, 232–239.
- Zhao, H., Gao, J., Zhao, G., Fan, J., Wang, Y., Wang, Y., 2013. Environmental fabrication of novel SnO₂-Sb/carbon aerogel electrode for ultrasonic electrochemical oxidation of perfluorooctanoate with high catalytic efficiency, *Applied Catal. B: Environ.* 136–137, 278–286.
- Liao, C., Kang, S., Wu, F., 2001. Hydroxyl radical scavenging role of chloride and bicarbonate ions in the H₂O₂/UV process. *Chemosphere.* 44, 1193–1200.
- Yao, J. J., Gao, N. Y., Li, C., Li, L., Xu, B., 2010. Mechanism and kinetics of parathion degradation under ultrasonic irradiation. *J. Hazard. Mater.* 175, 138–145.
- Panda, D., Manickam, S., 2017. Recent advancements in the sonophotocatalysis (SPC) and doped-sonophotocatalysis (DSPC) for the treatment of recalcitrant hazardous organic water pollutants. *Ultrason. Sonochem.* 36, 481–496.
- Senthilkumar, P., Sivakumar, M., Pandit, A.B., 2000. Experimental quantification of chemical effects of hydrodynamic cavitation, *Chem. Eng. Sci.* 55, 1633–1639.

Sivakumar, M., Pandit, A. B., 2002. Wastewater treatment: a novel energy efficient hydrodynamic cavitation technique, *Ultrason. Sonochem.* 9, 123-131.

Patil, P. N., Gogate, P. R., 2012. Degradation of methyl parathion using hydrodynamic cavitation: effect of operating parameters and intensification using additives, *Sep. Purif. Technol.* 95, 172–179.

Chapter 4

Heterogeneous Sono-Fenton treatment of Decabromodiphenyl ether (BDE-209): Debromination mechanism and transformation pathways

Abstract

Polybrominated diphenyl ethers, used as flame retardants are a cause of concern over the past several years, due to their toxicity, bioaccumulation and widespread distribution. In this work, the combination of ultrasound and advanced Fenton process was investigated for the degradation of Decabromodiphenyl ether (BDE-209). The effect of pollutant concentration, solution pH, ultrasonic power density and loading of Fenton's reagent on the extent of BDE-209 degradation were studied. The results indicated an enhancement in the degradation of BDE-209 during Sono-Fenton treatment, leading to a complete degradation within 80 min of treatment, whereas only 40 % and 25 % degradation were achieved during US and Fenton treatment respectively. To understand the degradation mechanism, analytical techniques including High performance liquid chromatography and Gas chromatography mass spectroscopy were employed to monitor the concentrations of parent compound along with degradation products. The degradation mechanism was proposed based on the identified degradation products. Total organic carbon (TOC) analysis demonstrated 60 % TOC removal within 80 min of treatment time. The obtained results suggest that the initiation of BDE-209 degradation during Sono-Fenton treatment followed thermal decomposition at bubble-vapor interface along with reductive debromination at the surface of iron, accompanied by oxidative degradation of lower brominated congeners at liquid bulk. This work illustrated an effective method for the removal of BDE-209 and providing an efficient wastewater treatment solution for recalcitrant pollutants.

4.1 Introduction

Polybrominated diphenyl ethers (PBDEs), also referred as brominated flame retardants, are widely used since 1970 in numerous products, including furniture, electrical equipment, textiles and other household accessories (US EPA, 2014). The presence of PBDEs have been detected in air, sediments, surface water, fish, marine animals and even in humans, indicating PBDEs emission into environment via various routes (US EPA, 2014; Chen et al., 2007; Hites, 2004). Following the wide distribution and environmental persistence of PBDEs (US EPA, 2013), they have emerged as contaminants of concern, which are associated with endocrine disruption, neurodevelopmental toxicity, hepatic toxicity in humans and mammals (Darnerud et al., 2001). Decabromodiphenyl ether (BDE-209) is the major industrial PBDE product with a global demand of 54,800 tons out of 67,000 tons PBDEs in 1999 and reaching a production of 56,000 tons in 2003 even after the limitations imposed by several countries on the application of PBDEs (Alaee et al., 2003; Peng et al., 2009; Andersson et al., 2006). Environmental protection agency (EPA) has classified BDE-209 as a possible human carcinogen (ATSDR, 2004).

Considering BDE-209's persistency, an extensive occurrence in environment and toxic nature, an effective wastewater treatment technique is required for its elimination. Biodegradation has demonstrated effectiveness in the removal of BDE-209 (Shih et al., 2012; Zhou et al., 2007; Chou et al., 2013; Gerecke et al., 2005), but longer duration of treatment time and further disposal of the biotic waste are major drawbacks. Photocatalysis was reported to be successful for BDE-209 removal (An et al., 2008; Stapleton and Dodder, 2008; Christiansson et al., 2009), however, the requirement of intense UV light limits its environmental remediation application. Advanced oxidation processes (AOPs), such as ultrasonic irradiation, has been employed for the removal of pesticides, dyes, surfactants and phenolic compounds (Kidak and Ince, 2006; Sivasankar and

Moholkar, 2009), but combination of different AOPs has been reported to be more efficient compared to individual oxidation process (Panda and Manickam, 2017; Bagal and Gogate, 2014). Numerous reports on coupled Sono-Fenton based treatment indicated its effectiveness in pollutant removal (Patil and Gogate, 2015; Jawale and Gogate, 2018). Conventional Fenton process utilizes FeSO_4 as the major source of Fe^{2+} (Lin and Lo, 1997), but associated key issues such as consumption of reagent and generation of chemical sludge, can be addressed via nZVI application as the alternative Fenton heterogeneous reagent. ElShafei et al. (2017) reported successful degradation of nonylphenol by ultrasonic assisted heterogeneous Fenton like oxidation using nZVI as a catalyst. The advanced heterogeneous Fenton process (AFP) employs zero valent iron (mZVI/nZVI) in conjunction with H_2O_2 , preferably under acidic conditions, which leads to Fenton chain reaction via corrosion of metal iron (Bremner et al., 2006).

US, Fenton and US/Fenton degradation of BDE-209 have been investigated in the present work to illustrate the effect of combined process. Optimum operational parameters were decided with respect to the highest degradation rate. To monitor BDE-209 concentration during treatment and to identify the degradation products, High performance liquid chromatography (HPLC) and Gas chromatography-mass spectrometry (GC-MS) analysis were conducted. To understand the extent of BDE-209 mineralization, total organic carbon (TOC) analysis has been performed. This report has demonstrated the effectiveness of combined US/Fenton treatment for the best possible degradation of recalcitrant BDE-209 as compared to US or Fenton's treatment only.

4.2 EXPERIMENTAL

4.2.1 Materials

BDE-209 [Decabromodiphenyl ether ($\text{C}_{12}\text{Br}_{10}\text{O}$), 98%, CAS Number 1163-19-5], Methanol (HPLC grade), Hydrogen peroxide (analytical grade, 30% w/w), Potassium hydrogen phthalate

(>99%), Tetrahydrofuran (THF), acetonitrile, N-hexane and Sodium bicarbonate (99.5%) were purchased from Sigma Aldrich (Malaysia). A standard solution of 39 PBDE congeners mixture was obtained from Cambridge Isotope Laboratories (Andover, MA). Nano zero valent iron metal powder (>99.5%, <45 nm) was obtained from Sigma Aldrich (Malaysia). Ultra-pure deionized water of 15 M Ω . cm resistivity was obtained from a water purification system (PURELAB Option-R, ELGA, UK) and was used throughout experiment. Agilent nylon syringe filter of 0.45 μ m pore size and 5 ml syringes were purchased from IT Tech Research (M) Sdn. Bhd. (Malaysia).

4.2.2 Experiment methodology

The reaction solutions were prepared by diluting an appropriate amount of BDE-209 stock solution (200 mg/L in THF) with Milli-Q water. Each treatment (US/Fenton, US, Fenton) was performed in a 100-mL reactor using a 20-kHz ultrasonic probe (CPX 750, 750 W, Cole-Parmer Instruments, Illinois, USA), whereas the addition of required amount of hydrogen peroxide and iron powder to the solution was performed during US/Fenton process. Sonication was conducted in pulse mode and calorimetric procedures (Koda et al., 2003) were adopted to verify the actual ultrasonic power and the energy dissipated by the transducer into the solution. Appropriate quantity of H₂SO₄ and/or NaOH was used for pH adjustments. The temperature of reaction mixture solution was maintained at 25 \pm 5 °C using a chiller (Julabo Labortechnik GmbH, Germany). Experiments were conducted up to 120 min and a powerful magnet was used at the bottom of glass reactor to retain nZVI. Samples were withdrawn by using a syringe at regular intervals followed by filtration through 0.45 μ m membrane for analysis. Subsequently nZVI particles were separated following centrifugation for 10 min. N-hexane was used to extract BDE-209 in aqueous solutions (1:1, v/v) and the nZVI particles were subjected to extraction via acetonitrile to completely desorb the adsorbed BDE-209 or its degradation products if present. All extractions were performed thrice, and the combined

extract was dehydrated by anhydrous sodium sulfate. Prior to GC-MS analysis the combined extracts were concentrated to 1 mL by rotary evaporation.

4.2.3 Analytical methods

The concentration of BDE-209 was monitored by a HPLC system (Agilent 1200 infinity), equipped with an online degasser, quaternary LC pump (infinity model 1260), an infinity 1260 VWD UV detector for separation on a CORTECS™ C18 column (4.6 mm × 100 mm, 2.7 μm). Standards were used for optimization of HPLC parameters, which have been followed for the entire analysis. The Agilent ChemStation software was used for instrument control, data acquisition and data analysis. The mobile phase was composed of solvent A (methanol) and solvent B (ultrapure water) in 95:5 ratio. The column chamber was kept at 30 °C and BDE-209 was monitored at a wavelength of 235 nm. The injection volume and flow rate were 20 μL and 1.2 mL/min respectively. The retention time of BDE-209 was 8.12 min and the run time was 12 min. The quantification was performed by constructing a calibration curve of BDE-209 standard.

Identification of products was conducted by GC-MS (Perkin Elmer CLARUS SQ8 S/CLARUS 680) equipped with a PerkinElmer Elite 5-MS capillary column (length: 30 m, I. D: 0.25 mm, Film thickness: 0.25μm). Helium gas of chromatographic grade was used as a carrier gas. The injector temperature was at 300 °C, the flow rate was 1.0 mL/min and the injection volume was 1 μL. The oven temperature was at 100 °C for 3 min, which was then increased at 5 °C/min to 310 °C and was finally hold for 15 min. The GC interface and the source were at 300 °C and 250 °C respectively. The scan range was 60 to 1100 amu.

To determine the mineralization of BDE-209, the decay in total organic carbon content was monitored using a TOC analyzer (Shimadzu TOC 5050A) equipped with an ASI5000 autosampler. Prior to analysis, all the liquid samples, including blanks and standards were acidified to pH 2

using hydrochloric acid and instrument calibration was performed using potassium hydrogen phthalate standards. The inorganic carbon was removed by sparging the samples with air.

4.2.4 Debromination rate constants

The pseudo-first-order model was used to illustrate the debromination of BDE-209 by US/Fenton treatment, which can be expressed as follows (Eq. (19)):

$$C_t = C_0 e^{-kt} \quad (19)$$

Where, k is the apparent rate constant and C_0 , C_t are the concentrations of BDE-209 at time “0” and “t” respectively. The mean value along with standard deviations obtained from triplicate experiments are reported.

4.3 Results and discussion

HPLC and GC-MS analysis were performed for three modes of treatments (US, Fenton, US/Fenton) and the extent of degradation was compared. During all types of treatment, BDE-209 concentration declined with treatment time, but only 40 % and 25 % decline in concentration was achieved via US and Fenton treatment (Fig. 4.2), which indicates the recalcitrant nature of BDE-209 towards US or Fenton treatment for rapid transformation. However, during the combined US/Fenton treatment, a comparatively faster degradation of BDE-209 was observed, leading to 92 % decline in the concentration within 60 min of treatment.

GC-MS analysis was performed in full scan mode and retention time along with mass spectra of respective new peaks were compared with authentic standards, but due to the lack of some standards, certain lower brominated congeners were identified qualitatively via NIST library match. Selected Ion Monitoring (SIM) was also performed for target ion (m/z 799) to determine

BDE-209 concentration over treatment time. Fig. 4.1 illustrates the GC-MS chromatogram of BDE-209 during US/Fenton treatment.

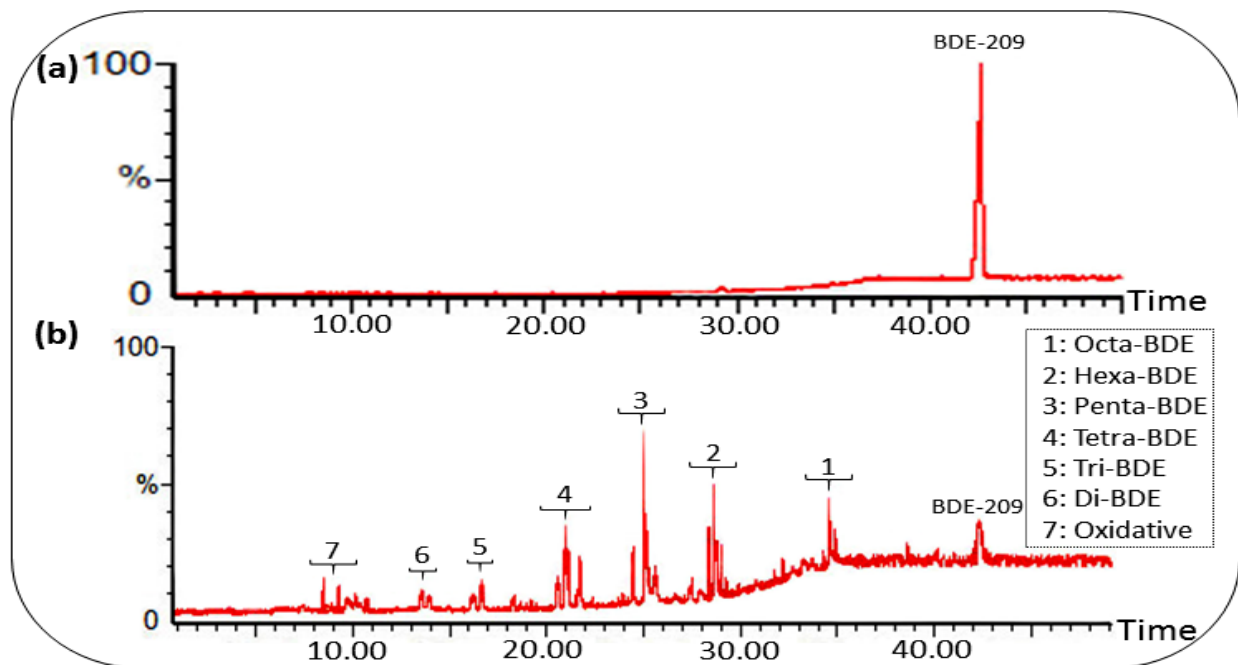


Figure 4.1. Chromatograms of BDE-209 full scan analysis at (a) 0 min (b) 60 min of treatment

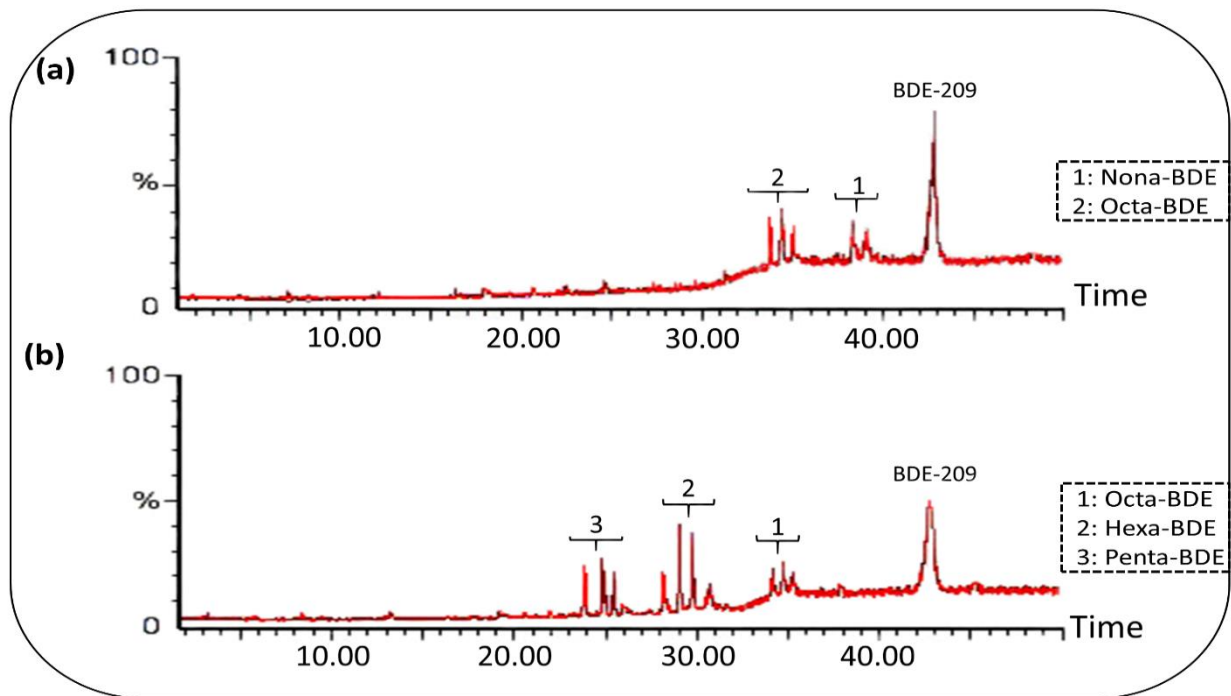


Figure 4.2. Chromatograms of BDE-209 full scan analysis at 80 min of (a) Fenton and (c) US treatment

Fig. 4.3 plots the percentage of TOC removal within 80 min of US/Fenton treatment. The TOC removal was up to 60 % at optimum conditions, indicating mineralization of BDE-209 during the combined treatment.

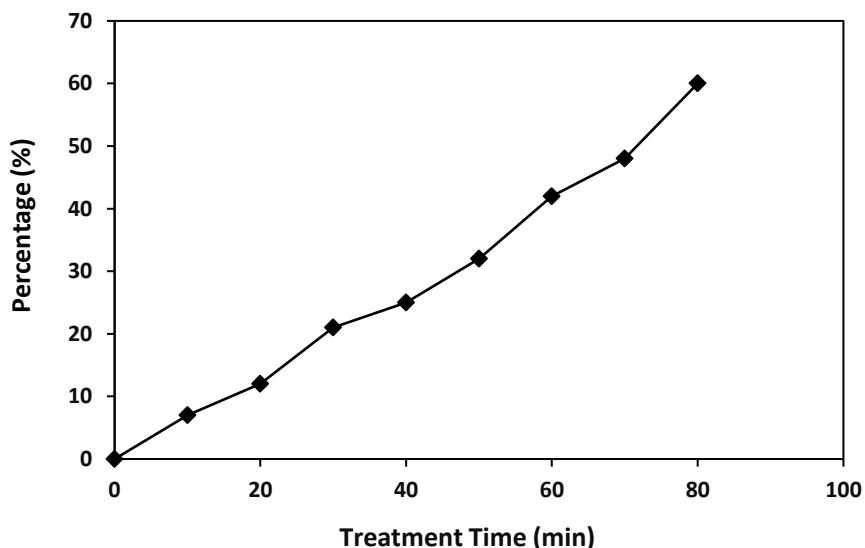


Figure 4.3. TOC removal of BDE-209 within 80 min of treatment (Experimental conditions: initial concentration: 20 mg/L; power density: 420 W; pH: 2; H₂O₂ loading: 150 mg/L; nZVI loading: 1 mg/L)

4.3.1 Degradation pathways and possible mechanism

During US treatment of BDE-209, the appearance of only Octa, Hexa and Penta-BDE congeners rather than any Nona and Hepta-BDE degradation products indicated a thermal decomposition mediated debromination of parent compound leading to indiscriminate removal of bromine, rather than a sequential reductive debromination of BDE-209, whereas during Fenton's treatment, sequential reductive debromination has resulted in the appearance of Nona and Octa-BDE within 60 min of treatment. During only US or Fenton treatment, the absence of lower brominated congeners within the defined treatment time, indicated the recalcitrant nature of BDE-209 towards either of the treatments. Shi et al. (2015) also reported similar mechanism indicating BDE-209 could not be effectively degraded in 20 h by conventional oxidizing agents such as Fenton's reagent, KMnO₄ and ozone.

Considering US/Fenton treatment, Octa-BDE first appeared after 20 min, whereas Hexa-BDE, Penta-BDE and Tetra-BDE appeared after 40 min of treatment, which remained in considerable amounts up-to 60 min, following gradual decrease in concentration with treatment time. Meanwhile, the amounts of Tri-BDE and Di-BDE gradually increased with the treatment time, but their concentration decreased rapidly. Lower brominated degradation products were observed to disappear faster than higher brominated degradation products, indicating rapid dehalogenation. The detection of oxidative products along with lower brominated congeners (Table 4.1), indicated simultaneous reductive and oxidative process to be occurring for lower brominated products.

Table 4.1. Retention time of the chemical standards in the GC-MS

Number	Congeners	Retention time (min)	(% abundance)
1	BDE-7	13.45	85
2	BDE-15	13.97	82
3	BDE-17	16.24	84
4	BDE-28	16.91	88
5	BDE-66	20.92	91
6	BDE-77	21.15	93
7	BDE-100	24.43	84
8	BDE-99	25.12	95
9	BDE-126	25.72	89
10	BDE-154	27.44	78
11	BDE-153	28.75	97
12	BDE-138	28.84	84
13	BDE-156	29.52	81
14	BDE-197	34.94	76
15	BDE-196	34.71	92
16	BDE-203	34.93	94
17	BDE-209	42.45	97
18	Phenol	8.450	80
19	<i>p</i> -Hydroquinone	10.14	77

The detection of lower brominated congeners and oxidative products such as Phenol and *p*-Hydroquinone during US/Fenton treatment demonstrates the successive hydroxylated oxidation of Mono-BDEs as the final stage of transformation and hence indicating the enhanced debromination of BDE-209 during the combined treatment. Based on the identification of degradation products during combined US/Fenton treatment, the degradation pathway is proposed as represented in Fig. 4.4.

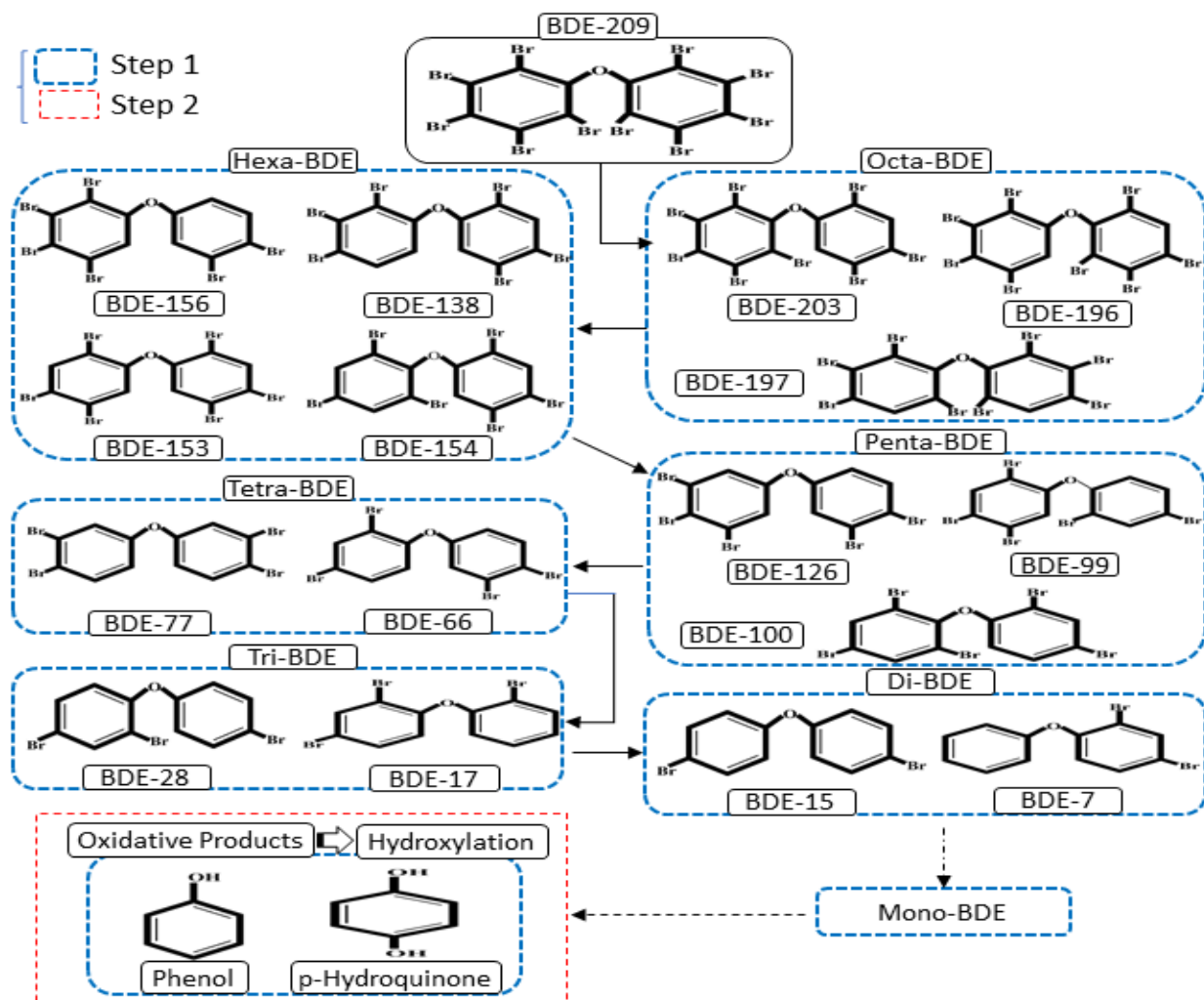


Figure 4.4. The proposed degradation pathways of BDE-209 during US/Fenton treatment

A two-step degradation pathway is proposed for BDE-209 degradation via successive elimination of bromine atoms as the first step of debromination, leading to the formation of lower brominated

congeners and oxidative degradation of lower brominated congeners as the second step. The role of Fenton's reagent can be understood by considering the fact that Nano zero valent iron (nZVI) exhibits high Fenton-like oxidative activity towards lower brominated diphenyl ethers and halogenated organic compounds (Xu et al., 2013; Xu and Wang, 2011; Luo et al., 2011), whereas less effective towards fully brominated diphenyl ethers such as BDE-209, due to their extremely stable symmetrical structure. After the removal of halides from the aromatic ring, it was found that halogenated compounds provide less resistance towards oxidative degradation (Monserrate and Haggblom, 1997). Luo et al. (2011) reported that diphenyl ether can be mineralized effectively in a Fe/Ag/H₂O₂ system subjected to ultrasound treatment and Lin et al. (2014) demonstrated PCB28 degradation via Fenton-like oxidation process using goethite, indicating that reactive radicals are only capable of attacking lower brominated BDEs along with water soluble halogenated organic compounds. Also, heterogeneous reaction on iron surface could simultaneously results in reductive debromination of parent BDE-209 and short chain congeners. Our experimental outcomes confirmed the previously stated results that additional active radicals generated by Fenton's reagent promoted further debromination and degradation of lower brominated degradation products. Overall, the initial decomposition of BDE-209 is proposed to be a function of both interfacial thermal decomposition during sonolysis along with reductive debromination of parent compound at nZVI surface, following successive hydroxylation along with oxidation of lower brominated congeners at liquid bulk and bubble interfacial region. The increased probability of simultaneous oxidative and reductive debromination of lower brominated congeners at liquid bulk and at nZVI surface can be attributed to their enhanced aqueous solubility (Table 4.2) compared to the parent compound.

Table 4.2. The aqueous solubility of PBDE congeners

PBDE congener	Aqueous solubility (mol/L)
209	1.28×10^{-10}
203	4.69×10^{-10}
190	5.63×10^{-9}
138	1.20×10^{-8}
99	3.55×10^{-8}
47	9.44×10^{-8}
17	1.26×10^{-6}
7	1.06×10^{-5}
1	2.90×10^{-5}

4.3.2 Effect of initial concentration on degradation

The initial concentration of pollutant is one of the important factors to determine its extent of degradation under specific experimental conditions. The concentration of BDE-209 was varied from 10 to 100 mg/L while maintaining pH at 2, power density of 420 W, 150 mg/L of H₂O₂ loading and with an iron loading of 0.5 mg/L. The degradation rate hindered from 0.019 min⁻¹ to 0.005 min⁻¹ for an increase in the concentration from 20 to 100 mg/L (Fig. 4.5), demonstrating 20 mg/L to be the optimum value.

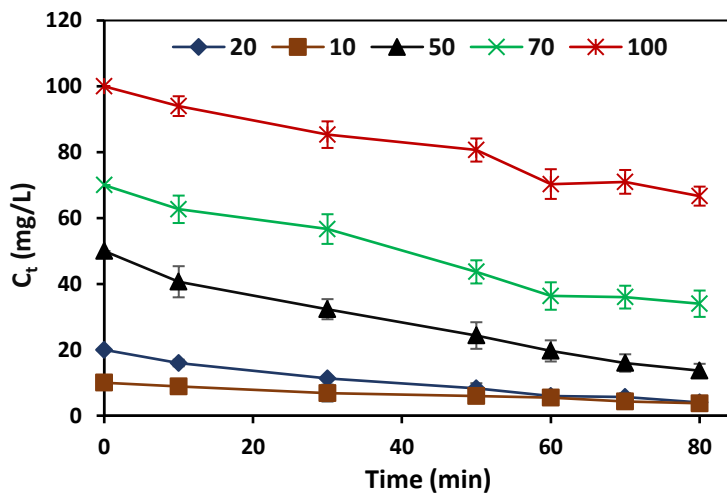


Figure 4.5. Degradation of BDE-209 at different initial concentration: (■) 10, (◆) 20, (▲) 50, (×) 70, (✱) 100 mg/L (Experimental conditions: power density: 420 W; pH: 2; H₂O₂ loading: 150 mg/L; nZVI loading: 0.5 mg/L)

Above the optimum concentration of pollutant, the surface of bubbles is expected to be saturated and hence a decline in the degradation rate was witnessed, whereas at lower concentration a decline in the degradation rate indicates lesser evaporation of pollutant into the bubble-vapor interfacial region (Panda and Manickam, 2017). Also, the decline in degradation rate can be attributed to the inactiveness of nZVI surface for being fully occupied at higher pollutant concentration. Similarly, Khataee et al. (2016) reported the importance of optimum pollutant concentration for US/Fenton removal of Reactive Red 84.

4.3.3 Effect of solution pH on degradation

Experiments were conducted in the pH range of 2-10 at 20 mg/L BDE-209 (initial concentration), while maintaining 150 mg/L of H₂O₂ loading, iron loading of 0.5 mg/L and ultrasonic power density of 420 W. As demonstrated in Fig. 4.6, the degradation rate constant (*k*) increases up to 0.019 min⁻¹ (Table 4.3) with the decrease in pH value, which reached the maximum at pH 2.

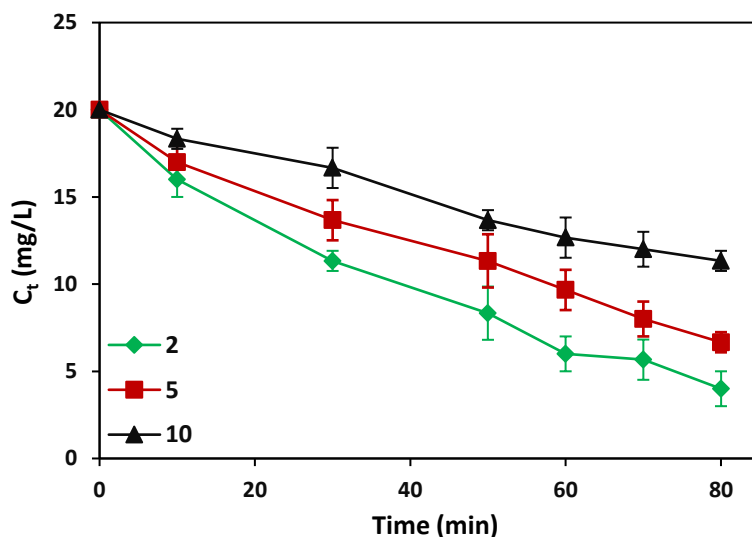


Figure 4.6. Degradation of BDE-209 at various solution pH: (◆) 2, (■) 5, (▲) 10 (Experimental conditions: initial concentration: 20 mg/L; power density: 420 W; H₂O₂ loading: 150 mg/L; nZVI loading: 0.5 mg/L)

The enhancement in degradation under lower pH values could be due to higher amount of ferrous ion production as iron powder is easily dissolved in acid solution and the associated production of

higher amount of hydroxyl radicals as the outcome (Walling, 1975). Also, the higher production of ferrous ion can be attributed to the removal of outer iron oxide layer of nZVI and the subsequent enhanced oxidation of inner Fe⁰ part (Eq. (20)) at low pH.



Due to hydrophobic (log K_{ow}: 6.26) and semi-volatile nature of BDE-209 (Henry's constant: 1.62 x 10⁻⁶ atm m³/mol), it is expected to be present at bubble vapor interfacial region rather than at liquid bulk or bubble core. Also, at acidic pH, the BDE-209 constituents are present in molecular form rather than the ionic form and hence the transport of neutral species of BDE-209 to the interfacial region enhances, leading to faster thermal decomposition. Previous reports suggested that a faster sonolytic degradation of semi-volatile and non-volatile organic pollutants was observed at low pH, due to the increased hydrophobicity of protonated species leading to higher accumulation of molecules at the interfacial region of the cavitation bubble (Wei et al., 2016).

4.3.4 Effect of ultrasonic power density on degradation

As illustrated in Fig. 4.7, the effect of acoustic power on BDE-209 degradation rate was monitored by varying power density between 150 to 450 W, while initial concentration of BDE-209, loading of Fenton's reagent, and pH value were kept constant at optimum values following the previous section.

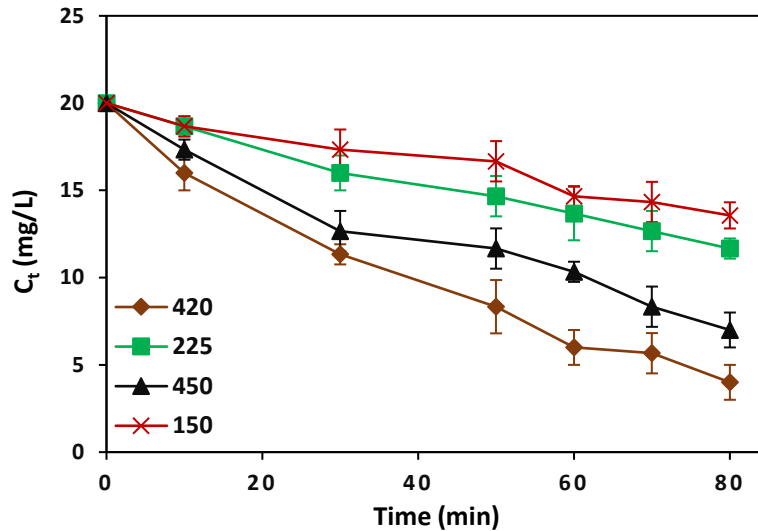


Figure 4.7. BDE-209 degradation at various ultrasound power density: (×) 150 (■) 225 (◆) 420 (▲) 450 W (Experimental conditions: initial concentration: 20 mg/L; pH: 2; H₂O₂ loading: 150 mg/L; nZVI loading: 0.5 mg/L)

The application of ultrasound during US/Fenton process not only creates effective radicals required for the degradation but also continuously cleans the surface of iron powder to avoid the accumulation of pollutants and to promote further surface reactions (Namkung et al., 2008). Also, ultrasonic irradiation results in faster dissolution of iron, resulting in larger surface area and enhanced mass transfer rate of organic pollutants between the liquid phase and the surface of iron powder. The corrosion of metal iron and mixing intensity of solution enhances with the increase in ultrasonic powder density due to the high pressure and turbulence generated during bubble collapse event (Hung et al., 2000). The degradation rate increased with the increase in power density up-to 420 W, beyond which a decline in the degradation rate was observed, which could be attributed to the coalescence of bubbles at higher power levels, leading to lower efficiency of energy transfer into the reaction solution (Bagal and Gogate, 2014).

4.3.5 Effect of Fenton's reagent loading on degradation

Oxidation process that utilizes activation of H₂O₂ by the addition of iron powder is termed as Fenton's oxidation, which was effective in the removal of several pollutants in water. Since,

hydroxyl radicals are being generated by the sonolysis of water, adding iron powder in the presence of hydrogen peroxide in acid solutions produces ferrous ions, which would later react with hydrogen peroxide to generate hydroxyl radicals (Walling, 1975), resulting in the enhancement of the degradation efficiency of pollutant. As the generation of hydroxyl radicals is dependent on hydrogen peroxide and the concentration of iron loading, the optimum value affects the degradation efficiency. To decide the optimum loading of Fenton's reagent, different sets of experiments were conducted for H₂O₂ addition between 50 to 200 mg/L and iron powder addition between 0.5 to 2 mg/L. Figs. 4.8 and 4.9 illustrate the effect of H₂O₂ and iron loading on the degradation of BDE-209 respectively.

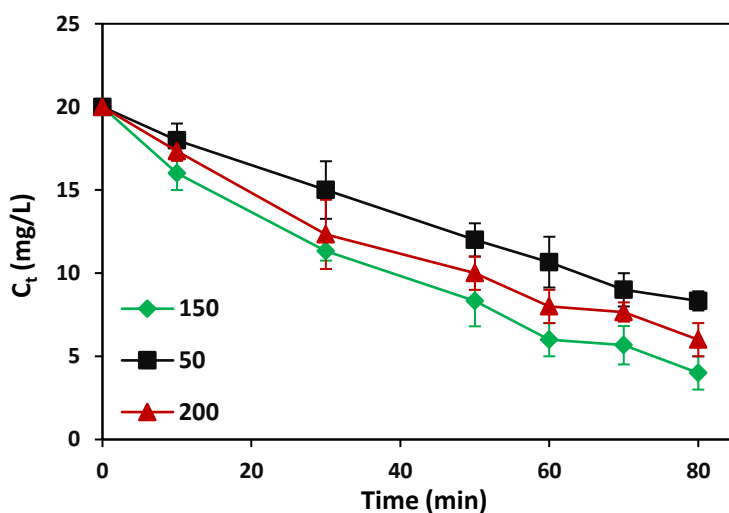


Figure 4.8. BDE-209 degradation at various H₂O₂ loading: (■) 50, (◆) 150, (▲) 200 mg/L (Experimental conditions: initial concentration: 20 mg/L; power density: 420 W; pH: 2; nZVI loading: 0.5 mg/L)

It could be seen that the degradation rate constant increased up-to a loading of 150 mg/L H₂O₂ and an iron loading of 1 mg/L beyond which the rate declines (Table 4.3), which could be attributed to the production of larger number of ferrous ions that act as hydroxyl radical scavenger.

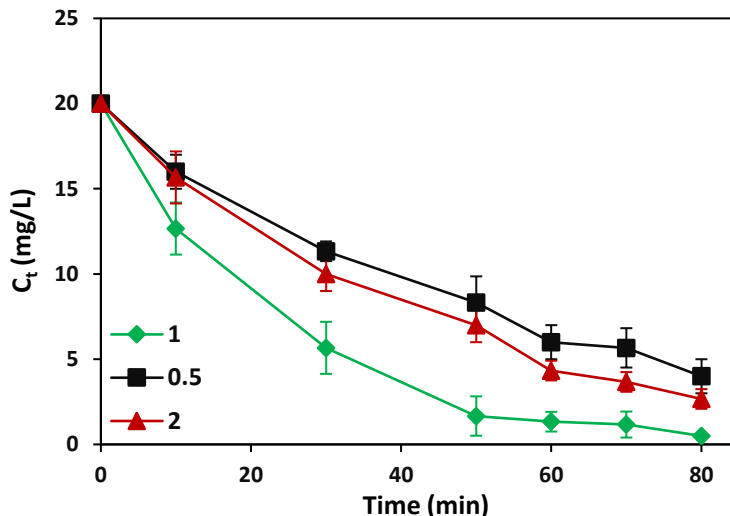


Figure 4.9. BDE-209 degradation percentage at various nZVI loading: (■) 0.5 (◆) 1 (▲) 2 mg/L (Experimental conditions: initial concentration: 20 mg/L; power density: 420 W; pH: 2; H₂O₂ loading: 150 mg/L)

Addition of either nZVI or H₂O₂ beyond the optimum loading could result in the scavenging of •OH radicals and the formation of perhydroxyl radical (HOO•), resulting in a rapid interaction among HO₂ radicals to generate H₂O₂ and thereby reducing the presence of oxidative radicals.

Table 4.3. Pseudo-first-order rate constants for the degradation of BDE-209 under different operational parameters

Parameter		k (min ⁻¹)	R ²
BDE-209 concentration (mg/L)	10	0.012	0.98
	20	0.019	0.99
	50	0.016	0.99
	70	0.010	0.97
	100	0.005	0.97
pH	2	0.019	0.99
	5	0.013	0.98
	10	0.007	0.99
Power density (W)	150	0.005	0.97
	225	0.006	0.99
	420	0.019	0.99
	450	0.012	0.97
H ₂ O ₂ loading (mg/L)	50	0.011	0.99
	150	0.019	0.99
	200	0.015	0.99

nZVI loading (mg/L)	0.5	0.019	0.99
	1	0.045	0.98
	2	0.025	0.99

4.4 Control experiments

Control experiments in the presence of nZVI only, H₂O₂ only and US/nZVI were performed to verify their effect on BDE-209 degradation. While only marginal degradation was observed during the addition of H₂O₂ alone, a 18 % degradation was witnessed for nZVI, which indicates the recalcitrant nature of BDE-209 precursor compounds towards oxidation at the early stage of degradation. The combination of US/nZVI has resulted in 64 % degradation (Table 4.5) within 80 min of treatment under optimum parameters.

To compare the extent of Ferrous ion generation during Fenton only and the combined US/Fenton after 60 min, evaluations were performed for the pH range of 2-10, while maintaining H₂O₂ loading of 150 mg/L and ultrasonic power density of 420 W. The concentration of Fe²⁺ in the aqueous solution was highest at pH 2, which indirectly indicates that the iron oxide shell was fully dissolved and Fe⁰ was oxidized. It is assumed that the degradation of BDE-209 during the combined US/Fenton treatment, would initiate via thermal decomposition at the bubble-vapor interfacial region with simultaneous reduction at nZVI surface, following oxidative degradation at later stage. To obtain information regarding the reaction zones, sodium bicarbonate was chosen which is a free radical scavenger for the bulk phase solution. Different sets of experiments were conducted for the loading of sodium bicarbonate i.e. 1 g/L, 3 g/L and 5 g/L, while maintaining all other optimum parameters. The extent of degradation decreased up to 27 % (Table 4.4) in the presence of bicarbonate ions for 5 g/L loading, indicating simultaneous radical driven reaction in the bulk phase during combined US/Fenton process, which could be attributed to the oxidation of lower

brominated congeners. Fig. 4.10. demonstrates the effect of radical scavenger on BDE-209 degradation.

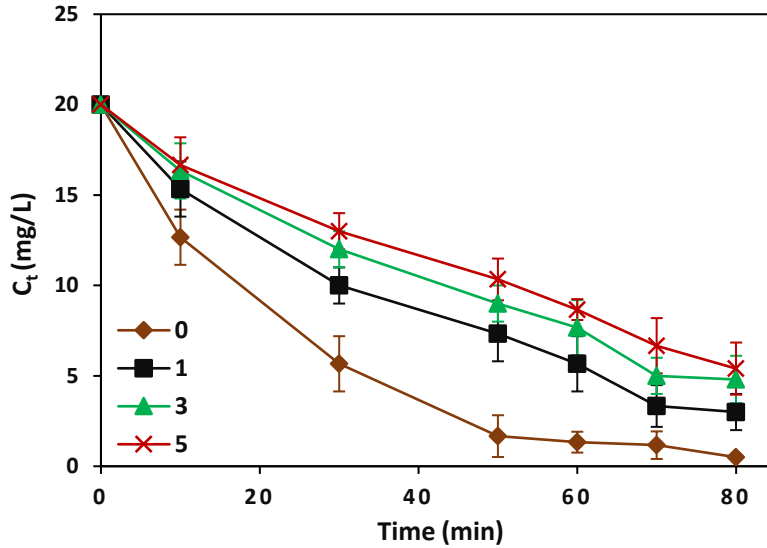


Figure 4.10. Degradation of BDE-209 at various loadings of sodium bicarbonate: (◆) 0, (■) 1, (▲) 3, (×) 5 g/L (Experimental conditions: initial concentration: 20 mg/L; power density: 420 W; pH: 2; H₂O₂ loading: 150 mg/L, nZVI loading: 1 g/L)

Table 4.4. Effect of addition of radical scavenger on the extent of degradation and kinetic rate constants

Sodium bicarbonate loading (g/L)	Extent of degradation (%)	Rate constant k (min ⁻¹)	R ²
0	100	0.045	0.98
1	85	0.023	0.98
3	76	0.018	0.98
5	73	0.016	0.98

4.5 Comparison of degradation efficiency with different processes

The synergistic effect of combined US/Fenton treatment on the degradation of BDE-209 was calculated considering the rate constants obtained from the individual treatment methods of US and Fenton along with overall US/Fenton. The synergy index (*f*) of the coupled method was calculated by the following Eq. (21) (Panda and Manickam, 2017).

$$\text{Synergy index } (f) = \frac{k_{(US+Fenton)}}{k_{(US)}+k_{(Fenton)}+k_{(nZVI+US)}} = \frac{0.045}{0.007+0.004+0.012} = 1.96 \quad (21)$$

Where $k_{(US)}$, $k_{(Fenton)}$, and $k_{(US+Fenton)}$ are the reaction rate constants of US, Fenton and US/Fenton respectively.

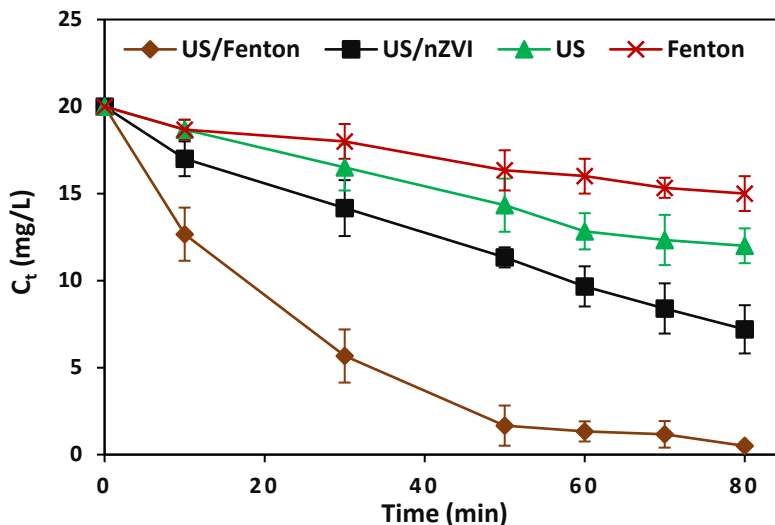


Figure 4.11. The (◆) US/Fenton, (■) US/nZVI, (▲) US and (×) Fenton processes of BDE-209 degradation

During the combined process (US/Fenton), the degradation rate constant ($k = 0.045 \text{ min}^{-1}$) of BDE-209 was found to be higher than the sum of the rate constants of individual processes. Table 4.5 provides comparison among individual treatments with respect to the synergistic effect.

Table 4.5. Comparison of the combined process of US/Fenton with individual process (US and Fenton)

Initial concentration of BDE-209: 20 mg/L; pH: 2; ultrasound power density: 420 W; nZVI loading: 1 mg/L; H ₂ O ₂ loading: 150 mg/L				
System	Extent of degradation (%)	Rate constant, k (min ⁻¹)	R ²	Synergistic index (f)
Only Fenton	25	0.004	0.98	-
Only US	40	0.007	0.99	-
US/nZVI	64	0.012	0.99	-
US/Fenton	100	0.045	0.98	1.96

The results indicated a very high synergistic effect ($f \sim 1.96$) during the US/Fenton treatment of BDE-209 at optimum conditions, which could be attributed to the simultaneous effect of ultrasound and Fenton's reagent for both pyrolytic as well as oxidative degradation of pollutants.

4.6 Conclusions

The combined US/Fenton treatment demonstrated a complete transformation of BDE-209 into lower brominated congeners and oxidative products, which was proposed to follow a two-stage transformation mechanism. The results indicated the appearance of debrominated congeners during US and Fenton's treatment alone, whereas the appearance of lower brominated congeners along with oxidative products during combined US/Fenton process, clarifies the role of both US and Fenton reagent for the enhancement in degradation process. The complete transformation of BDE-209 within 80 min of treatment, illustrates the importance of acidic solution pH, optimum ultrasonic power density along with an optimum loading of Fenton's reagent.

4.7 References

- US EPA, 2014. Technical fact sheet – polybrominated diphenyl ethers (PBDEs) and polybrominated biphenyls (PBBs), 1–5.
- Chen, D., Mai, B., Song, J., Sun, Q., Luo, Y., Luo, X., Zeng, E. Y., Hale, R. C., 2007. Polybrominated diphenyl ethers in birds of prey from northern china, *Environ. Sci. Technol.* 41, 1828–1833.
- Hites, R. A., 2004. Polybrominated diphenyle ethers in the environment and in people: a meta-analysis of concentrations, *Environ. Sci. Technol.* 38, 945–956.
- US EPA, 2013. Contaminants of emerging concern (CECs) in fish: polybrominated diphenyl ethers (PBDEs), Office of Water.
- Darnerud, P. O., Eriksen, G. S., Jóhannesson, T., Larsen, P. B., Viluksela, M., 2001. Polybrominated diphenyl ethers: occurrence, dietary exposure, and toxicology, *Environ. Health Perspect.* 109, 49–68.
- Alaee, M., Arias, P., Sjodin, A., Bergman, A., 2003. An overview of commercially used brominated flame retardants, their applications, their use patterns in different countries/regions and possible modes of release, *Environ. Int.* 29, 683–689.
- Peng, X., Tang, C., Yu, Y., Tan, J., Huang, Q., Wu, J., Chen, S., Mai, B., 2009. Concentrations, transport, fate, and releases of polybrominated diphenyl ethers in sewage treatment plants in the pearl river delta, South China, *Environ. Int.* 35, 303–309.
- Andersson, P. L., Oberg, K., Örn, U., 2006. Chemical characterization of brominated flame retardants and identification of structurally representative compounds, *Environ Toxicol Chem.* 25, 1275–1282.
- ATSDR, 2004. Public health statement for polybrominated diphenyl ethers (PBDEs).

- Shih, Y. H., Chou, H. L., Peng, Y. H., Chang, C. Y., 2012. Synergistic effect of microscale zerovalent iron particles combined with anaerobic sludges on the degradation of decabromodiphenyl ether, *Bioresour. Technol.* 108, 14–20.
- Zhou, J., Jiang, W., Ding, J., Zhang, X., Gao, S., 2007. Effect of tween 80 and β -cyclodextrin on degradation of decabromodiphenyl ether (BDE-209) by white rot fungi, *Chemosphere* 70, 172–177.
- Chou, H. L., Chang, Y. T., Liao, Y. F., Lin, C. H., 2013. Biodegradation of decabromodiphenyl ether (BDE-209) by bacterial mixed cultures in a soil/water system, *Int. Biodeterior. Biodegrad.* 85, 671–682.
- Gerecke, A. C., Hartmann, P. C., Heeb, N. V., Kohler, H. P. E., Giger, W., Schmid, P., Zennegg, M., Kohler, M., 2005. Anaerobic degradation of decabromodiphenyl ether, *Environ. Sci. Technol.* 39, 1078–1083.
- An, T., Chen, J., Li, G., Ding, X., Sheng, G., Fu, J., Mai, B., O’Shea, K. E., 2008. Characterization and the photocatalytic activity of TiO₂ immobilized hydrophobic montmorillonite photocatalysts: degradation of decabromodiphenyl ether (BDE 209), *Catal. Today* 139, 69–76.
- Stapleton, H. M., Dodder, N. G., 2008. Photodegradation of decabromodiphenyl ether in house dust by natural sunlight, *Environ. Toxicol. Chem.* 27, 306–312.
- Christiansson, A., Eriksson, J., Teclechiel, D., Bergman, Å., 2009. Identification and quantification of products formed via photolysis of decabromodiphenyl ether, *Environ. Sci. Pollut. Res.* 16, 312–321.
- Kidak, R., Ince, N., 2006. Ultrasonic destruction of phenol and substituted phenols: a review of current research, *Ultrason. Sonochem.* 13, 195–199.

- Sivasankar, T., Moholkar, V. S., 2009. Physical insights into the sonochemical degradation of recalcitrant organic pollutants with cavitation bubble dynamics, *Ultrason. Sonochem.* 16, 769–781.
- Panda, D., Manickam, S., 2017. Recent advancements in the sonophotocatalysis (SPC) and doped-sonophotocatalysis (DSPC) for the treatment of recalcitrant hazardous organic water pollutants, *Ultrason. Sonochem.* 36, 481–496.
- Bagal, M. V., Gogate, P. R., 2014. Wastewater treatment using hybrid treatment schemes based on cavitation and Fenton chemistry: a review, *Ultrason. Sonochem.* 21, 1–14.
- Patil, P. N., Gogate, P. R., 2015. Degradation of dichlorvos using hybrid advanced oxidation processes based on ultrasound, *J. Water Process Eng.* 8, e58–e65.
- Jawale, R. H., Gogate, P. R., 2018. Combined treatment approaches based on ultrasound for removal of triazophos from wastewater, *Ultrason. Sonochem.* 40, 89–96.
- Lin, S.H., Lo, C.C., 1997. Fenton process for treatment of desizing wastewater, *Water Res.* 31, 2050–2056.
- ElShafei, G. M. S., Yehia, F. Z., Eshaq, G., ElMetwally, A. E., 2017. Enhanced degradation of nonylphenol at neutral pH by ultrasonic assisted heterogeneous fenton using nano zero valent metals, *Sep. Purif. Technol.* 178, 122–129.
- Bremner, D. H., Burgess, A. E., Houllé, D., Namkung, K. C., 2006. Phenol degradation using hydroxyl radicals generated from zero-valent iron and hydrogen peroxide, *Appl. Catal. B: Environ.* 63, 15–19.
- Koda, S., Kimura, T., Kondo, T., Mitome, H., 2003. A standard method to calibrate sonochemical efficiency of an individual reaction system, *Ultrason. Sonochem.* 10, 149–156.

- Shi, J., Qu, R., Feng, M., Wang, X., Wang, L., Yang, S., Wang, Z., 2015. Oxidative degradation of decabromodiphenyl ether (BDE 209) by potassium permanganate: reaction pathways, kinetics, and mechanisms assisted by density functional theory calculations, *Environ. Sci. Technol.* 49, 4209–4217.
- Xu, J., Tan, L., Baig, S.A., Wu, D., Lv, X., Xu, X., 2013. Dechlorination of 2,4-dichlorophenol by nanoscale magnetic Pd/Fe particles: effects of pH, temperature, common dissolved ions and humic acid, *Chem. Eng. J.* 231, 26–35.
- Xu, L., Wang, J., 2011. A heterogeneous fenton-like system with nanoparticulate zero-valent iron for removal of 4-chloro-3-methyl phenol, *J. Hazard. Mater.* 186, 256–264.
- Luo, S., Yang, S., Xue, Y., Liang, F., Sun, C., 2011. Two-stage reduction/subsequent oxidation treatment of 2,2',4,4'-tetrabromodiphenyl ether in aqueous solutions: kinetic, pathway and toxicity, *J. Hazard. Mater.* 192, 1795–1803.
- Monserrate, E., Haggblom, M. M., 1997. Dehalogenation and biodegradation of brominated phenols and benzoic acids under iron-reducing, sulfidogenic, and methanogenic conditions, *Appl. Environ. Microbiol.* 63, 3911–3915.
- Lin, Z. R., Ma, X. H., Zhao, L., Dong, Y. H., 2014. Kinetics and products of PCB28 degradation through a goethite-catalyzed fenton-like reaction, *Chemosphere.* 101, 15–20.
- Khataee, A., Gholami, P., Vahid, B., 2016. Heterogeneous sono-fenton-like process using nanostructured pyrite prepared by Ar glow discharge plasma for treatment of a textile dye, *Ultrason. Sonochem.* 29, 213–225.
- Walling, C., 1975. Fenton's reagent revisited, *Accounts Chem. Res.* 8, 125–131.
- Wei, Z., Spinney, R., Ke, R., Yang, Z., Xiao, R., 2016. Effect of pH on the sonochemical degradation of organic pollutants, *Environ. Chem. Lett.* 14, 163–182.

Namkung, K. C., Burgess, A. E., Bremner, D. H., Staines, H., 2008. Advanced Fenton processing of aqueous phenol solutions: a continuous system study including sonication effects, *Ultrason. Sonochem.* 15, 171–176.

Hung, H. M., Ling, F. H., Hoffmann, M.R., 2000. Kinetics and mechanism of the enhanced reductive degradation of nitrobenzene by elemental iron in the presence of ultrasound, *Environ. Sci. Technol.* 34, 1758–1763.

Chapter 5

Sonolytic mineralization of Hexabromocyclododecane: kinetics and influencing factors

Abstract

Hexabromocyclododecane (HBCD), a brominated flame retardant, is under the list of Stockholm convention of persistent organic pollutants of concern. The sonochemical degradation of HBCD in aqueous media has been investigated using a 20-kHz probe type sonicator with power inputs from 150 to 450 W. The degradation rate was determined as a function of concentration of HBCD, bulk phase temperature, pH, ultrasonic power density and the addition of H₂O₂. At optimum operating conditions, the degradation rate constant (k) was determined to be 0.118 min⁻¹. High performance liquid chromatography was employed for the quantification of parent compound, which indicated the complete disappearance of HBCD within 40 min of sonochemical treatment. Gas chromatography mass spectroscopy analysis was performed for the identification of transformed products. Total organic carbon (TOC) analysis demonstrated a removal of 72 % TOC, indicating mineralization of HBCD. The obtained results suggested the degradation of HBCD to follow thermal decomposition at the bubble-vapor interface as the dominant pathway along with free radical attack and recombination of short chain intermediates as successive steps of transformation. A *Daphnia magna* bioassay was performed to evaluate the ecotoxicity of HBCD and its transformed products. Overall, the outcomes of this study clearly demonstrate that HBCD can be effectively removed by sonochemical treatment.

5.1 Introduction

Hexabromocyclododecane (HBCD), widely used as a flame retardant has been listed under the Stockholm Convention (2013), as a persistent organic pollutant. HBCD has been used in the coating of textiles, in high-impact polystyrene (PS) for electrical equipment along with PS based consumer products, as an additive of expanded and extruded polystyrene foams (Covaci et al., 2006; Marvin et al., 2011) and as flame retardant. Currently, HBCD is regarded as the third highest brominated flame retardant used after tetrabromobisphenol-A and decabromodiphenyl ether (Alaee et al., 2003). Considering the wider usage, the principal release of HBCD to the environment might result from numerous routes such as emissions during production, leaching from consumer goods or by disposal (Marvin et al., 2011; Arnot et al., 2009). The higher bioaccumulation potential, environmental persistency and the toxic effects of HBCD on humans, wildlife as well as on aquaculture livestock have marked it as a ubiquitous contaminant (Ronisz et al., 2004). The screening level risk assessments conducted by United Nations Environment Program and Stockholm Convention acknowledged its persistence, bioaccumulative and toxic nature (Marvin et al., 2011; Birnbaum and Staskal, 2004).

Due to severe health impacts and worldwide presence of HBCD, the employment of an effective wastewater treatment technique is of significance for its elimination. Even though biodegradation (Davis et al., 2006) and degradation by autochthonous microflora (Stiborova et al., 2015) have been reported to be successful in the removal of HBCD, but the requirement of comparatively longer duration of treatment is a major drawback. Faster degradation of HBCD by zero valent iron (Tso and Shih, 2014) and mechanochemical treatment (Zhang et al., 2014) have also been reported, but mineralization has not been achieved yet. Photodegradation demonstrated a HBCD removal of 54.8 % within 80 min of treatment (Zhou et al., 2014), indicating the incompetence of photolysis

based advanced oxidation process as well. On this context, in our investigation, the proposed sonochemical treatment provides advantages over the previously employed techniques that include faster and effective removal of HBCD with efficient utilization of energy. Several investigations on sonochemical degradation of recalcitrant organic pollutants such as DDT, diclofenac etc. indicated the competence of sonolysis in achieving a successful removal (Thangavadivel et al., 2009; Chowdhury and Viraraghavan, 2009; Naddeo et al., 2010).

In the present work, the sonochemical treatment of HBCD has been performed to investigate the degradation pathways and the extent of mineralization. High performance liquid chromatography (HPLC) and Gas chromatography-mass spectrometry (GC-MS) have been employed to monitor the concentration of parent compound and to identify the transformed products, respectively. The quantification of parent compound was performed considering an external calibration curve with respect to HPLC data. Total organic carbon (TOC) analysis has been performed to illustrate the extent of HBCD mineralization. In addition, the toxicity of HBCD and its products generated during the sonochemical treatment were assessed. We believe that this is the first reported investigation on the sonochemical treatment of HBCD for its successful removal.

5.2 EXPERIMENTAL

5.2.1 Materials

Hexabromocyclododecane (HBCD, $C_{12}H_{18}Br_6$, 99%), n-hexadecane (99%, employed for extraction and injection solvent for gas chromatography), acetonitrile (HPLC grade, $\geq 99.9\%$), methanol (HPLC grade, $\geq 99.9\%$), Potassium hydrogen phthalate ($>99\%$) and Hydrogen peroxide (H_2O_2 , 30%) were purchased from Sigma Aldrich (Malaysia). All aqueous solutions were prepared with high purity water (Milli-Q water). Agilent nylon syringe filter of $0.45\ \mu m$ pore size and 5 ml syringes were purchased from IT Tech Research (M) Sdn. Bhd. (Malaysia).

5.2.2 Sonochemical experiments

For sonication, a co-solvent approach of using methanol along with water was adopted because of low aqueous solubility of HBCD. Extraction of the sonicated samples by n-hexane was performed before GC-MS analysis due to the limitation of analytical instrument. HBCD solutions were prepared by dissolving 50 mg of HBCD in 100 ml methanol followed by the addition of ultrapure water to achieve a final solution concentration of 160 to 270 μM . Sonochemical treatment was performed in a 100-mL reactor using a 20 kHz ultrasonic probe (Cole-Parmer Instruments, Illinois, USA) and the applied ultrasonic power range was varied between 150 to 450 W. The temperature of reaction mixture was maintained between 15 to 40 $^{\circ}\text{C}$ using a chiller. Sonication was performed in the pH range of 3 to 14. Sonochemical treatment was conducted for 60 min and aliquots were withdrawn at every 10 min interval for HPLC, GC-MS and TOC analysis. The treated solutions were neutralized with 2N NaOH (Merck) for toxicity assays. Each experiment was repeated three times and standard deviation of the triplicate experiments were included in the corresponding figure.

5.3 Chemical analysis

5.3.1 HPLC analysis

The analysis of HBCD was performed using an Agilent HPLC system equipped with an online degasser, quaternary LC pump (Agilent infinity model 1260), an Agilent infinity 1260 VWD UV detector for the separation on a CORTECSTM C18 column (4.6 mm \times 100 mm, 2.7 μm). The HBCD elution was carried out at a column temperature of 25 $^{\circ}\text{C}$ using an isocratic gradient composed of solvent A (acetonitrile) and solvent B (water) in 80:20 ratio and the detection was carried out at a wavelength of 215 nm. The injection volume and flow rate were 20 μL and 1 ml/min respectively. The retention time of HBCD was 4 min. The Agilent ChemStation software

was used for instrument control, data acquisition, and data analysis. Calibration curves were constructed at five concentration levels and analyzed in triplicate.

5.3.2 GC-MS analysis

The transformed products of HBCD were determined qualitatively using GC-MS equipped with a PerkinElmer Elite 5-MS capillary column (length: 30 m, I.D: 0.25 mm, Film thickness: 0.25 μ m). The injector temperature was at 250 °C and the flow rate was 1.0 mL/min. The oven temperature was at 150 °C for 0.5 min, which was then increased at 15 °C/min to 300 °C, and then sustained at this temperature for 5 min. The detector temperature was at 345 °C and the GC interface along with ion source temperatures were at 250 °C. Total run time was 15 min and HBCD retention time was 13.18 min.

5.3.3 Mineralization study

To determine the extent of HBCD mineralization, the decay in total organic carbon content was monitored using a TOC analyzer (Shimadzu TOC 5050A) equipped with an ASI5000 autosampler. Prior to analysis, all liquid samples, including blanks and standards were acidified to pH 2 using hydrochloric acid and instrument calibration was performed using potassium hydrogen phthalate standards. The inorganic carbon was removed by sparging the samples with air.

5.3.4 Ecotoxicity assessment

Toxicity measurements were performed using Daphtoxkit FTM magna toxicity test for samples collected at regular intervals during the treatment. This test is based on the observation of the *Daphnia magna* immobilization after 24 hours of exposure to the untreated and treated samples. Toxicity analysis was conducted according to the ISO 6341 (1996) standard protocol.

5.4 Results and discussion

In the present investigation, HPLC chromatogram (Fig. 5.1) indicated a gradual decrease in the concentration of HBCD and a complete disappearance of the parent compound within 40 min of treatment time.

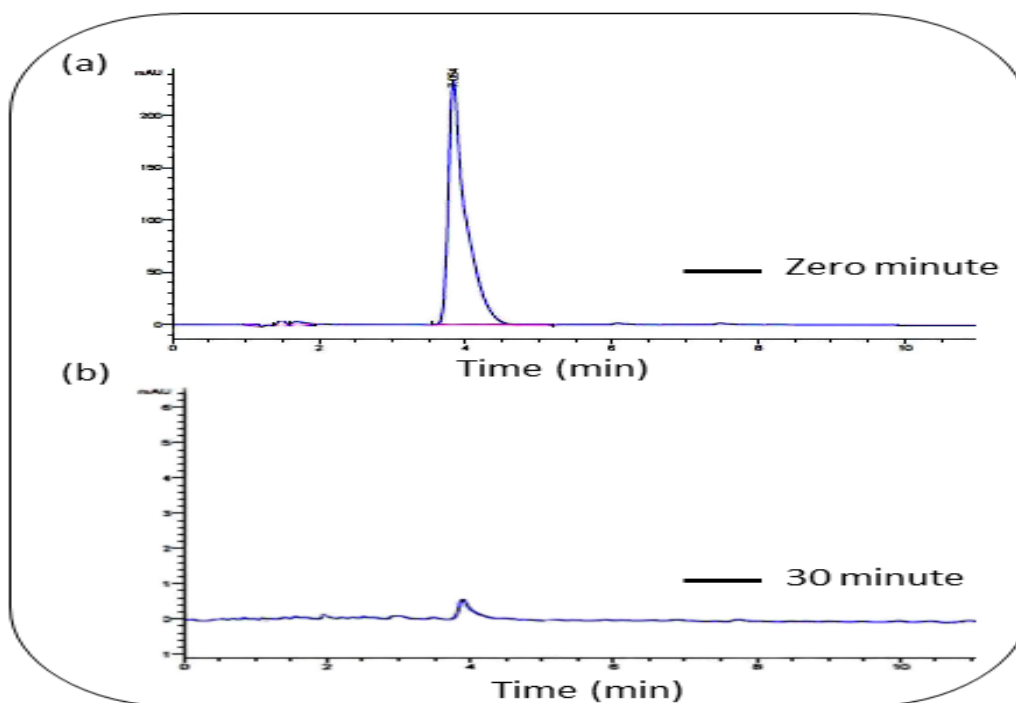


Figure 5.1. HPLC chromatograph of HBCD at (a) 0 min (b) 30 min of treatment

Eight transformed products of HBCD have been detected during GC-MS analysis (Table 1). 2-(1-Bromo-2-ethoxy-p-methoxy-phenethyl)-3-phenyl-quinazolin-4(3H)-one ($C_{25}H_{23}BrN_2O_3$), 1,2-Bromooctadecanal ($C_{18}H_{35}BrO$), I-Leucine, N-(2-bromobenzoyl)-decyl ester ($C_{23}H_{36}BrNO_3$), 11,13-Dimethyl-12-tetradecen-1-ol acetate ($C_{18}H_{34}O_2$), 12-methyl-E,E-2,13-octadecadien-1-ol ($C_{19}H_{36}O$), 13-heptadecyn-1-ol ($C_{17}H_{32}O$), 2-Hexadecanol ($C_{16}H_{34}O$), Z,Z-2,5-Pentadecadien-1-ol ($C_{15}H_{28}O$) were identified after 10 min of sonication (Fig. 5.2).

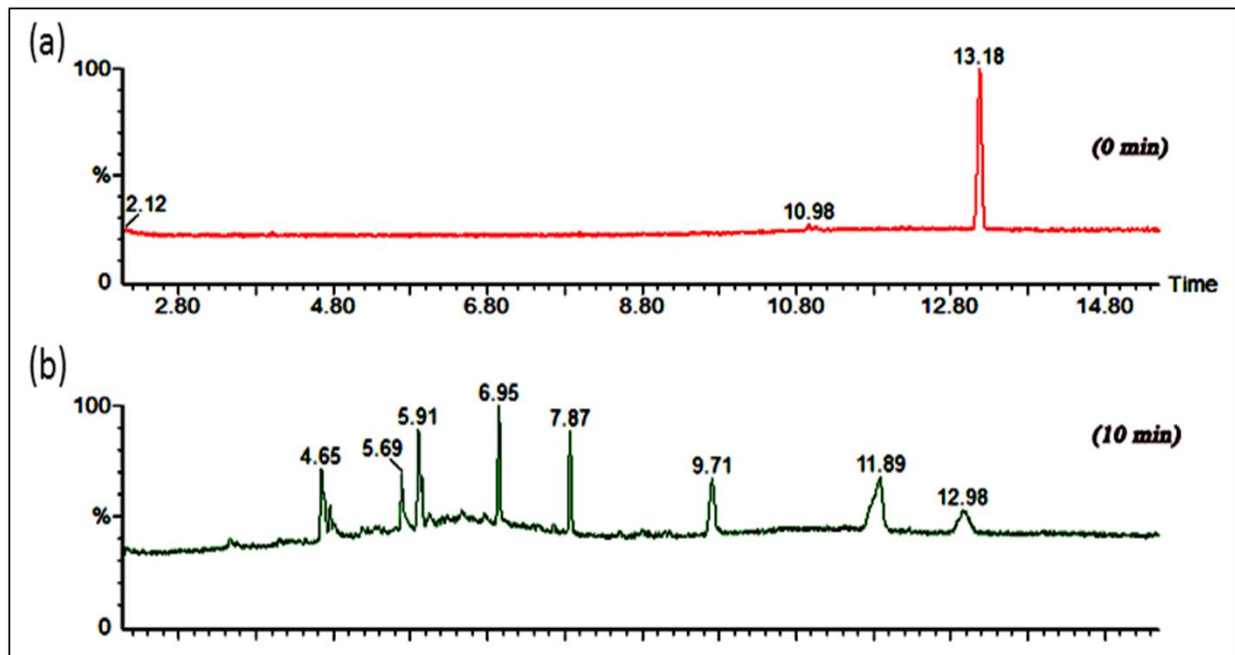


Figure 5.2. Chromatographic representation of (a) HBCD standard (b) transformed products

However, additional transformed products having lower molecular weight and/or vapor pressure compared to n-hexane may be present because of their coelution with the extraction solvent and due to low solubility in n-hexane to be extracted for GC-MS analysis. Also, poor ionization of numerous degradants during mass spectroscopy analysis can be attributed to the presence of additional undetected products. Table 5.1 indicates the estimated water solubility, Log P, retention time and molecular weight of the identified transformed products, justifying the detection of only hydrophobic products. The identified transformed products of HBCD during GC-MS analysis and the possible reaction pathways are represented in Fig. 5.3.

Table 5.1. GC-MS retention time and spectral characteristics of HBCD transformed products

Compound	Molecular weight	Retention time (min)	Similarity (%)	Solubility (25 °C) (mg/L)	Log P
C ₁₅ H ₂₈ O	224	4.65	81	1.146	5.65
C ₁₆ H ₃₄ O	242	5.69	78	0.1727	6.87
C ₁₇ H ₃₂ O	252	5.91	82	0.2046	6.47
C ₁₉ H ₃₆ O	280	6.95	80	0.01357	7.38
C ₁₈ H ₃₄ O ₂	282	7.20	78	0.006017	7.01
C ₁₈ H ₃₅ BrO	347	9.71	83	0.00102	8.42
C ₂₃ H ₃₆ BrNO ₃	453	11.89	84	-	-
C ₂₅ H ₂₃ BrN ₂ O ₃	478	12.98	86	-	-

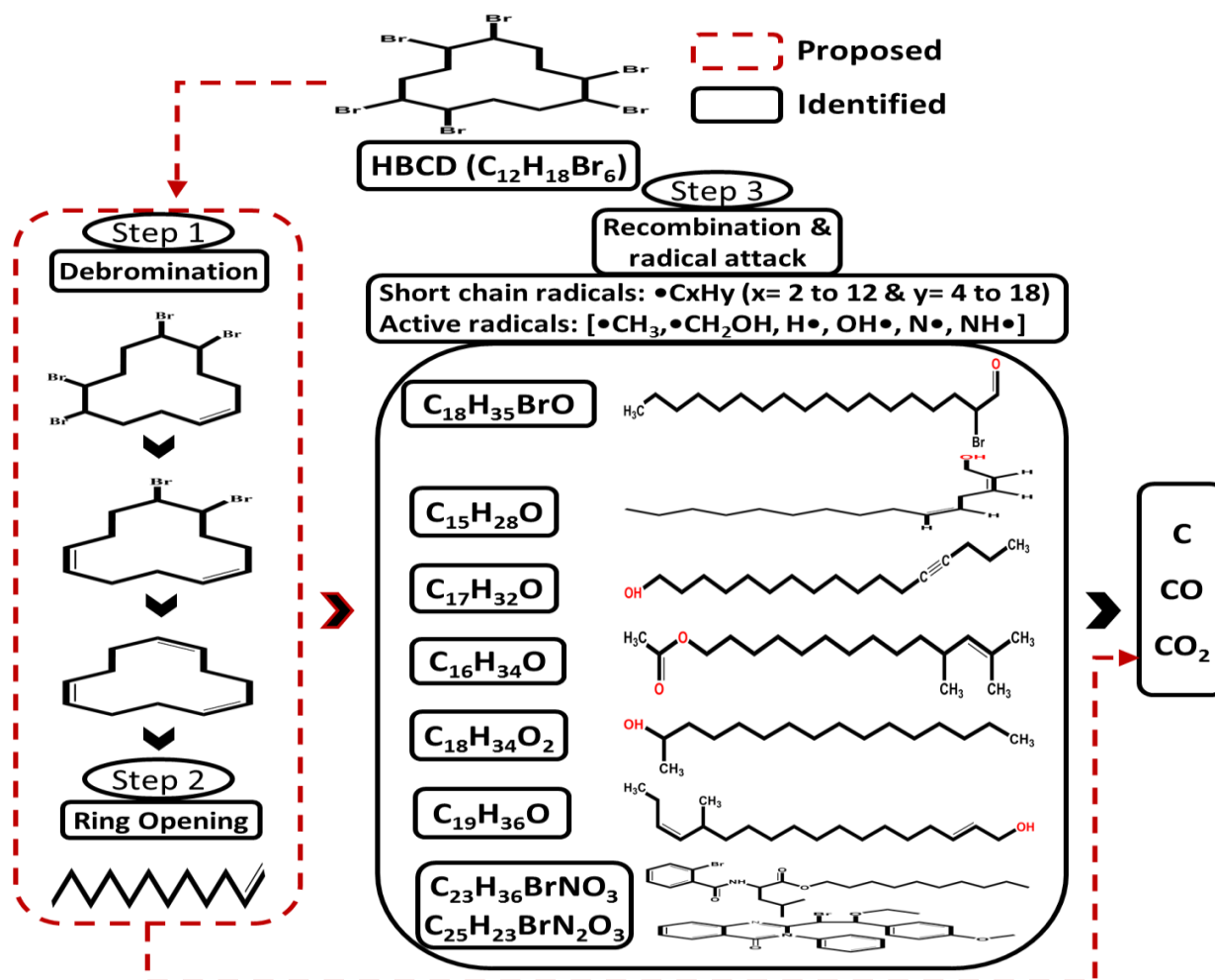


Figure 5.3. Proposed transformation of HBCD during sonolysis. Dashed line represents the proposed pathways, whereas the solid line represents the identified products during GC-MS analysis

The transformation of HBCD under ultrasonication is proposed to follow a three-step mechanism that includes: (1) the pyrolytic cleavage/thermal decomposition of vicinal bromine; (2) formation of ring opening products followed by the formation of short chain intermediates at the bubble-vapor interfacial region where the pressure gradients and temperatures are still high enough to induce thermal effects; (3) recombination of short chain radicals ($\bullet\text{C}_x\text{H}_y$: x = No of carbon atoms, y = No of hydrogen atoms) along with the attack of numerous radicals ($\text{H}\bullet$, $\bullet\text{OH}$, $\bullet\text{CH}_3$) at the interfacial region and at the bulk liquid medium. Thermal decomposition of HBCD is proposed to follow respective bond dissociation energy order (Table 5.2) for bond cleavage. Since the vapor pressure of HBCD is 4.7×10^{-7} mm Hg (Table 5.3), it falls under the category of gas/particulate mixture (EPA, 2014) and thus the transport of larger amount of HBCD into the bubble-liquid interfacial region is expected in comparison to its presence at bulk liquid phase during the cavitation event.

Table 5.2. Individual chemical bonds of HBCD and their corresponding bond dissociation energies

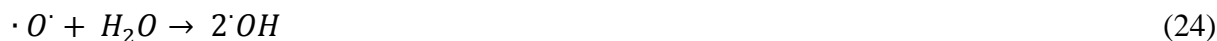
Bond	Bond dissociation energy (kJ/mol)
C-Br	280
C-H	337.2
C-C	607

Table 5.3. Properties of HBCD

Compound	MW	V	Log K_{ow}	V_p	W_s	HLC	pKa
HBCD	641.7	6×10^{-5}	5.625	4.7×10^{-7}	3.4	1.167×10^{-4}	Not expected to dissociate under normal environmental conditions

*MW: molecular weight, g/mol; V: volatility, Pa (21°C); Log K_{ow} : octanol-water partition coefficient
 V_p : vapor pressure, mmHg (20°C); W_s : water solubility, $\mu\text{g/L}$ (25°C);
HLC: Henry's law constant, $\text{atm}\cdot\text{m}^3/\text{mol}$; pKa: dissociation constant*

Volatility of pollutants plays a vital role in deciding the predominant cavitation degradation region. Sivasankar and Moholkar (2009) reported the degradation of phenol, chlorobenzene, nitrobenzene, p-nitrophenol and 2,4-dichlorophenol based on their water solubility and volatility. Reported results suggested that phenol is not expected to evaporate into the bubble due to its nonvolatile nature and hence the degradation mechanism of phenol is expected to follow hydroxylation, whereas chlorobenzene is expected to evaporate into the bubble and undergo pyrolytic decomposition due to its volatile and hydrophobic nature. But semi-volatile (Table 5.3) and hydrophobic pollutants such as HBCD are expected to follow bubble-liquid interfacial region as the predominant region of degradation with mixed probability of thermal decomposition and free radical attack. Sonolysis is known to generate hydroxyl radicals following the dissociation of water molecules (Eqn.22) and numerous reactive radical species (Yao et al., 2010) due to the sonolytic cleavage of dissolved oxygen and nitrogen in the solution (Eqns. 23-25).



As proposed in Fig. 5.3, the preliminary degradation of HBCD could have resulted in the formation of partially debrominated intermediates and completely debrominated products at the bubble-vapor interfacial region via cleavage of vicinal bromine. The second stage of degradation is proposed to form HBCD ring opening products via thermal decomposition of aromatic ring, following simultaneous radical attack to generate numerous recombined transformed products such as $C_{18}H_{35}BrO$, $C_{18}H_{34}O_2$, $C_{19}H_{36}O$, $C_{17}H_{32}O$, $C_{16}H_{34}O$, $C_{15}H_{28}O$ either in the bubble interfacial region or in the bulk liquid phase with the formation of C, CO and CO_2 as end products.

Products such as $C_{25}H_{23}BrN_2O_3$ and $C_{23}H_{36}BrNO_3$ indicate the active role of N_2 and radical attack on the degraded products of HBCD. Addition of additives such as methanol other than H_2O_2 or Fenton's reagent has been reported to enhance the degradation of pollutants significantly as methanol generates $\bullet CH_3$, $\bullet CH_2OH$ and $\bullet OH$ radicals (Neta et al., 1996; Gonzalez et al., 2007), which has been assumed to play a similar role in HBCD degradation in our study. A higher rate of Rhodamine 6G degradation has also been reported with the addition of methanol (Bokhale et al., 2014). The thermolysis of methanol can generate the following species (Eqns. 26,27).



Alegria et al. (1989) reported the formation of several carbon centered radicals ($\bullet C$, $\bullet CH$, $\bullet CH_2$) during the sonolysis of surfactants such as dodecyl sulfate, dodecyltrimethylammonium bromide, n-octyl- β -D-glucopyranoside (OGP). Tauber et al. (1999) reported the formation of t-butanol-derived radicals, following subsequent recombination to form 2,5-dimethylhexane-2,5-diol as the transformed product during sonolysis of anoxic aqueous solutions of t-butanol. Also, Yao et al. (2010) reported the generation of $\bullet C_2H_5$ short chain radicals and their subsequent recombination with other degraded products during sonolysis of parathion. However, the actual transformation pathway of HBCD is too complex to draw all possible routes because of the generation of numerous ring opening products along with recombination that may occur concurrently.

Black carbonaceous particles were observed visually after 40 min of sonication in pulse mode under optimized parameters, indicating the generation of carbon during the sonochemical treatment of HBCD. The generation of C, CO along with CO_2 as end products must have taken place according to the proposed scheme (Fig. 5.3). The formation of carbonaceous particles via pyrolytic conditions during sonolysis are consistent with the results observed by Hart et al. (1990)

and González-García et al. (2010), where they observed the formation of carbonaceous particles during sonolysis of acetylene and chlorinated organocompounds.

Fig. 5.4 plots the percentage of TOC removal within 40 min of sonochemical treatment, demonstrating the extent of HBCD mineralization. The TOC removal was up to 72 % at optimum conditions, indicating a significant mineralization of HBCD during sonochemical treatment.

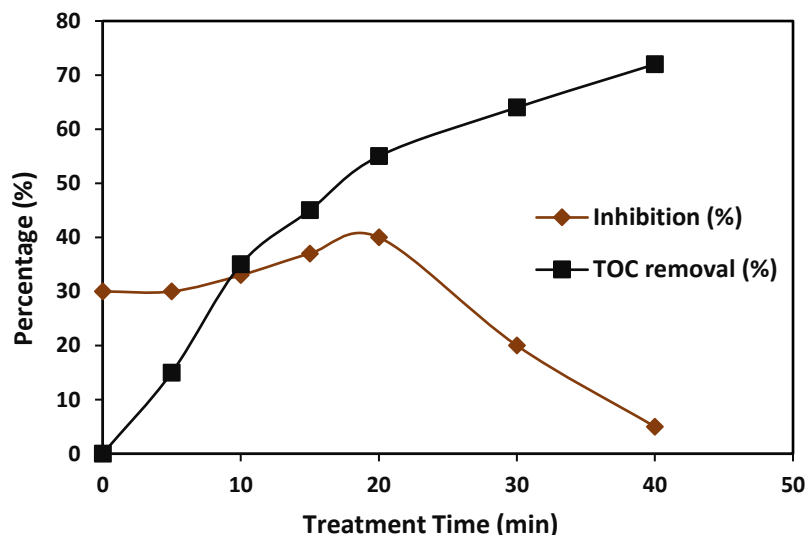


Figure 5.4. HBCD, (◆) (%) Inhibition of *Daphnia magna* and (■) TOC removal (%)

Toxicity evaluation of HBCD has resulted in 30 % immobilization of *Daphnia magna* for the untreated samples, whereas 40 % immobilization for the 20 min treated samples after 24 h of exposure. The initial degradation of HBCD may have led to the formation of more toxic debrominated products as compared to the parent compound, leading to an increase in *Daphnia magna* immobilization with treatment time. Fig. 5.4 shows the comparison in percentage of *Daphnia magna* inhibition for the untreated HBCD to treated solution after 24 h of exposure. During sonochemical process, the acute toxicity again dropped after 20 min, reaching 5 % immobility at the end of 40 min of treatment which could be attributed to further degradation of toxic intermediates. Due to the complicated nature of transformed products, it was difficult to

figure out the individual responsible degradant for the substantial increase in toxicity. It should be noted that the concentration of HBCD employed in the current study is much higher than the nominal concentration of EPA, which demonstrated no acute toxicity within 48 h of exposure to *Daphnia magna* (EPA, 2014).

5.4.1 Reaction kinetics of HBCD

The pseudo-first-order kinetic model was used to evaluate the effect of operational parameters on HBCD degradation. Based on Eqn. 28, plots of C_t versus irradiation time (t) were produced (Fig. 5.5-5.9) according to the HPLC data obtained during different operational parameters.

$$C_t = C_0 e^{-kt} \quad (28)$$

where, k is the measured degradation rate constant and C_0 , C_t are the concentrations of HBCD at time “0” and “ t ” respectively.

Considering all the studied parameters during the sonochemical treatment of HBCD, the experimental data fit well to the pseudo-first-order model. Table 5.4 lists the values of pseudo-first order degradation rate constant (k), and the linear regression coefficient (R^2) for all operating parameters. The highest rate of HBCD removal was obtained after the addition of hydrogen peroxide, while maintaining other essential parameters at their optimum values.

5.4.2 Effect of initial concentration on the degradation HBCD

The extent of pyrolytic destruction of semi-volatile pollutants is dependent on their concentration and hydrophobicity, which define their ability to migrate towards the bubble-liquid interface (Serpone et al., 1994). The concentration of HBCD was varied from 160 to 270 μM while maintaining the operating temperature at 30 $^\circ\text{C}$, pH at 3, power density of 375 W and 20 ppm H_2O_2 loading. The degradation rate enhanced up to an initial concentration of 200 μM , beyond which a decline in the rate was witnessed.

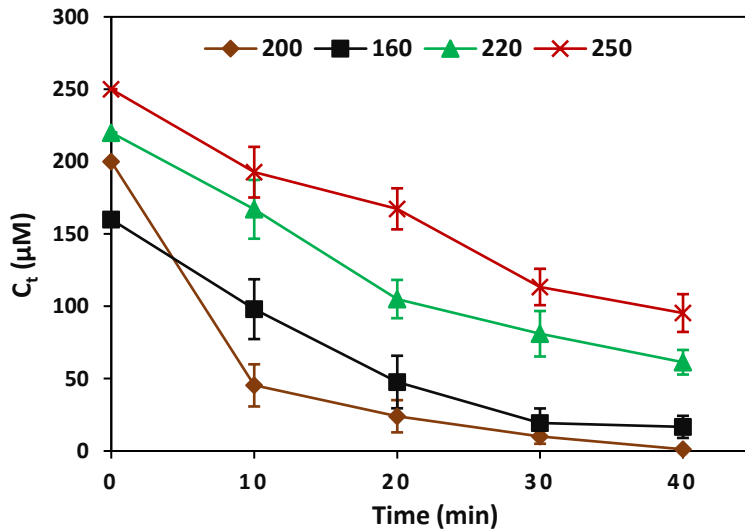


Figure 5.5. Degradation of HBCD at various initial concentrations: (■) 160, (◆) 200, (▲) 220, (×) 250 μM

At the initial concentrations of 160 μM and 200 μM , the results indicated a degradation rate constant of 0.061 min^{-1} and 0.118 min^{-1} (Table 5.4) respectively. The degradation rate scarcely increased beyond the optimum concentration of 200 μM . Similarly, Mendez-Arriaga et al. (2008) observed an optimum concentration of 5 mg/L for Ibuprofen followed by a relatively constant degradation rate at higher concentrations.

5.4.3 Effect of acoustic power on degradation

The extent of applied ultrasonic power is a vital factor in the sonochemical degradation of pollutants, as it can alter the generation of number of active cavitation bubbles (Merouani et al., 2010). The effect of acoustic power on HBCD degradation was monitored by varying the power (150-450 W) at an operating solution temperature of 30 $^{\circ}\text{C}$, while maintaining the concentration of HBCD at 200 μM , pH of 3 and a H_2O_2 loading of 20 ppm. Fig. 5.6 illustrates the power dependence of HBCD on its degradation.

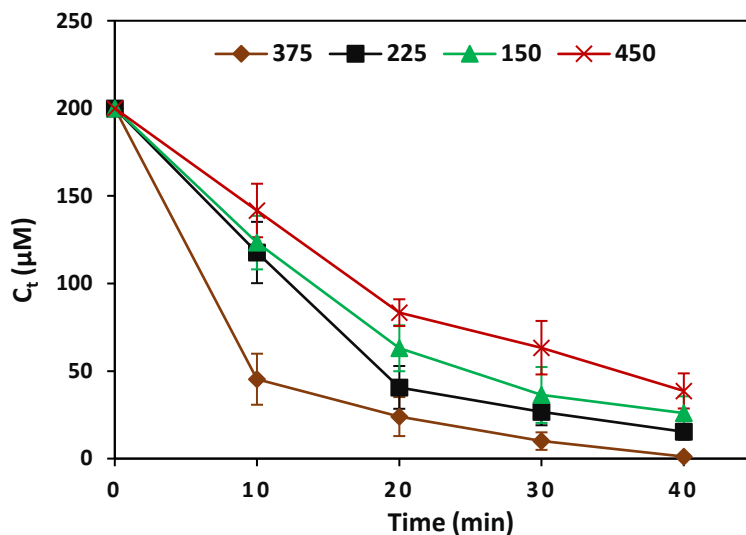


Figure 5.6. Degradation of HBCD at different ultrasonic power levels: (▲)150, (■) 225, (◆) 375, (×) 450 W

The calculated pseudo first order rate constant was 0.118 min^{-1} for an acoustic power of 375 W. It is evident that the rate constants increased with a rise in acoustic power up to 375 W beyond which a decline in the degradation rate was observed. By increasing the power up to the optimum value, the energy of cavitation enhanced following more violent implosion. It has been reported that an increase in the acoustic intensity up to a maximum value of 8.4 W/cm^2 and 110 W/cm^2 enhanced the degradation rate of Ofloxacin (Hapeshi et al., 2013) and Nitrotoluenes (Chen and Huang, 2011) respectively, beyond which a decline in the degradation was observed.

5.4.4 Effect of operating temperature on the degradation of HBCD

A change in the operating temperature affects the cavitation intensity owing to the variation in the physiochemical properties of the liquid medium (Golash and Gogate, 2012). By using the cooling system, the operating temperature was controlled to vary over a range of 15-40 °C, while maintaining the concentration of HBCD at 200 μM, pH of 3, power density of 375 W and H_2O_2 loading of 20 ppm. The operating temperature of 30 °C has been found to be optimum for the highest rate of HBCD degradation.

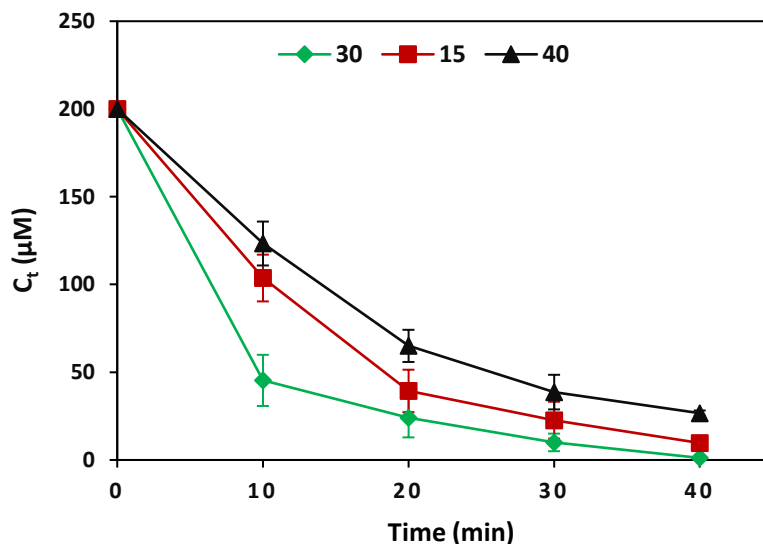


Figure 5.7. Degradation of HBCD at different temperatures: (■) 15 °C, (◆) 30 °C, (▲) 40 °C

Varying the operating temperature affects the formation of type of cavities (gaseous or vaporous) as well as affecting the kinetic rate constant of the components subjected to degradation (Evgenidou et al., 2005). Previous studies on bubble dynamics indicated that a linear decrease in the collapse pressure is witnessed with a rise in the bulk liquid temperature (Gogate et al., 2003; Gogate and Pandit, 2004). Vichare et al. (2000) reported similar observations during the energy analysis of collapsing bubble, which illustrates that the released energy during the collapse of vaporous cavity is lesser than gaseous cavity. The degradation of 4-chlorophenol enhanced at a lower operating temperature (Jiang et al., 2006). Bhatnagar and Cheung (1994) and Wu et al. (1992) observed that the degradation of trichloroethylene (TCE) and carbon tetrachloride was not affected with a change in the temperature between 7-20 °C and 20-60 °C, respectively, whereas Destailats et al. (2000) reported that the sonochemical degradation of TCE increased with a rise in the temperature. At high temperature, semi-volatile or nonvolatile molecules may migrate easily from the bulk solution to the interfacial region, but at the same time a decline in the bubble collapse

intensity could result, hence demonstrating that optimum temperature for the highest rate of degradation is pollutant-specific.

5.4.5 Effect of change in pH

Sonochemical degradation of HBCD was conducted at different solution pH in the range of 3-14 at an operating temperature of 30 °C, while maintaining HBCD concentration of 200 μM, power density of 375 W and H₂O₂ loading of 20 ppm. The highest rate of HBCD degradation was achieved at pH 3 (Fig. 5.8), which can be attributed to the faster transport of short chain intermediates towards bubble interfacial region due to their enhanced hydrophobic nature at acidic conditions.

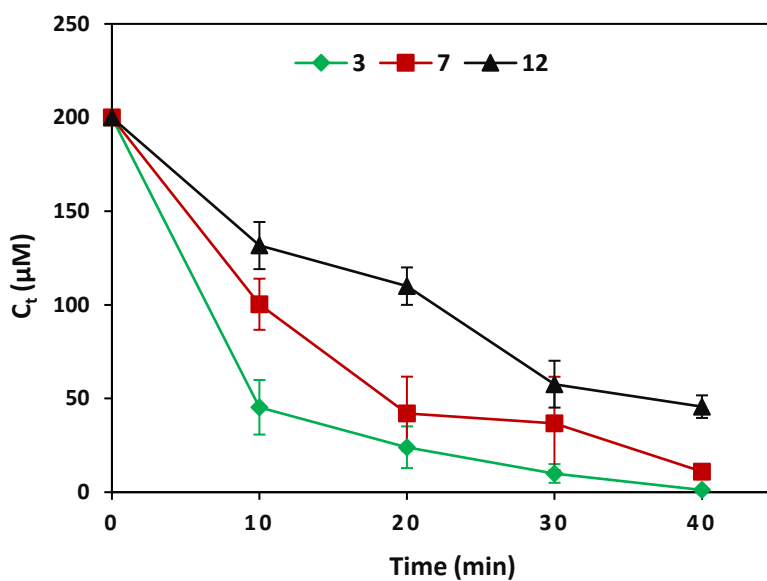


Figure 5.8. Degradation of HBCD at different pH: (◆) 3, (■) 7, (▲) 12

Even though HBCD does not undergo ionization, the enhancement in degradation rate at lower pH could be attributed to the change in the properties of degraded products. Several previous reports suggested that a faster sonolytic degradation was observed at low pH for semi-volatile and non-volatile organic pollutants, owing to the increased hydrophobicity of protonated species, resulting in an enhanced accumulation of molecules at the bubble interfacial region (Wei et al., 2016).

5.4.6 Effect of addition of H₂O₂

In the presence of ultrasonic irradiation, hydrogen peroxide was observed to dissociate into hydroxyl radicals (Eqn. 29), thereby acting as an additional source of free radicals. Also, it can act as a scavenger of the generated free radicals (Eqn. 30) beyond the optimum concentration.



HBCD is known to be recalcitrant towards hydroxylation and to verify the effect of H₂O₂ on HBCD degradation, the concentration of H₂O₂ was varied over the range of 10-50 ppm, while maintaining the operating temperature at 30 °C, concentration of HBCD at 200 μM, power density of 375 W and pH at 3. Addition of H₂O₂ up to 20 ppm loading enhanced the degradation rate of HBCD (Fig. 5.9), indicating that the short chain intermediates must have gone through significant radical attack via simultaneous hydroxylation at the interface and at bulk region. Beyond the optimum loading of 20 ppm, the degradation rate was hindered, illustrating the scavenging effect of H₂O₂ on the generated hydroxyl radicals.

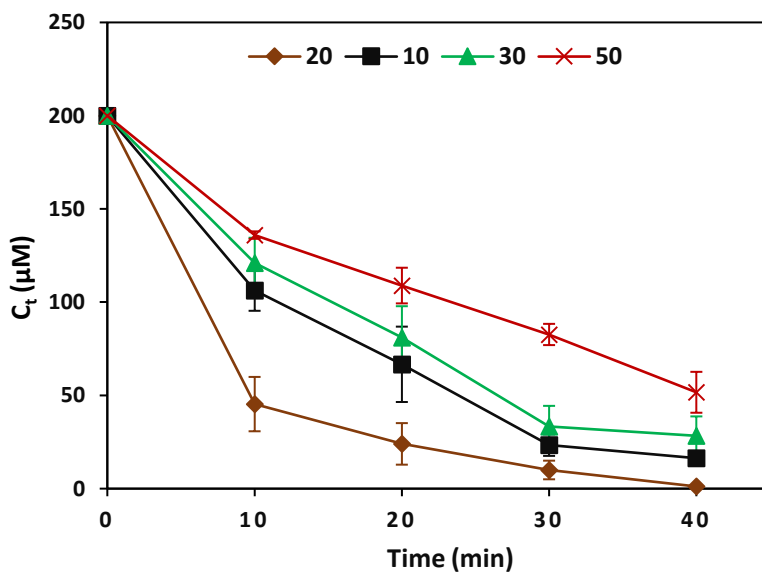


Figure 5.9. Degradation of HBCD at different H₂O₂ loading: (■) 10, (◆) 20, (▲) 30, (×) 50 ppm

Control experiments were also conducted considering an identical dosage of H₂O₂ to understand its effect on HBCD in the absence of sonochemical treatment. No degradation product was detected in the absence of sonication, justifying the recalcitrant nature of HBCD towards hydroxylation.

Table 5.4. Pseudo-first-order rate constants for the degradation of HBCD under different operational parameters

Parameter		k (min ⁻¹)	R ²
Initial concentration (μM)	160	0.061	0.967
	200	0.118	0.957
	220	0.033	0.989
	250	0.025	0.981
Acoustic Power (W)	150	0.053	0.989
	225	0.066	0.978
	375	0.118	0.957
	450	0.041	0.992
Solution temperature (°C)	15	0.076	0.994
	30	0.118	0.957
	40	0.052	0.993
pH	3	0.118	0.957
	7	0.068	0.960
	12	0.038	0.973
H ₂ O ₂ loading (ppm)	10	0.065	0.980
	20	0.118	0.957
	30	0.052	0.968
	50	0.032	0.984

5.5 Conclusions

The sonochemical treatment has demonstrated to be an effective and efficient technique for the removal of HBCD. The outcomes demonstrated a complete disappearance of HBCD within 40 min of treatment under optimum parameters of 375 W acoustic power, 30 °C solution temperature, pH of 3, 200 μM pollutant concentration and for the 20 ppm H₂O₂ addition. GC-MS analysis

indicated the formation of transformed products. TOC removal reached 72 % within 40 min of sonication at optimum conditions, which illustrated a significant mineralization of HBCD. The first step of HBCD degradation is proposed to follow thermal decomposition at bubble liquid interface following radical attack and recombination of short chain intermediates at the later stage of transformation.

5.6 References

- Stockholm Convention on Persistent Organic Pollutants. Depository notifications: C.N.934. 2013. TREATIES-XXVII.15 (amendment to annex A), United Nations (UN). <https://treaties.un.org/doc/Publication/CN/2013/CN.934.2013-Eng.pdf>.
- Covaci, A., Gerecke, A. C., Law, R. J., Voorspoels, S., Kohler, M., Heeb, N.V., Leslie, H., Allchin, C. R., Boer, J. D., 2006. Hexabromocyclododecanes (HBCDs) in the environment and humans: a review, *Environ. Sci. Technol.* 40, 3679-3688.
- Marvin, C. H., Tomy, G. T., Armitage, J. M., Arnot, J. A., McCarty, L., Covaci, A., Palace, V., 2011. Hexabromocyclododecane: current understanding of chemistry, environmental fate and toxicology and implications for global management, *Environ. Sci. Technol.* 45, 8613-8623.
- Alaee, M., Arias, P., Sjodin, A., Bergman, A., 2003. An overview of commercially used brominated flame retardants, their applications, their use patterns in different countries/regions and possible modes of release, *Environ. Int.* 29, 683–689.
- Arnot, J., McCarty, L., Armitage, J., Toose-Reid, L., Wania, F., Cousins, I., 2009. An evaluation of hexabromocyclododecane (HBCD) for persistent organic pollutant (POP) properties and the potential for adverse effects in the environment, *Eur. Brominated Flame Retard. Ind. Panel.*
- Ronisz, D., Finne, E. F., Karlsson, H., Forlin, L., 2004. Effects of the brominated flame retardants hexabromocyclododecane (HBCDD) and tetrabromobisphenol-A (TBBPA), on hepatic enzymes and other biomarkers in juvenile rainbow trout and feral eelpout, *Aquat. Toxicol.* 69, 229–245.
- Birnbaum, L. S., Staskal, D. F., 2004. Brominated flame retardants: cause for concern?, *Environ.*

- Health Perspect. 112, 9-17.
- Davis, J. W., Gonsior, S. J., Markham, D. A., Friederich, U., Hunziker, R. W., Ariano, J. M., 2006. Biodegradation and product identification of [14C] hexabromocyclododecane in wastewater sludge and freshwater aquatic sediment, *Environ. Sci. Technol.* 40, 5395–5401.
- Stiborova, H., Vrkoslavova, J., Pulkrabova, J., Poustka, J., Hajslova, J., Demnerova, K., 2015. Dynamics of brominated flame retardants removal in contaminated wastewater sewage sludge under anaerobic conditions, *Sci. Total Environ.* 533, 439–445.
- Tso, C.P., Shih, Y.H., 2014. The transformation of hexabromocyclododecane using zerovalent iron nanoparticle aggregates, *J. Hazard. Mater.* 277, 76–83.
- Zhang, K., Huang, J., Wang, H., Liu, K., Yu, G., Deng, S., Wang, B., 2014. Mechanochemical degradation of hexabromocyclododecane and approaches for the remediation of its contaminated soil, *Chemosphere* 116, 40–45.
- Zhou, D., Wu, Y., Feng, X., Chen, Y., Wang, Z., Tao, T., Wei, D., 2014. Photodegradation of hexabromocyclododecane (HBCD) by Fe(III) complexes/H₂O₂ under simulated sunlight. *Environ. Sci. Pollut. Res.* 21, 6228–6233.
- Serpone, N., Terzian, R., Hidaka, H., Pelizzetti, E., 1994. Ultrasonic induced dehalogenation and oxidation of 2-, 3-, and 4-chlorophenol in air-equilibrated aqueous media. Similarities with irradiated semiconductor particulates, *J. Phys. Chem.* 98, 2634-2640.
- Mendez-Arriaga, F., Torres-Palma, R. A., Petrier, C., Esplugas, S., Gimenez, J., Pulgarin, C., 2008. Ultrasonic treatment of water contaminated with ibuprofen, *Water Res.* 42, 4243–4248.
- Merouani, S., Hamdaoui, O., Saoudi, F., Chiha, M., 2010. Sonochemical degradation of rhodamine B in aqueous phase: effects of additives, *Chem. Eng. J.* 158, 550–557.
- Thangavadivel, K., Megharaj, M., Smart, R. S. C., Lesniewski, P. J., Naidu, R., 2009. Application

- of high frequency ultrasound in the destruction of DDT in contaminated sand and water, *J. Hazard. Mater.* 168, 1380–1386.
- Chowdhury, P., Viraraghavan, T., 2009. Sonochemical degradation of chlorinated organic compounds, phenolic compounds and organic dyes - a review, *Sci. Total Environ.* 407, 2474–2492.
- Naddeo, V., Belgiorno, V., Kassinos, D., Mantzavinos, D., Meric, S., 2010. Ultrasonic degradation, mineralization and detoxification of diclofenac in water: optimization of operating parameters, *Ultrason. Sonochem.* 17, 179–185.
- ISO 6341, 1996. Water quality determination of the inhibition of the mobility of daphnia magna straus (cladocera, crustacea)-acute toxicity test.
- EPA, 2014. Flame retardant alternatives for hexabromocyclododecane (HBCD), EPA Publication 740R14001.
- Sivasankar, T., Moholkar, V. S., 2009. Physical insights into the sonochemical degradation of recalcitrant organic pollutants with cavitation bubble dynamics, *Ultrason. Sonochem.* 16, 769–781.
- Yao, J.J., Gao, N. Y., Deng, Y., Ma, Y., Li, H. J., Xu, B., Li, L., 2010. Sonolytic degradation of parathion and the formation of byproducts, *Ultrason. Sonochem.* 17, 802–809.
- Neta, P., Grodkowski, J., Ross, A.B., 1996. Rate constants for reactions of aliphatic carbon-centered radicals in aqueous solution, *J. Phys. Chem. Ref. Data* 25, 709–1050.
- Gonzalez, M. C., Le Roux, G. C., Rosso, J. A., Braun, A. M., 2007. Mineralization of CCl₄ by the UVC – photolysis of hydrogen peroxide in the presence of methanol, *Chemosphere* 69, 1238–1244.
- Bokhale, N. B., Bomble, S. D., Dalbhanjan, R. R., Mahale, D. D., Hinge, S. P., Banerjee, B. S.,

- Mohod, A. V., Gogate, P. R., 2014. Sonocatalytic and sonophotocatalytic degradation of rhodamine 6G containing wastewaters, *Ultrason. Sonochem.* 21, 1797–1804.
- Alegria, A. E., Lion, Y., Kondo, T., Riesz, P., 1989. Sonolysis of aqueous surfactant solutions: probing the interfacial region of cavitation bubbles by spin trapping, *J. Phys. Chem.* 93, 4908–4913.
- Tauber, A., Mark, G., Schuchmann, H. P., Sonntag, C. V., 1999. Sonolysis of tert-butyl alcohol in aqueous solution, *J. Chem. Soc. Perkin Trans. 2.* 6, 1129–1136.
- Yao, J. J., Gao, N. Y., Li, C., Li, L., Xu, B., 2010. Mechanism and kinetics of parathion degradation under ultrasonic irradiation, *J. Hazard. Mater.* 175, 138–145.
- Hart, E. J., Fischer, C. H., Henglein, A., 1990. Pyrolysis of acetylene in sonolytic cavitation bubbles in aqueous solution, *J. Phys. Chem.* 94, 284-290.
- González-García, J., Sáez, V., Tudela, I., Díez-García, M. I., Deseada Esclapez, M., Louisnard, O., 2010. Sonochemical treatment of water polluted by chlorinated organocompounds. A review, *Water* 2, 28–74.
- Hapeshi, E., Fotiou, I., Fatta-Kassinos, D., 2013. Sonophotocatalytic treatment of ofloxacin in secondary treated effluent and elucidation of its transformation products, *Chem. Eng. J.* 224, 96–105.
- Chen, W. S., Huang, S. C., 2011. Sonophotocatalytic degradation of dinitrotoluenes and trinitrotoluene in industrial wastewater, *Chem. Eng. J.* 172, 944–951.
- Golash, N., Gogate, P. R., 2012. Degradation of dichlorvos containing wastewaters using sonochemical reactors, *Ultrason. Sonochem.* 19, 1051–1060.
- Evgenidou, E., Fytianos, K., Poulios, I., 2005. Semiconductor-sensitized photodegradation of dichlorvos in water using TiO₂ and ZnO as catalysts, *App. Cat. B: Environ.* 59, 81–89.

- Gogate, P. R., Wilhelm, A. M., Pandit, A. B., 2003. Some aspects of the design of sonochemical reactors, *Ultrason. Sonochem.* 10, 325–330.
- Gogate, P. R., Pandit, A. B., 2004. Sonochemical reactors: scale up aspects, *Ultrason. Sonochem.* 11, 105–117.
- Vichare, N. P., Senthilkumar, P., Moholkar, V. S., Gogate, P. R., Pandit, A. B., 2000. Energy analysis in acoustic cavitation, *Ind. Eng. Chem. Res.* 39, 1480–1486.
- Jiang, Y., Petrier, C., Waite, T. D., 2006. Sonolysis of 4-chlorophenol in aqueous solution: effects of substrate concentration, aqueous temperature and ultrasonic frequency, *Ultrason. Sonochem.* 13, 415–422.
- Bhatnagar, A., Cheung, H. M., 1994. Sonochemical destruction of chlorinated C1 and C2 volatile organic compounds in dilute aqueous solution, *Env. Sci. Tech.* 28, 1481-1486.
- Wu, J. M., Huang, H. S., Livengood, C. D., 1992. Ultrasonic destruction of chlorinated compounds in aqueous solution, *Environ. Prog. Sus. Energy* 11, 195-201.
- Destailats, H., Colussi, A. J., Joseph, J. M., Hoffmann, M. R., 2000. Synergistic effect of sonolysis combined with ozonolysis for the oxidation of azobenzene and methyl orange, *J. Phys. Chem. A.* 104, 8930-8935.
- Wei, Z., Spinney, R., Ke, R., Yang, Z., Xiao, R., 2016. Effect of pH on the sonochemical degradation of organic pollutants, *Environ. Chem. Lett.* 14, 163–182.

Chapter 6

Kinetics and mechanism of low frequency ultrasound driven elimination of trace level aqueous Perfluorooctanesulfonic acid and Perfluorooctanoic acid

Abstract

Perfluorinated surfactants such as Perfluorooctanesulfonic acid (PFOS) and Perfluorooctanoic acid (PFOA) are the most investigated persistent organic pollutants due to their adverse health concerns and inertness in elimination. The sonochemical treatment of PFOX (PFOS and PFOA) in aqueous media has been investigated using a 20-kHz transducer type sonicator with power inputs from 150 to 375 W. The degradation rate was determined as a function of concentration of PFOX, bulk phase temperature, pH and ultrasonic power density. Liquid chromatography mass spectroscopy analysis indicated the complete disappearance of PFOX within 80 min of treatment. Change in the bulk phase temperature from the optimum value of 20 °C indicated detrimental effect on the degradation rate and decline in the ultrasonic power decreased PFOX degradation rate. The reaction rate increased with an increase in the concentration of PFOX in the range of 20-220 pM indicating a pseudo first order kinetics, beyond which a decline in the degradation rate was witnessed. The obtained results suggest that the degradation of PFOX followed thermal decomposition at bubble-vapor interface as the dominant pathway followed by the pyrolysis of intermediates inside the bubble.

6.1 Introduction

Perfluorooctanoic acid (PFOA) and perfluorooctanesulfonic acid (PFOS), altogether called PFOX, are under the family of perfluorinated surfactants. PFOX has been used in various applications including cosmetics, stain repellants, fabric protectors, preparation of insecticides, textile treatment, production of firefighting foams and in various photolithographic chemicals in semiconductor industries for the past 50 years (German 2014; EFSA 2008). Additionally, PFOA finds its dominant use as an emulsifier for the polymerization of fluoropolymers such as polytetrafluoroethylene (PTFE or Teflon). The higher bioaccumulation potential, environmental persistency and the toxic effects of PFOX on humans, wildlife as well as on aquaculture livestock have marked it as a ubiquitous contaminant. PFOX is associated with adverse health concerns such as tumor development, gastrointestinal irritation, body weight reduction, weariness, liver damage and development of cancer among various living species (US EPA 2014; US EPA 2016; ASTDR 2009). The median concentration of PFOX in surface water was reported to be in 3 ng/L, whereas in wastewater treatment effluent the concentrations are 24 ng/L and 11 ng/L for PFOA and PFOS respectively (Zareitalabad et al. 2013).

PFOX is recalcitrant towards oxidation and resistant to conventional treatment technologies due to their unique physiochemical properties leading to more thermally stable and a weakly polarizable structure (Goss 2008; Goss 2006; 3M 1999; Vecitis et al. 2009). Even though technologies such as nanofiltration, reverse osmosis and activated carbon etc. were effective in PFOX removal from wastewater, but subsequent incineration of the adsorbent medium is necessary for the complete destruction of PFOX. Advanced oxidation processes utilizing hydroxyl and oxygen radicals such as alkaline ozonation, peroxone or Fenton's reagent have demonstrated to be relatively ineffective for the elimination of PFOX (Vecitis et al. 2009). Sonochemical based

wastewater treatment was successful in the complete removal of PFOX at higher sonication frequency (200 kHz-1 MHz) for the concentrations range of 10 nM to 500 μ M (Rodriguez-Freire et al. 2015; Cheng et al. 2010; Vecitis et al. 2008; Moriwaki et al. 2005), whereas low frequency (40 kHz) sonication in combination with carbonate radical, sulfate ions had shown moderate effectiveness for PFOA (120 nM-120 μ M) removal (Phan Thi et al. 2014; Lin et al. 2015). As the presence of PFOX in the contaminated water/wastewater matrix are reported to be in trace level only (6-58 pM), the effectiveness of low frequency ultrasound (20 kHz) for the elimination of low concentration PFOX needs to be investigated, which could lead to a greater energy efficient sonochemical wastewater treatment.

In the present work, low frequency driven sonochemical treatment of PFOX has been investigated. The effect of operational parameters such as ultrasonic power, pH, initial concentration and solution temperature on the extent of PFOX degradation was also examined. The degradation by-products of PFOX were monitored and quantified by liquid chromatography tandem mass spectroscopy (LC-MS/MS). Considering complications in quantitation and detection of trace level of PFOX via LC/MS analysis, our investigation has demonstrated the necessary precautions to be implemented during analysis.

6.2 EXPERIMENTAL

6.2.1 Materials

Perfluorooctanoic acid ($C_8HF_{15}O_2$, PFOA, 99%), Perfluorooctanesulfonate ($C_8F_{17}SO_3K$, PFOS, 99%), Perfluoroheptanoic acid (PFHpA, $C_7F_{13}COOH$, 99%), Perfluorohexanoic acid (PFHxA, $C_6F_{11}COOH$, 97%), Perfluoropentanoic acid (PFPA, C_5F_9COOH , 97%), Heptafluorobutyric acid (PFBA, C_4F_7COOH , 99%) and Pentafluoropropionic acid (PFPrA, C_3F_5COOH , 97%), Trifluoroacetic acid (TFA, CF_3COOH , 99%), Tert-butyl alcohol, N-hexane, Methanol (HPLC

grade) and Ammonium acetate (HPLC grade) were purchased from Sigma Aldrich (Malaysia). All these chemicals were used as-received without further purification. All aqueous solutions were prepared with high purity water (Milli-Q water). Agilent nylon syringe filter of 0.45 μm pore size and 5 ml syringes were purchased from IT Tech Research (M) Sdn. Bhd. (Malaysia).

6.2.2 Sonochemical experiments

The stock solutions were prepared by dissolving PFOX in Milli-Q water and was stored at 2 °C. Working standard solutions were prepared regularly by the dilution of stock in water to a desired concentration range from 20 to 2000 pM. Sonochemical experiments were performed in a 100-mL reactor using a 20 kHz ultrasonic probe (Cole-Parmer Instruments, Illinois, USA) and the applied ultrasonic power range was varied between 150 to 375 W. The temperature of reaction mixture was maintained between 10-40 °C using a chiller. Sonication was performed in the pH range from 2 to 7. Appropriate quantity of H₂SO₄ and/or NaOH was used for pH adjustments. Sonication was performed for 120 min and aliquots were withdrawn at regular intervals for LC-MS analysis. Each experiment was repeated three times and the standard deviation of the triplicate experiments are included in the corresponding figure.

6.3 Chemical analysis

6.3.1 LC-MS analysis

PFOX samples were placed into polypropylene vials (1.5 ml) instead of glass vials owing to the potential loss of analyte due to the adsorption to the glass wall. Also, the Teflon septa of vials were replaced to avoid PTFE contamination. 20 μL of collected samples were injected onto a Varian 212-LC for separation on a CORTECSTM C18 column (4.6 mm \times 100 mm, 2.7 μm). The HPLC separation was carried out at a column temperature of 40 °C using a gradient composed of solvent A (methanol) and solution B (5 mM aqueous ammonium acetate). The gradient expressed as

changes in solvent A was as follows: 0-1.0 min, 30% A; 1.0 to 7.0 min, 30 to 90% A; 7.0 to 10.0 min, 90% to 30% A. The flow rate was 200 $\mu\text{L}/\text{min}$. Considering the properties of PFOX including polarity, acidity and electronegativity, negative ESI interface was adopted as the ion source for ionization and LC effluents were analyzed with a Varian 320-MS. Single ion monitoring was performed for the precursor ion of PFOS ($m/z=499$) and PFOA ($m/z=413$) and the ESI mass spectra was obtained. The electrospray conditions were as follows: nitrogen curtain gas flow: 10.0 L/min; API drying gas: 20 psi at 200 $^{\circ}\text{C}$; API nebulizing gas: 40 psi; Detector: 1900 V; Needle potential: -4500 V; Shield potential: -600 V.

PFOX was quantified by multiple reaction monitoring (MRM) using the most abundant precursor/product ion transitions ($499 \rightarrow 80$ for PFOS and $413 \rightarrow 369$ for PFOA), whereas the second MRM transitions ($499 \rightarrow 99$ for PFOS and $413 \rightarrow 169$ for PFOA) were used as qualifiers. The primary MRM transitions were used for the quantification, while the secondary transitions were used for the ion ratio confirmation to eliminate false positive results. The product ion of PFOA with the m/z value of 368.9 was generated via the decarboxylation of the precursor ion, whereas for PFOS its product ion with the m/z value of 79.7 was SO_3^- . The parameters of MS segment were as follows: Capillary voltage (V): PFOS: -95 and PFOA: -45; CID gas: 2.4 mTorr. The observed detection signal was very less for PFOA at the optimal fragmentor voltage of PFOS (200V). PFOA is relatively fragile and its precursor signal drops off at 160 V, while PFOS is considered to be harder than PFOA to break apart and thereby exhibiting a higher fragmentor voltage compared to PFOA. The optimum ionization and fragmentation conditions for PFOS and PFOA were as follows: PFOS and PFOA: Dwell time (ms):100; PFOS transition ($499 \rightarrow 99$) & ($499 \rightarrow 80$): Fragmentor energy (V): 200; Collision energy (eV): ($499 \rightarrow 99$):48 and ($499 \rightarrow 80$):49; PFOA transition ($413 \rightarrow 369$) & ($413 \rightarrow 169$): Fragmentor energy (V): 80; Collision energy (eV):

(413→369): 8.5 and (413→169): 16. Good signal to noise ratio (S/N) was obtained after following essential precautions to avoid unwanted background contamination. The sonochemical products of PFOX were measured by LC/MS/MS in MRM mode. Calibration curves for perfluoro compounds at concentrations from 1 pg/mL to 10 ng/mL were constructed and good linearity was observed.

6.3.2 Precautions during detection

Reported data suggested that perfluorinated compounds (PFCs) could be present in LC systems, for example, in the tubes of chromatographic system and at degasser membrane (Lee et al. 2008), resulting in the interference which is difficult to eliminate. Depending on the analytical conditions, PFOA could be present in the online degasser and in the flow line, which may accumulate in the analytical column (Shimadzu 2011). Also, PTFE components of labware and LC instrument such as autosampler needle as well as mobile phases are the dominant sources of PFC contamination. Also, elevated base line and unknown interference peaks could result in the MRM transitions, because of the identical molecular weight of some of the carboxylic acids as compared to PFOA. Several blank samples of reagent (MeOH or MeOH/water) were injected to the LC-MS system prior to the sample analysis to reduce the unwanted interference of PFCs and the background contamination was evaluated with reference to the signal response. Detection of PFOX during initial blank injection can be attributed to the possible absorption of PFOX onto the surface of pre-column pipeline and the particles packed in the chromatographic column (Tang et al. 2014). The problem was resolved by relatively high initial proportion of organic mobile phase (30% MeOH) and comparatively higher end time elution with 100% MeOH followed by a longer stabilization run time.

6.4 Results and discussion

Degraded products of PFOX were identified within 40 min of sonolysis under the same parameters followed for PFOX standard (Figure 6.1) and the disappearance of intermediates after 80 min of sonication demonstrates the complete removal of PFOX. The LC/MS/MS acquisition was performed in MRM mode by following the transitions m/z 413.0-369 (PFOA), m/z 363-319 (PFHpA), m/z 313-269 (PFHxA), m/z 263-219 (PFPA), m/z 213-169 (PFBA), m/z 163-119 (PFPrA) and m/z 113-69 (TFA) for sonicated PFOS samples, which confirmed the formation of degradation products corresponding to Perfluorooctanoic acid (PFOA), Perfluoroheptanoic acid (PFHpA), Perfluorohexanoic acid (PFHxA), Perfluoropentanoic acid (PFPA), Heptafluorobutyric acid (PFBA), Pentafluoropropionic acid (PFPrA), Trifluoroacetic acid (TFA) respectively. The sonicated solution of PFOA was also monitored following the MRM transitions of m/z 363-319, m/z 313-269, m/z 263-219, m/z 213-169, m/z 163-119 and m/z 113-69 respectively and the appearance of degraded products confirmed the identical degradation mechanism of PFOA as compared to PFOS. The difference of m/z between these peaks are 50 and could be assigned to $\text{CF}_3(\text{CF}_2)_n\text{COO}^-$ ($n = 0-6$) ions because of the formula weight of CF_2 as 50. It could be anticipated that the ions were formed by the dissociation of CF_2 from PFOX. Figure 6.1 shows the total ion chromatogram (TIC) of PFOX along with the MRM transition spectra of its degraded products.

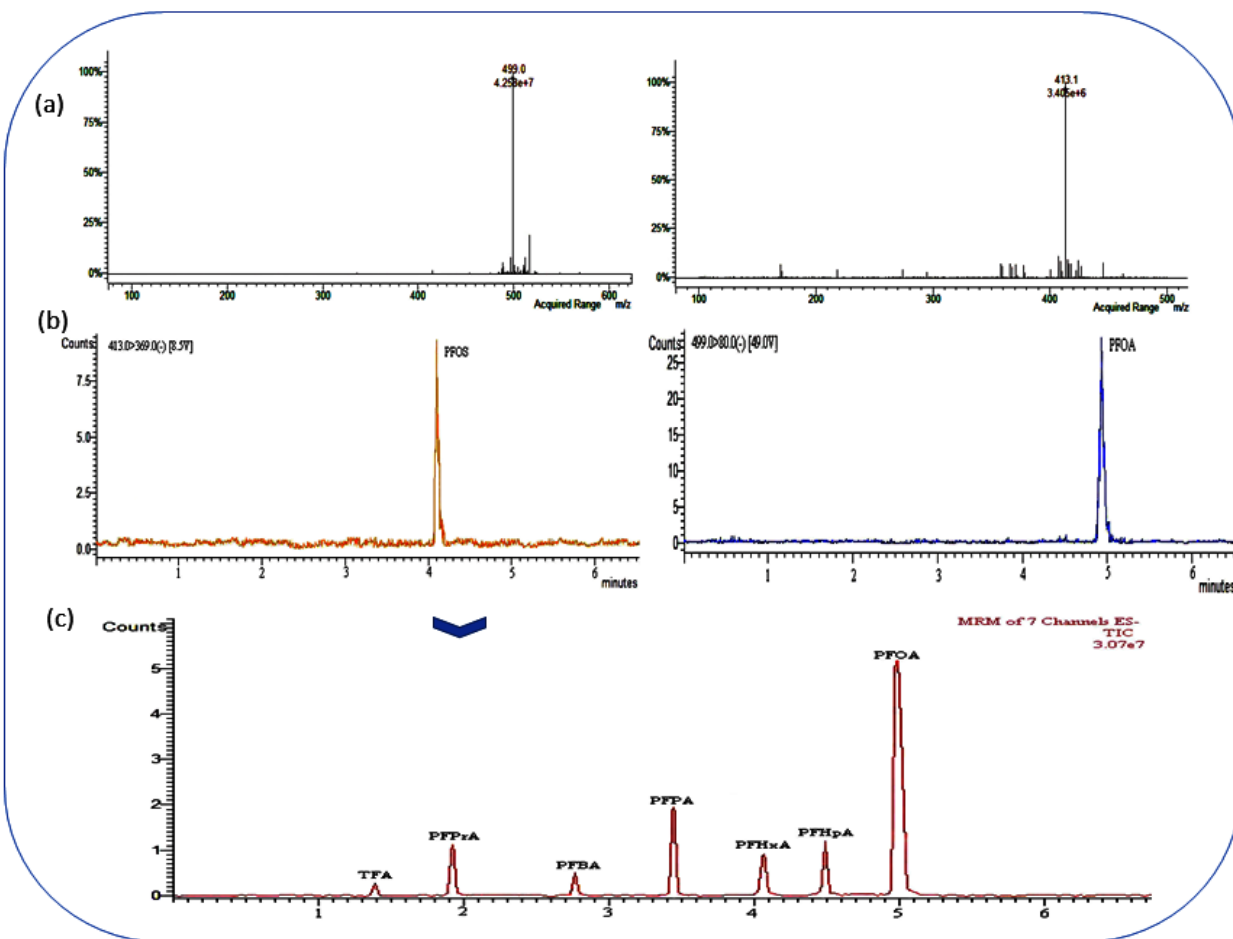


Figure 6.1. Chromatographic representation of (a) ESI mass spectra of PFOS and PFOA parent ions (b) MRM spectra of PFOS and PFOA (c) MRM spectra of degraded products of PFOS after 60 min of sonication

As both PFOS and PFOA molecules have a hydrophobic (perfluoroalkyl) and a hydrophilic group (acid), they are considered to be anionic surfactants. Since PFOX is considered as nonvolatile, pyrolysis inside the bubble should be excluded. PFOX coupled with its small Henry's constant precludes its diffusive transfer to the bubble vapor phase. Thus, interfacial pyrolytic decomposition appears to be the primary pathway for the sonochemical degradation of PFOX. Therefore, it could be assumed that most of the PFOX molecules are pyrolyzed at the gas-liquid interfacial region resulting in complete mineralization. The identified degraded products of PFOX via LC-MS/MS

and the possible degradation pathways in consideration of cavitation bubble mechanism are represented in Fig. 6.2.

To verify the degradation mechanism of PFOX, sonolysis in the presence of tert-butyl alcohol (TBA) was also conducted, which is known as free radical scavenger of the gaseous regions and/or interfacial regions (Song et al. 2006). PFOX degradation rate inhibited a little in the presence of TBA for both loading (0.5 & 5 mM), indicating the degradation mechanism to be thermal decomposition driven rather than being radical dependent.

Conceptually, interfacial pyrolysis can be considered into two fundamental steps. The first step involves the diffusion and adsorption of PFOX to a transiently cavitating bubble-liquid interface followed by a second step involving thermal decomposition at the interfacial region along with the pyrolytic degradation of intermediates inside the bubble core. The pyrolytic degradation of PFOS at the bubble-water interface involves the loss of part of ionic sulfonate functional group leading to the formation of short chain fluorinated intermediates. These fluorinated intermediates are expected to enter the bubble core and undergo a series of pyrolytic reactions leading to C1 fluoro-radicals and the gradual conversion of C1 fluoro-radicals into carbon monoxide, carbon dioxide, HF, and fluoride ion. The obtained results suggest that the primary intermediates produced during PFOX degradation seem to have much shorter half-lives than their precursors, which can be attributed to the high Henry's constant values (Table 6.1) of the intermediates as compared to their precursors, resulting in faster evaporation of degraded intermediates into the bubble core. Similar observations had been reported by Vecitis et al. (2008), demonstrating the faster degradation of intermediates as compared to the parent compound of PFOX.

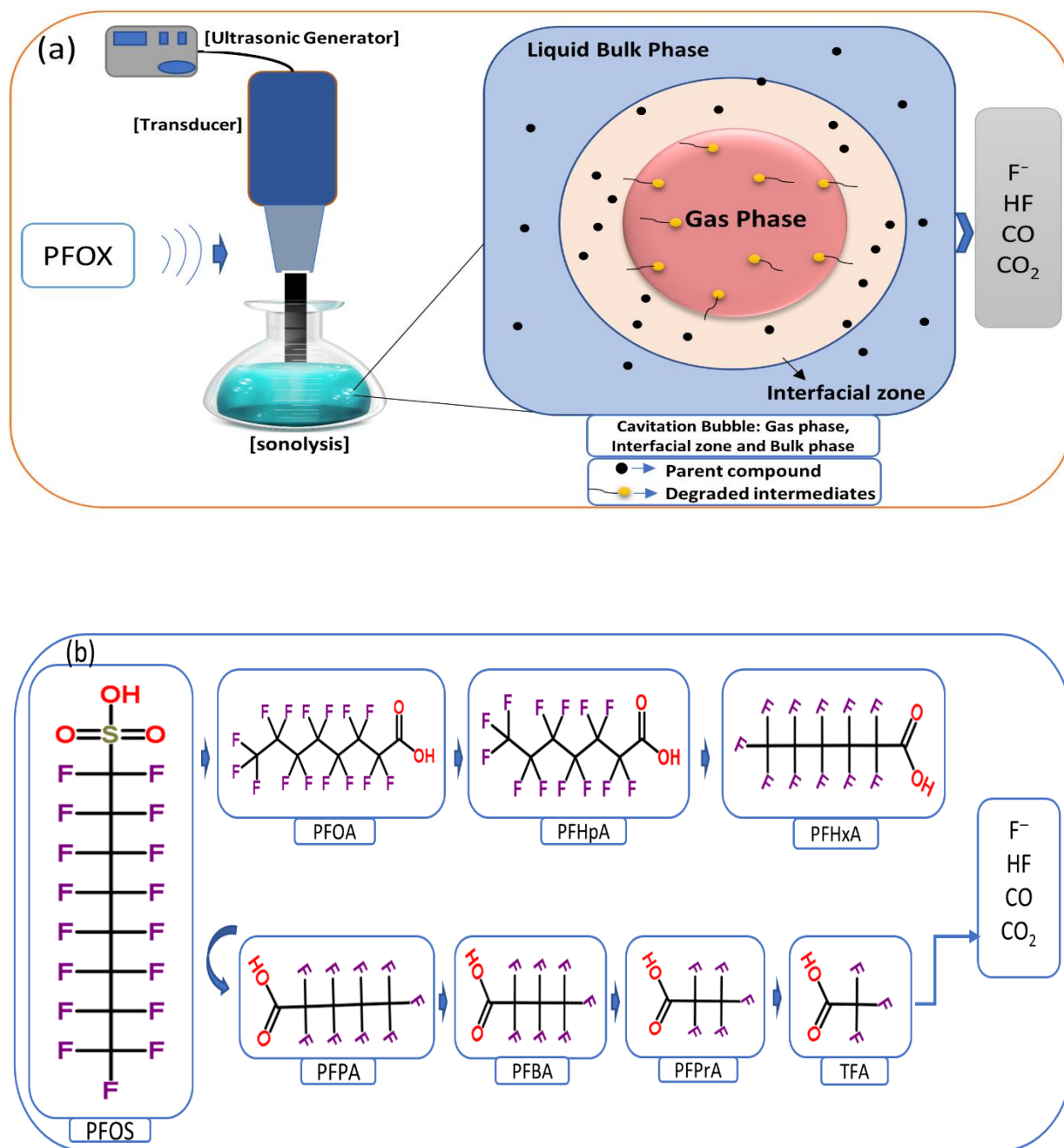


Figure 6.2. (a) Cavitation bubble and PFOX degradation: adsorption and thermal decomposition of PFOX parent compound at bubble-bulk interfacial zone and pyrolytic degradation of intermediates inside the bubble core (gas phase) (b) The products identified by LC-MS/MS and the proposed degradation pathways of PFOS under ultrasonic irradiation

Table 6.1. Henry's constants of PFOX and their degradants

Compound	Henry's constants (atm·m ³ /mol)
PFOS	1.85 × 10 ⁻¹¹
PFOA	2.02 × 10 ⁻¹⁰
Perfluoroheptanoic acid (PFHpA)	2.22 × 10 ⁻¹⁰
Perfluorohexanoic acid (PFHxA)	2.51 × 10 ⁻¹⁰
Perfluoropentanoic acid (PFPA)	3.22 × 10 ⁻¹⁰
Heptafluorobutyric acid (PFBA)	4.99 × 10 ⁻⁵
Pentafluoropropionic acid (PFPrA)	3.47 × 10 ⁻⁶
Trifluoroacetic acid (TFA)	1.24 × 10 ⁻⁷

6.4.1 Significance of low frequency for the trace level elimination of PFOX

The relationship between frequency, the size of bubble and final temperature generated within the bubble can be explained by a simplified numerical assumption (Eqn. 31).

$$T_f = T_0 \left(\frac{R_{max}}{R_0} \right)^{3(\gamma-1)} \quad (31)$$

T_0 and T_f are the temperatures of the bulk liquid and final temperature of the gas within the bubble, whereas R_0 and R_{max} are the initial and maximum bubble radius and γ is the ratio of specific heat capacities (C_p/C_v) of the gas/vapor mixture. It demonstrates the changes in the generation of temperature with frequency during the collapse of bubble since T_f is proportional to the cube of its fractional change in the radius of bubble. Usually a bubble of initial radius R_0 grows for a few acoustic cycles until it reaches a maximum value R_m , which is at least two to three times of its initial radius following a collapse during the next acoustic compression half cycle. As the frequency of sonication increases, R_m decreases and the time available for bubble nucleation and growth also decreases, which leads to a less violent bubble collapse (Riesz et al. 1985; Merouani and Hamdaoui 2016).

Bubbles excited by low frequency waves are reported to have a resonance radius of ~170 μm (at 20 kHz), resulting in stable cavities with an average life-time of ~10 μs (Ince et al. 2001). Hence during low frequency cavitation, the collapse stage is delayed until the elapse of a number of compression and rarefaction cycles, during which adequate solutes can accumulate at the interfacial region (Ince et al. 2001). The extent of pyrolytic destruction of non-volatile pollutants is directly related to their concentration and hydrophobicity, which govern their ability to migrate towards the bubble and/or to accumulate at the bubble–liquid interface (Serpone et al. 1994). Alegria et al. (1989) investigated the site of degradation of non-volatile surfactants by ultrasonic irradiation using 50 kHz and reported that surfactants orient themselves radially in the interfacial region with their polar head groups pointing to the bulk solution. At higher concentrations, the adsorptive tendency of non-volatile solutes on non-polar surfaces of bubbles was verified by the exhibition of saturation type kinetics, typical of Langmuirian behavior (Serpone et al. 1994), which can be applied for PFOX of higher concentrations leading to rapid saturation at the interfacial region, making low frequency sonication ineffective. But in case of trace level concentration of PFOX, the solute can evade the saturation phenomena and can be effectively degraded at the interfacial sheath, where pressure gradients and temperatures are still high enough to induce thermal effects.

6.4.2 Reaction kinetics of PFOX

The pseudo-first-order kinetic model was used to evaluate the effect of operational parameters on the degradation of PFOX. Based on Eqn. 32, plots of C_t versus irradiation time (t) were made as shown in Fig. 6.3.

$$C_t = C_0 e^{-kt} \quad (32)$$

Where, k is the measured rate constant and C_0 , C_t are the concentrations of PFOX at time “0” and “t” respectively.

6.4.3 Effect of initial concentration of PFOX on its degradation

The initial concentration of pollutant is one of the significant factors affecting the efficiency of degradation. While several reported results suggest a decline in the degradation rate with an increase in the initial concentration of the pollutant, some of the investigations reported that an optimum concentration of the pollutant led to the highest rate of degradation (Chowdhury and Viraraghavan 2009; Panda and Manickam 2017; Vecitis et al. 2008). The extent of pyrolytic destruction of semi-volatile or non-volatile pollutants is dependent on their concentration and hydrophobicity, which define their ability to migrate towards the bubble-liquid interface and to accumulate (Serpone et al. 1994). The concentration of PFOX was varied from 20 to 2000 pM while maintaining the operating temperature at 20 °C, power density of 375 W and pH at 2. The degradation enhanced up to an initial concentration of 220 pM of PFOS and 180 pM of PFOA beyond which a decline in the degradation rate was witnessed, indicating as the optimum concentration for the highest rate of degradation. Under identical conditions, the rate constant of PFOA was higher than PFOS (Table 6.2) and a complete disappearance of PFOA was observed within 70 min of treatment, indicating faster removal of PFOA as compared to PFOS. Above the optimum concentration of PFOX, the surface of bubbles is expected to be saturated and hence a decline in the degradation rate was witnessed.

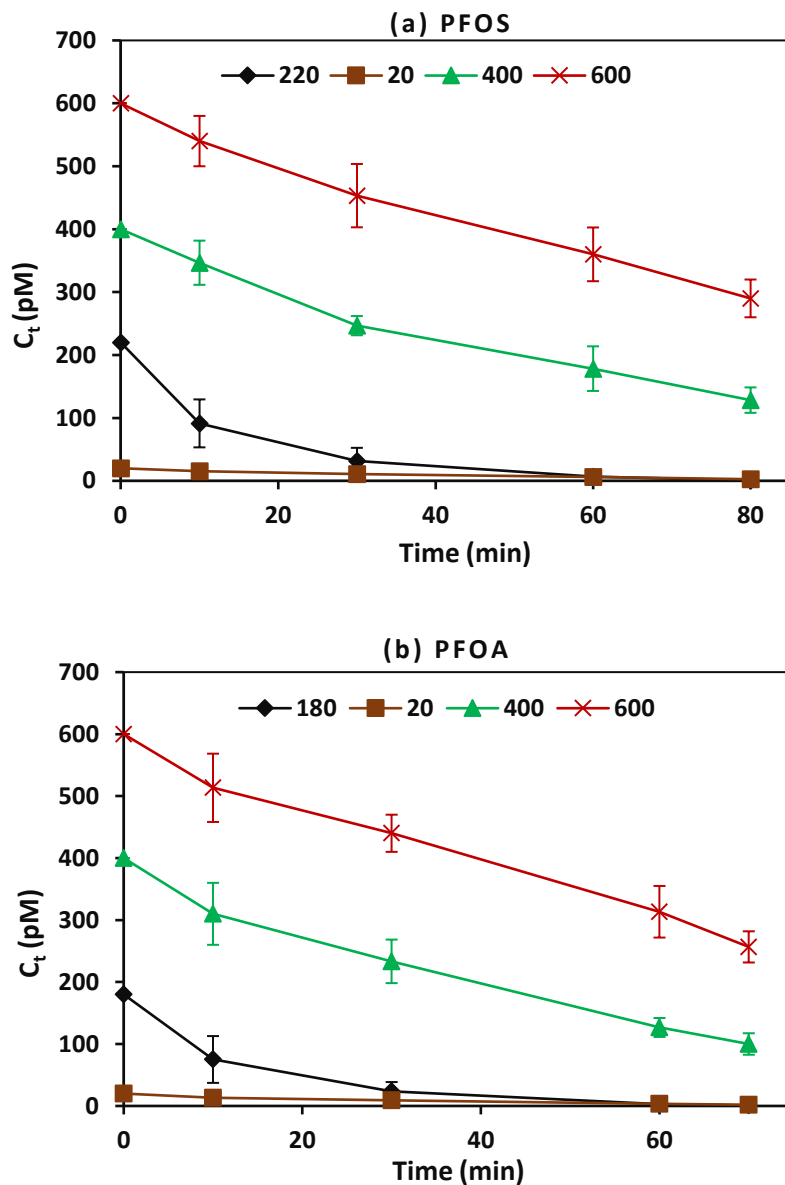


Figure 6.3. Degradation of PFOX at various initial concentrations (a) PFOS, (b) PFOA

Vecitis et al. (2008) reported that at higher concentrations ($>20 \mu\text{M}$), excess PFOS cannot evaporate into cavitation bubbles following the saturation of bubble-water interfacial adsorption sites, which lead to a decline in the degradation efficiency (Yang et al. 2013). Similarly, Mendez-Arriaga et al. (2008) observed an optimum concentration of 5 mg/L for Ibuprofen followed by a relatively constant degradation rate at higher concentrations.

Table 6.2. Pseudo-first-order rate constants for PFOX under different initial concentration

Concentration (pM)		k (min ⁻¹)		R ²	
PFOS	PFOA	PFOS	PFOA	PFOS	PFOA
20	20	0.024	0.031	0.96	0.98
220	180	0.068	0.075	0.97	0.98
400	400	0.014	0.019	0.99	0.99
600	600	0.009	0.011	0.99	0.98

6.4.4 Effect of operating temperature on degradation

The operating temperature of the solution plays a vital role in the degradation of pollutants during cavitation-based processes. A change in the operating temperature during cavitation affects the cavitation intensity owing to the variation in the physiochemical properties of the liquid medium (Golash and Gogate 2012). By using the cooling system, the operating temperature was controlled to vary over a range of 10-40 °C, while maintaining the concentration of PFOX at 200 pM, power density of 375 W and pH of 2. The operating temperature of 20 °C has been found to be optimum for the degradation of PFOX and the obtained results suggest that increasing temperature beyond an optimum value resulted in a significant decrease in the degradation efficiency. Varying the operating temperature affects the cavitation intensity and the type of cavities formed (gaseous or vaporous) as well as affecting the kinetic rate constant of the components subjected to degradation (Evgenidou et al. 2005). Previous studies on bubble dynamics indicated that a linear decrease in the collapse pressure is witnessed with a rise in the bulk liquid temperature (Gogate et al. 2003).

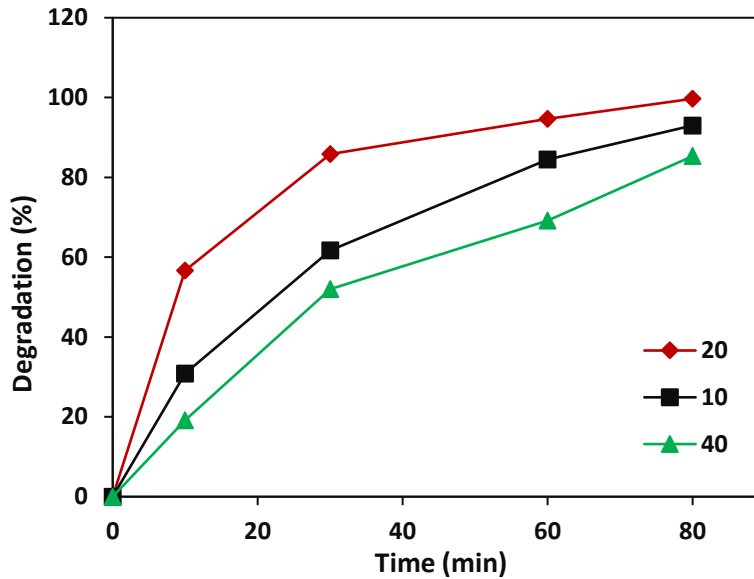


Figure 6.4. Degradation of PFOX at different temperatures: (■) 10 °C, (◆) 20 °C, (▲) 40 °C

At high temperature, PFOX migrates easily from the bulk solution to the interfacial regions, but at the same time a decline in the bubble collapse intensity could result with a rise in temperature. Similarly, Lin et al. (2015) and Yang et al. (2013) reported the detrimental effect of higher sonochemical reaction temperatures on the degradation of PFOX.

6.4.5 Effect of acoustic power on degradation

The extent of applied ultrasound power is one of the vital factors in the sonochemical degradation of pollutants, as it can alter the generation of number of active cavitation bubbles (Merouani et al. 2010). The correlation between sonochemical reactions and the applied power can be illustrated as follows: (1) the rate and the generation of number of active bubbles increase with an increase in the power density, (2) an increase in the size (R_m) of individual bubbles with an increase in power. An increase in R_m results in higher collapse temperature because of the conversion of higher available potential energy into heat (Kanthale et al. 2008). (3) Mixing intensity increases with an increase in the power density because of the turbulence produced from cavitation effects. The

effect of acoustic power on the degradation of PFOX was monitored by varying the power (150-410 W) at an operating temperature of 20 °C, at PFOX concentration of 200 pM, and at pH 2 to decide the optimum conditions. Fig. 6.5 shows the average degradation of PFOS and PFOA (PFOX) with respect to the change in power density.

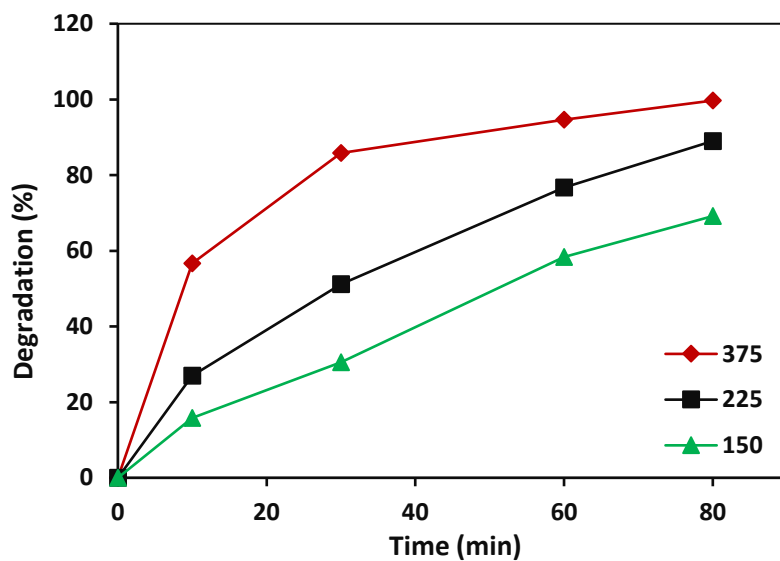


Figure 6.5. Degradation of PFOX at different ultrasonic power levels: (▲) 150, (■) 225, (◆) 375 W

It is evident that the rate constants increased with an increase in acoustic power up to 375 W beyond which a decline in the degradation rate was observed. By increasing the power, the energy of cavitation enhanced following a more violent implosion up to the optimum value. It has been reported that an increase in the acoustic intensity up to a maximum of 8.4 W/cm² and 110 W/cm² enhanced the degradation efficiency of Ofloxacin and Nitrotoluenes (Panda and Manickam 2017), beyond which a decline in the degradation was observed. The optimum power dissipation and its effectiveness in pollutant removal are dependent on the reactor configuration and the pollutant employed, beyond which cavitation events may be affected or reduced marginally.

6.4.6 Effect of pH on the degradation of PFOX

The pH of the reaction solution plays a vital role in deciding the rate and the extent of degradation of pollutants. Sonochemical degradation of PFOX was conducted for solution pH in the range of 2-7, at an operating temperature of 20 °C, while maintaining the power density of 375 W and an initial concentration of 200 μM of PFOX. While the highest rate of removal efficiency was observed under acidic conditions (Fig. 6.6), but only a marginal change in the degradation rate was witnessed at higher pH. Owing to low pKa values of PFOS and PFOA (Table 6.3), PFOX will be present in the ionized forms in the pH range of 2-7 and hence the degradation mechanism followed a similar pattern at different pH values.

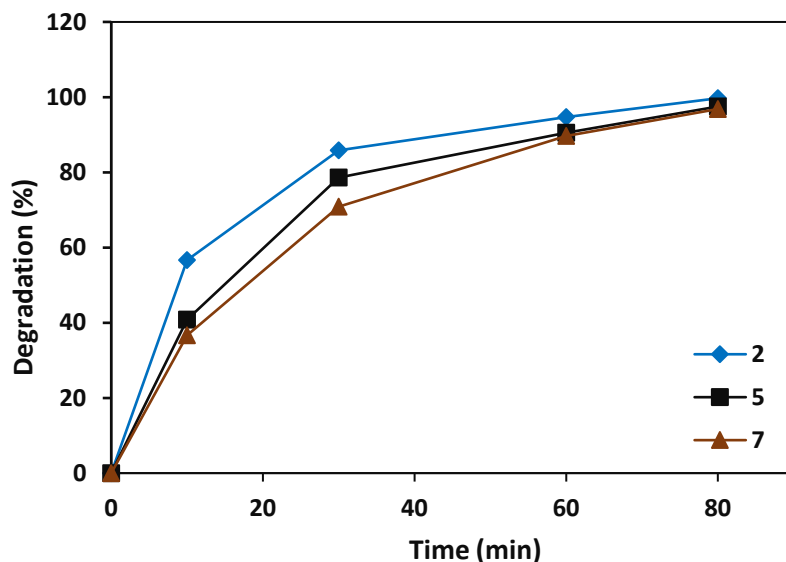


Figure 6.6. Degradation of PFOX at different pH: (◆) 2, (■) 5, (▲) 7

Table 6.3. pKa values of PFOX and their degradants

Compound	pKa
PFOS	<1.0
PFOA	- 0.5 to 2.8
Perfluoroheptanoic acid (PFHpA)	-2.29
Perfluorohexanoic acid (PFHxA)	-0.16
Perfluoropentanoic acid (PFPA)	0.31
Heptafluorobutyric acid (PFBA)	0.4
Pentafluoropropionic acid (PFPrA)	0.18
Trifluoroacetic acid (TFA)	0.3

6.5 Conclusions

In the present study, the degradation of low concentration/trace level of PFOX by low frequency (20 kHz) ultrasound has been investigated. The main conclusions observed from this investigation are:

- Low frequency sonochemical treatment has been proven to be advantageous over the previously employed techniques such as faster removal rate along with complete removal of trace level of PFOX with efficient utilization of energy.
- The gas/liquid interfacial region is the most effective site for the degradation of PFOX.
- LC-MS/MS analysis demonstrated the degradation of PFOX with the detection of 7 short chain intermediates and indicated the complete removal of PFOX within 80 min of sonication.

6.6 References

- German, T., 2014. Annex xv restriction report proposal for a restriction PFOA-related substances, European Chem. Agency 1, 340.
- EFSA, 2008. Perfluorooctane sulfonate (PFOS), perfluorooctanoic acid (PFOA) and their salts: scientific opinion of the panel on contaminants in the food chain, 653, 1–131.
- US EPA, 2014. Health effects document for perfluorooctane sulfonate (PFOS), 208.
- US EPA, 2016. Health effects support document for perfluorooctanoic acid (PFOA).
- ASTDR, 2009. Toxicological profile for perfluoroalkyls, 4.
- Zareitalabad, P., Siemens, J., Hamer, M., Amelung, W., 2013. Perfluorooctanoic acid (PFOA) and perfluorooctanesulfonic acid (PFOS) in surface waters, sediments, soils and wastewater - a review on concentrations and distribution coefficients, *Chemosphere* 91, 725–732.
- Goss, K., 2008. The pKa values of PFOA and other highly fluorinated carboxylic acids, *Environ. Sci. Technol.* 42, 456–458.
- Goss, K., Bronner, G., 2006. What is so special about the sorption behavior of highly fluorinated compounds?, *J. Phys. Chem. A.* 110, 9518–9522.
- 3M, 1999. The science of organic fluorochemistry.
- Vecitis, C. D., Park, H., Cheng, J., Mader, B. T., Hoffmann, M. R., 2009. Treatment technologies for aqueous perfluorooctanesulfonate (PFOS) and perfluorooctanoate (PFOA), *Front. Environ. Sci. Eng.* 3, 129-151.
- Rodriguez-Freire, L., Balachandran, R., Sierra-Alvarez, R., Keswani, M., 2015. Effect of sound frequency and initial concentration on the sonochemical degradation of perfluorooctane sulfonate (PFOS), *J. Hazard. Mater.* 300, 662–669.

- Cheng, J., Vecitis, C. D., Park, H., Mader, B. T., Hoffmann, M. R., 2010. Sonochemical degradation of perfluorooctane sulfonate (PFOS) and perfluorooctanoate (PFOA) in groundwater: kinetic effects of matrix inorganics, *Environ. Sci. Technol.* 44, 445–450.
- Vecitis, C. D., Park, H., Cheng, J., Mader, B. T., Hoffmann, M. R., 2008. Kinetics and mechanism of the sonolytic conversion of the aqueous perfluorinated surfactants, perfluorooctanoate (PFOA), and perfluorooctane sulfonate (PFOS) into inorganic products, *J. Phy. Chem. A.* 112, 4261–4270.
- Moriwaki, H., Takagi, Y., Tanaka, M., Tsuruho, K., Okitsu, K., Maeda, Y., 2005. Sonochemical decomposition of perfluorooctane sulfonate and perfluorooctanoic acid, *Environ. Sci. Technol.* 39, 3388–3392.
- Phan Thi, L. A., Do, H. T., Lo, S. L., 2014. Enhancing decomposition rate of perfluorooctanoic acid by carbonate radical assisted sonochemical treatment, *Ultrason. Sonochem.* 21, 1875–1880.
- Lin, J. C., Lo, S. L., Hu, C. Y., Lee, Y. C., Kuo, J., 2015. Enhanced sonochemical degradation of perfluorooctanoic acid by sulfate ions, *Ultrason. Sonochem.* 22, 542–547.
- Chowdhury, P., Viraraghavan, T., 2009. Sonochemical degradation of chlorinated organic compounds, phenolic compounds and organic dyes - a review, *Sci. Total Environ.* 407, 2474–2492.
- Lee, P. J., Bernier, E. T., Fujimoto, G. T., Shia, J., Young, M. S., Di Gioia, A. J., 2008. Acquity UPLC system solution for quantifying trace levels of perfluorinated compounds with an acquity PFC analysis kit, Waters.
- Shimadzu, 2011. Analysis of PFCs in environmental water using triple quadrupole LC / MS / MS [LCMS-8030].

- Tang, C., Tan, J., Wang, C., Peng, X., 2014. Determination of perfluorooctanoic acid and perfluorooctane sulfonate in cooking oil and pig adipose tissue using reversed-phase liquid-liquid extraction followed by high performance liquid chromatography tandem mass spectrometry, *J. Chromatogr. A.* 1341, 50–56.
- Song, W., de La Cruz, A.A., Rein, K., O’Shea, K.E., 2006. Ultrasonically induced degradation of microcystin-LR and -RR: identification of products, effect of pH, formation and destruction of peroxides, *Environ. Sci. Technol.* 40, 3941–3946.
- Riesz, P., Berdahl, D., Christman, C. L., 1985. Free radical generation by ultrasound in aqueous and nonaqueous solutions, *Environ. Health Perspect.* 64, 233–252.
- Merouani, S., Hamdaoui, O., 2016. The size of active bubbles for the production of hydrogen in sonochemical reaction field, *Ultrason. Sonochem.* 32, 320–327.
- Ince, N. H., Tezcanli, G., Belen, R. K., Apikyan, I. G., 2001. Ultrasound as a catalyzer of aqueous reaction systems: the state of the art and environmental applications, *Appl. Catal. B: Environ.* 29, 167–176.
- Serpone, N., Terzian, R., Hidaka, H., Pelizzetti, E., 1994. Ultrasonic induced dehalogenation and oxidation of 2-, 3-, and 4-chlorophenol in air-equilibrated aqueous media. Similarities with irradiated semiconductor particulates, *J. Phys. Chem.* 98, 2634–2640.
- Alegria, A. E., Lion, Y., Kondo, T., Riesz, P., 1989. Sonolysis of aqueous surfactant solutions: probing the interfacial region of cavitation bubbles by spin trapping, *J. Phys. Chem.* 93, 4908–4913.
- Golash, N., Gogate, P. R., 2012. Degradation of dichlorvos containing wastewaters using sonochemical reactors, *Ultrason. Sonochem.* 19, 1051–1060.

- Evgenidou, E., Fytianos, K., Poullos, I., 2005. Semiconductor-sensitized photodegradation of dichlorvos in water using TiO₂ and ZnO as catalysts, *Appl. Catal. B Environ.* 59, 81–89.
- Gogate, P. R., Wilhelm, A. M., Pandit, A. B., 2003. Some aspects of the design of sonochemical reactors, *Ultrason. Sonochem.* 10, 325–330.
- Yang, S. W., Sun, J., Hu, Y., Cheng, J., Liang, X., 2013. Effect of vacuum ultraviolet on ultrasonic defluorination of aqueous perfluorooctanesulfonate, *Chem. Eng. J.* 234, 106–114.
- Mendez-Arriaga, F. Torres-Palma, R. A., Petrier, C., Esplugas, S., Gimenez, J., Pulgarin, C., 2008. Ultrasonic treatment of water contaminated with ibuprofen, *Water Res.* 42, 4243–4248.
- Merouani, S., Hamdaoui, O., Saoudi, F., Chiha, M., 2010. Sonochemical degradation of rhodamine B in aqueous phase: effects of additives, *Chem. Eng. J.* 158, 550–557.
- Kanthale, P., Ashokkumar, M., Grieser, F., 2008. Sonoluminescence, sonochemistry (H₂O₂ yield) and bubble dynamics: frequency and power effects, *Ultrason. Sonochem.* 15, 143–150.
- Panda, D., Manickam, S., 2017. Recent advancements in the sonophotocatalysis (SPC) and doped-sonophotocatalysis (DSPC) for the treatment of recalcitrant hazardous organic water pollutants, *Ultrason. Sonochem.* 36, 481–496.
- Vecitis, C. D., Park, H., Cheng, J., Mader, B. T., Hoffmann, M. R., 2008. Enhancement of perfluorooctanoate and perfluorooctanesulfonate activity at acoustic cavitation bubble interfaces, *J. Phys. Chem. C.* 112, 16850–16857.

Chapter 7

Overall discussion

To understand the overall outcomes of the PhD work, a relative comparison chart indicating achievements and discussion regarding vital factors necessary for pollutant degradation has been outlined in this chapter. Following sonochemical, HC and sono-Fenton treatment of pollutants in our study, Fig. 7.1 summarizes the extent of degradation under optimum conditions.

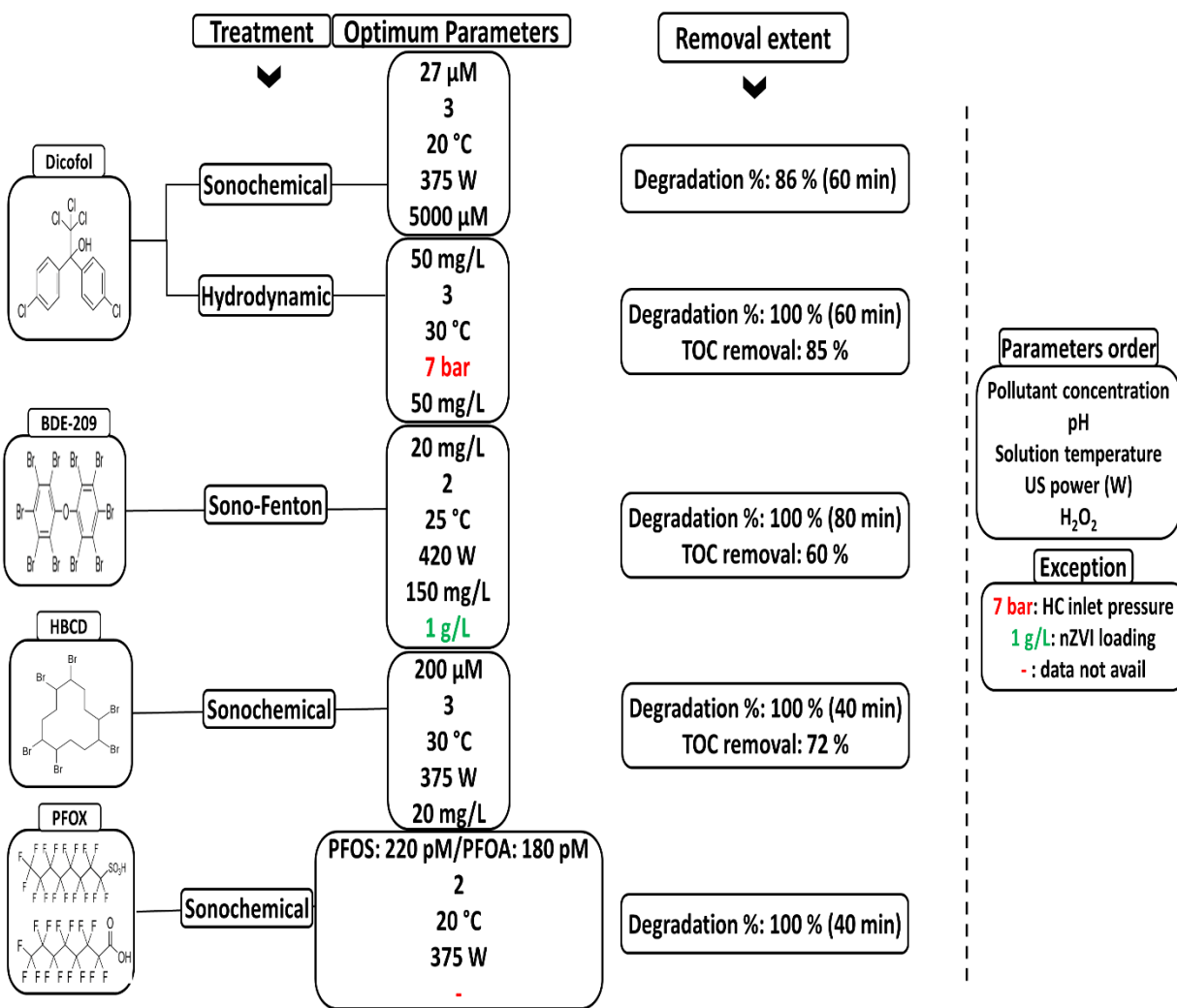


Fig. 7.1. Comparison chart

Efficiency of cavitation-based treatment depends on several operating parameters such as solution pH and temperature, concentration of pollutant and catalyst, addition of H₂O₂ and ultrasonic power density. Following our observation, the dependence of degradation rate on the initial concentration of pollutant can be categorized as follows:

- **Linear dependence:** Either an enhancement or a drop in the degradation rate with an increase in the concentration of pollutant.
- **Non-linear dependence:** An optimum concentration of pollutant up to which an augmentation in the degradation rate of pollutant can be observed, beyond which a fall in the degradation rate takes place.

Following outcomes of this research, it has been observed that the removal efficiency of pollutants followed non-linear dependence. The impact of initial pollutant concentration on the degradation rate is dependent on the nature of specific pollutant whether it's volatile, hydrophobic or hydrophilic. Semi-volatile and hydrophobic pollutants such as Dicofol, HBCD and BDE-209 apparently present in the interfacial region rather than in the cavities and hence mostly depend on the thermal decomposition driven degradation up to the optimum value.

We have witnessed varying degradation rate for the change in reaction solution pH value. The degradation of pollutants favored at an acidic pH and the degradation efficiency declined at basic environment. Summarizing the facts, following points are vital while deciding the effect of pH on degradation.

- The aqueous solubility of a pollutant.
- pKa values of the specific pollutant.

The addition of H₂O₂ as an external oxidizing agent affects the degradation of nonvolatile compounds as compared to volatile and semi-volatile compounds. According to the hypothesis,

degradation of Dicofol, BDE-209 etc. followed similar degradation pattern for H₂O₂ addition, indicating interfacial thermal decomposition to be the dominant degradation pathway. It can be attributed to the degradation of semi-volatile organic compounds which takes place at the vapor-liquid interface, while the degradation of nonvolatile compounds takes place in the liquid bulk solution.

To summarize the effect of solution temperature, we can conclude that an optimum temperature may exist for every individual pollutant which depends on its reactivity with hydroxyl radicals. The extent of applied ultrasound power and HC inlet pressure are also vital factors in the cavitation methods, as they can alter the generation of number of active cavitation bubbles. The optimum power dissipation and its effectiveness in pollutant removal are dependent on the reactor configuration and the pollutant under investigation. Beyond this optimum power dissipation, cavitation events may be affected or reduced marginally.

Chapter 8

Conclusions

In the overall investigation, five recalcitrant organic pollutants (Dicofol, HBCD, BDE-209, PFOS and PFOA) were subjected to sonochemical treatment, whereas hydrodynamic cavitation treatment was implemented for Dicofol. Different operational parameters such as solution pH, bulk phase temperature, initial concentration of pollutant, loading of hydrogen peroxide, ultrasonic power density, loading of Fenton's reagent, inlet pressure of HC and loading of radical scavenger were studied for the enhancement of degradation rate. This study identified the capacity of cavitation-based treatment for the removal of recalcitrant pollutant as compared to traditional wastewater treatment processes.

In Chapter 2, there was evidence that sonochemical treatment can effectively remove Dicofol. It was demonstrated that the removal efficiency reached maximum after considering optimum operational parameters such as initial pollutant concentration, ultrasonic power density, solution temperature, pH and the addition of H₂O₂. Furthermore, the effect of initial concentration of pollutant and ultrasonic power density were found to be significant. In general, the degradation rate hindered above and below 27 μM of an initial concentration of Dicofol, whereas an enhancement in the removal rate was observed with an increase in power density up to 375 W. Additionally, the solution pH and temperature both impact the removal efficiencies. A decrease in solution pH resulted in an enhancement in the degradation due to the easy transport of pollutants towards the bubble interfacial region. Based on radical scavenger test in this study, it was anticipated that thermal decomposition at bubble-vapor interface to be the dominant degradation mechanism. Sonochemical treatment is effective and promising for successful removal of harmful pesticides such as Dicofol and superior removal efficiency for other POPs is expected in the near future with the successful implementation of ultrasound-based wastewater treatment.

In Chapter 3, Hydrodynamic cavitation treatment demonstrated its effectiveness in complete removal of Dicofol within just 1 hr of treatment. It was determined that factors such as inlet pressure, initial concentration of Dicofol, solution temperature, pH and addition of H₂O₂ significantly impacted the removal efficiency. The degradation rate enhanced up to the inlet pressure of 7 bar, whereas the rate declined with an increase in the initial concentration of Dicofol from 50 to 100 mg/L. From the results, Hydrodynamic cavitation proved to be more effective in Dicofol removal than sonochemical treatment, with a degradation yield of 12 times higher than acoustic cavitation. Overall, the attempted hydrodynamic cavitation demonstrated successful and rapid removal of endocrine disruptive chemicals such as Dicofol and is expected to provide efficient solution for wastewater treatment.

Chapter 4 described the effect of combined US/Fenton treatment for BDE-209 degradation compared to individual processes (US and Fenton). Findings from this study showed that the removal rate enhanced during Sono-Fenton treatment with complete degradation of BDE-209 within 80 min of treatment which was dependent on solution pH, ultrasonic power density, and loading of Fenton's reagent. The removal efficiency was found to be only 40 % and 25 %, during US and Fenton treatment alone. During US/Fenton treatment, the degradation rate decreased from 0.019 min⁻¹ to 0.005 min⁻¹ for an increase in the initial concentration from 20 to 100 mg/L. Based on cavitation theory, it is known that increasing the pollutant concentration beyond the optimum value saturates the bubble surface, which could result in the decline in degradation rate. The detection of oxidative products such as Phenol and *p*-Hydroquinone along with lower brominated congeners, illustrated the role of both reductive and oxidative process during US/Fenton treatment. However, this research has demonstrated that application of ultrasound during the combined process provides additional reactive radicals, while preventing the agglomeration of pollutants at

the surface of iron as well. Overall, the combined US/Fenton treatment performed more effectively compared to individual treatments, demonstrating a synergy index (f) of 1.96. This new approach involving simultaneous application of US and Fenton treatment has great promise and capacity as an innovative tool for the elimination of numerous other PBDEs.

In Chapter 5, the sonochemical removal of HBCD has been illustrated, while considering the essential optimum parameters for the highest rate of degradation. This research has demonstrated that the highest rate of HBCD degradation was achieved under acidic conditions, where the rapid transport of precursor compound towards the interfacial region takes place. Additionally, the properties of detected transformed products of HBCD, indicated thermal decomposition at the bubble-vapor interface as the dominant degradation pathway, following radical attack and recombination of short chain intermediates at later stage of transformation. The high TOC removal (72 %) within 40 min of treatment demonstrated the mineralization of HBCD to be prominent during sonolysis. The *Daphnia magna* ecotoxicity assessment of HBCD, indicated the decline in toxicity after 40 min of treatment, which could be due to subsequent degradation of toxic intermediates with treatment time. This study confirms that the employment of sonochemical treatment should be further explored for the removal of hydrophobic pollutants to achieve successful mineralization.

Chapter 6 demonstrated the sonochemical treatment of PFOX (PFOS and PFOA), while discussing the necessary precautions to be undertaken during LC/MS analysis for quality assurance. The complete disappearance of PFOX was observed within 80 min of treatment under optimum operating conditions. Thermal decomposition at the bubble-vapor interface along with pyrolysis of short chain degraded products inside the bubble core were assumed to be the dominant degradation pathways. The significance of low frequency sonication for trace level removal of PFOX was

established to illustrate the degradation mechanism. Our study has systematically considered the crucial operating factors while investigating the removal of PFOX.

Recommendation

To obtain the highest pollutant removal efficiency under cavitation-based treatment, optimum values of solution temperature, ultrasound power density, initial concentration of pollutant with respect to sonication frequency, solution pH and inlet pressure of HC should be decided. Future investigations should also focus on the effect of sonication frequency on pollutant degradation, which could lead to a better understanding of the process. Understanding these mechanisms will not only lead to enhanced effectiveness and optimization of experimental parameters during the removal of pollutants, but also will bring future best practices to treat them effectively. Intensification in the generation of bubbles during cavitation-based methods via innovative reactor design and development of sun light driven cavitation reactor should also be explored. Implementation of cavitation-based treatment could lead to a promising wastewater treatment technique for the elimination of harmful pollutants. The need of low-cost wastewater treatment methods and large-scale commercialization require successful implementation of cavitation-based methods and hence ongoing research is anticipated for the advancement of cavitation treatment methods.